



REPUBLIC OF TURKEY
KARADENİZ TECHNICAL UNIVERSITY
GRADUATE SCHOOL OF HEALTH SCIENCES

DEPARTMENT OF MEDICAL MICROBIOLOGY

**RECOMBINANT PHAGE ENDOLYSINS
PRODUCTION AND INVESTIGATION OF
THEIR EFFICACY AGAINST
STAPHYLOCOCCAL BIOFILMS**

By

Mujib Abdulkadir ABDURAHMAN

IN PARTIAL FULFILLMENT OF THE
REQUIREMENTS FOR THE DEGREE OF DOCTOR
OF PHILOSOPHY IN MEDICAL MICROBIOLOGY

Prof. Dr. Ali Osman KILIÇ

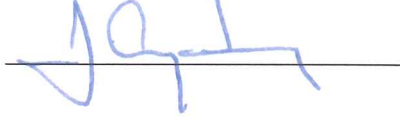
TRABZON-2018

APPROVAL

This dissertation satisfies all requirements for the degree of Doctor of Philosophy

Prof. Dr. Faruk AYDIN

Head of the Department of Medical Microbiology



The dissertation titled "Recombinant Phage Endolysins Production and Investigation of their Efficacy Against Staphylococcal Biofilms" prepared by Mujib Abdulkadir ABDURAHMAN, at the Department of Medical Microbiology, Graduate School of Health Sciences, Karadeniz Technical University, was examined for scope and scientific quality in accordance with the Karadeniz Technical University Rules and Regulations Governing Graduate Studies and accepted as Doctoral dissertation.

Supervisor Prof. Dr. Ali Osman KILIÇ



Committee members

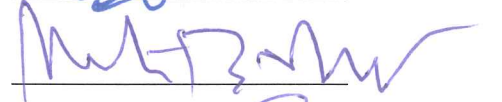
Prof. Dr. Ali Osman KILIÇ



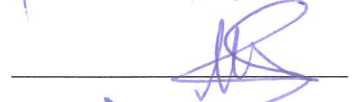
Prof. Dr. Zihni Açar YAZICI



Prof. Dr. Mehmet Ziya DOYMAZ



Prof. Dr. İlknur TOSUN



Dr. Tuba DİNÇER



Date : / / 2018

This dissertation has been approved by the board of Graduate School of Health Sciences, Karadeniz Technical University on / / with decision number of

.....

Prof. Dr. Ersan KALAY

Dean, Graduate School of Health Sciences

DECLARATION

I declare that this dissertation is written in accordance with the standards of the Karadeniz Technical University, Graduate School of Health Sciences thesis writing guide, I declare that the research contained in this dissertation, unless otherwise formally indicated within the text, is the original work of the author. The dissertation has not been previously submitted to this or any other university for a degree and does not incorporate any material already submitted for a degree.

02/05/2018

Mujib Abdulkadir ABDURAHMAN



Dedication

To my family, parents, sisters and brothers who have been constant sources of inspiration in my life and career.

ACKNOWLEDGMENTS

My sincerest gratitude goes to Allah (SWT). He has given me the strength; patience and hope that I needed to go through my studies.

I first and foremost, wish to thank my supervisor Prof. Dr. Ali Osman KILIÇ, as well as my co-supervisor Prof. Dr. İlknur TOSUN. I am very grateful for all your help, supervision and patience. The excellent advice and support have been invaluable in regards to both the laboratory work as well as the completion of my dissertation.

I would like to thank our department head Prof. Dr. Faruk AYDIN and other fantastic staff, in particular, Prof. Dr. Neşe KAKLIKKAYA, Assoc. Prof. Dr. Gulçin BAYRAMOĞLU, Assoc. Prof. Dr. Celal Kurtuluş BURUK and Assist. Prof. Dr. Esra ÖZKAYA for all their unfailing support and assistance.

I am very grateful to all staff members in Medical Biology Department, Prof. Dr. Ersan KALAY, Assist. Prof. Dr. Tuba DİNCER, Assist. Prof. Dr. Bayram TORAMAN, and all Research Assistants in the department including Idris ER, Cerren SARI, Asiye Buşra BOZ ER, Gülden BUDAK, Ceren SUMER for all their expertise, technical and instruments support, and for conversations and teaching me protein expression, DNA sequencing, and cell culture.

I would like to thank the following people both in specialist program and graduate program of our department for helping each time I was in need and for the excellent lab environment Dr. Erhan KONGUR, Dr. Rukiye AKYOL, Dr. Bünyamin KASAP, Dr. Şükran ÖNDER, Dr. Ahu REİS, Research Assistants Gülşen ULUÇAM ATAY, Merve CORA, İnci DURUKAN, Sana TABBOUCHE and Jaleel SAMANJE for your support and assistance. It was great sharing laboratory with you all during last five years.

I would like to express my special gratitude and thanks to Dr. Enis Fuat TÜFEKÇİ for his support in many aspects including laboratory work and his friendship from the very beginning of my arrival in Turkey.

I am very grateful to Prof. Dr. Şengül ALPAY KARAOĞLU (Recep Tayyip Erdogan University) for providing me mitomycin C and other technical support. I am also very thankful to İnci DURUKAN, Mona KHORSHIDTALAB, Prof. Dr. Ümit COBANOĞLU and Mehmet Ali ÖZDEŞ for their technical help to take TEM micrographs.

I would like to thank Fatih OZKALAY in Metallurgical and Materials Engineering department of Karadeniz Technical University; Assoc. Prof. Dr. Urartu ŐEKER, Research Assistants Musa Efe IŐILAK and Recep Erdem AHAN in National Nanotechnology Research Center of Bilkent University for their help to take SEM micrographs.

A very special gratitude to my beloved wife Semiir Hassen and my two-baby boys, Reyyan and Miraj, who provided through moral and expressive support in my life. I am also grateful to my other family members and friends who have supported me along the way.

Finally, I would like to thank Trkiye Scholarship for the grant throughout my Ph.D. study.

This project was supported by the Scientific Research Projects Coordination Unit of Karadeniz Technical University (Project number: TDK-2015-5340).

Mujib Abdulkadir ABDURAHAMAN

TABLE OF CONTENTS

	Page
INNER COVER PAGE	
APPROVAL	
DECLARATION	
DEDICATION	
ACKNOWLEDGMENTS	
TABLE OF CONTENTS	vii
LIST OF TABLES	xi
LIST OF FIGURES	xii
LIST OF ABBREVIATIONS	xv
1. ABSTRACT	1
2. ÖZET	2
3. INTRODUCTION AND AIMS	3
4. LITERATURE REVIEW	6
4.1. Overview of <i>Staphylococcus</i> species	6
4.1.1. <i>Staphylococcus aureus</i>	6
4.1.1.1. Cell wall Structure	7
4.1.1.2. Mechanism of <i>S. aureus</i> Pathogenicity	8
4.1.1.3. Epidemiology of <i>S. aureus</i>	9
4.1.2. <i>S. epidermidis</i> and other Coagulase Negative Staphylococci	10
4.2. Bacterial Biofilms	10
4.2.1. Stage of Biofilm Formation	11
4.2.2. Biofilms in Device Related Infections	12
4.2.3. Biofilm Control	13
4.3. Bacteriophages	14
4.3.1. Phage Structure	14
4.3.2. Phage Life Cycle	15
4.3.3. Prevalence, Isolation and Classification of Bacteriophages	16
4.3.4. Bacteriophage Therapy	19
4.4. Bacteriophage Endolysins	19
4.4.1. Structural and Biochemical Diversity of Endolysins	20

4.4.2. Applications of Endolysins	22
4.4.2.1. Endolysins as Therapeutic Agents	22
4.4.2.2. Application of Endolysins in Biofilm Removal	24
4.4.2.3. Endolysins in Veterinary and Food Applications	25
4.5. Production of Recombinant Proteins	25
5. MATERIALS AND METHODS	27
5.1. Materials	27
5.1.1. Bacterial Strains and Plasmids	27
5.1.2. Primers Used in the Study	28
5.1.3. Media, Growth Conditions, and Storage of Bacteria and Phages	28
5.1.4. Enzymes, Chemicals and Reagents	29
5.2. Methods	29
5.2.1. Bacterial Culture Conditions	29
5.2.2. Bioinformatics Search and Primer design	29
5.2.3. Genomic DNA Extraction from <i>S. aureus</i>	30
5.2.4. PCR Screening of Endolysin Genes in Genomic DNA of <i>S. aureus</i> Strains	30
5.2.5. Phage Isolation	30
5.2.6. Plaque Assay and Phage Purification	31
5.2.7. Phage Propagation and Concentrations	31
5.2.8. Imaging of Phages by Transmission Electron Microscopy	32
5.2.9. Determination of Phage Host Range	32
5.2.10. One-step Phage Growth Curve	33
5.2.11. Phage DNA Isolation	33
5.2.12. Restriction Enzyme Analysis of Phage DNA	33
5.2.13. Amplification of Endolysin Gene from Phage DNA by PCR	34
5.2.14. Agarose Gel Electrophoresis for Separation of DNA Fragment	34
5.2.15. Purification of PCR Products	34
5.2.16. Cloning and Transformation of Endolysin Genes	35
5.2.16.1. Preparation of Competent Cells	35
5.2.16.2. Cloning of PCR Products	35
5.2.16.3. Transformation of Recombinant Plasmids into <i>E. coli</i>	36
5.2.17. Plasmid DNA Isolation	36

5.2.18. Sequencing of Plasmid DNA	36
5.2.19. Transformation of Recombinant Plasmids into Expression Host	37
5.2.20. Expression of Endolysins	37
5.2.21. Preparation of Samples Before Running SDS Gels	37
5.2.22. Analysis of Expressed Endolysins by SDS-PAGE	38
5.2.23. Large Scale Production of Recombinant Endolysins	38
5.2.24. Purification of Recombinant Endolysin Proteins	39
5.2.25. Biological Activity of Recombinant Endolysins	39
5.2.26. Biochemical Characterization of Recombinant Endolysins	40
5.2.26.1. Heat Sensitivity Tests of Endolysins	40
5.2.26.2. Influence of pH on Endolysins	40
5.2.26.3. Effect of Divalent Metal Ions on Activity of Endolysins	40
5.2.27. Host Range Determination of Endolysins	41
5.2.28. <i>In vitro</i> Anti-biofilm Properties of Endolysins	41
5.2.28.1. Biofilm Disruption Test in Microtiter Plates	41
5.2.28.2. Biofilm Inhibition Assay in Microtiter Plates	42
5.2.28.3. Biofilm Removal Assay from Catheters	42
5.2.28.4. Prevention of Biofilm Formation on Catheters	43
5.2. 29. Scanning Electron Microscopy of Biofilms	43
5.2.30. <i>In Vitro</i> Cytotoxic Effects of Endolysins	44
5.2.30.1. Cytotoxicity Assay	44
5.2.31. Statistical Analysis	45
5.2.32. Phylogenetic Analysis	45
5.2.33. Sequence Variation Analysis	45
5.2.34. Structural Modeling	45
6. RESULTS	47
6.1. Screening Endolysin Gene in Genomic DNA of <i>S. aureus</i>	47
6.2. Phage Isolation	47
6.3. Transmission Electron Microscopy of Phages	48
6.4. Host Range Determination and Selection of Virulent Phages	50
6.5. One-Step Growth Curve	51
6.6. Analysis of Pahge DNA	52

6.7. PCR Amplification of Endolysin Genes from Phage DNA	53
6.8. Molecular Cloning of Endolysin Genes	54
6.9. Plasmid Sequencing	55
6.10. Pilot Expression of Endolysin proteins	60
6.11. Large Scale Expression of Endolysins	62
6.12. Purification and SDS-PAGE Analysis of Expressed Endolysins	62
6.13. Lytic Activity and Host Range Determination of Endolysins	64
6.14. Biochemical Characterization of Endolysins	68
6.15. Biofilm Inhibition and Disruption Capacity of Endolysins	70
6.15.1. Biofilm Disruption Assay Using Plate Staining Method	70
6.15.2. Prevention of Biofilm Formation Using Plate Staining Method	72
6.15.3. Biofilm Removal Assay from Catheters	72
6.15.4. Prevention of Biofilm Formation on Foley Catheters	74
6.16. Analysis of Biofilm Disruption by Scanning Electron Microscopy	75
6.17. Cytotoxicity Assessment on Growing Human Fibroblast Cells	79
6.18. Bioinformatics Analysis	79
6.18.1. Amino Acids Sequence Variation Analysis	79
6.18.2. Analysis of Modular Structure of Endolysin	81
6.18.3. Structural Modeling	82
7. DISCUSSION	84
8. CONCLUSION AND RECOMMENDATION	95
9. REFERENCES	98
10. ETHICAL COUNCIL APPROVAL	115
11. CURRICULUM VITAE	118

LIST OF TABLES

Table	Page
Table 1. The phage families based on morphology and genome characteristics	18
Table 2. Some examples of recombinant phage endolysins targeting pathogenic bacteria published in various articles	24
Table 3. List of primers used in this study	28
Table 4. Morphological characteristics of the seven phages isolated from clinical isolates	50
Table 5. Percent identity matrix of each endolysin with some other <i>S. aureus</i> phage endolysin genes found in the databases	58
Table 6. In vitro lytic efficacy of phages and its derived recombinant endolysin against <i>Staphylococcus</i> isolates originated from various clinical samples	66
Table 7. Percentage identity matrix to each individual endolysin obtained in this study	81

LIST OF FIGURES

Figure		Page
Figure 1.	Electron micrograph of <i>Staphylococcus aureus</i>	7
Figure 2.	Peptidoglycan units of <i>S. aureus</i> cell wall	8
Figure 3.	Virulence determination in <i>S. aureus</i>	9
Figure 4.	Stages of biofilm formation	12
Figure 5.	Generalized structure of tailed phage	15
Figure 6.	Bacteriophage life cycle	16
Figure 7.	Schematic representation of major phage group	18
Figure 8.	Schematic representation of mode of action of endolysin in the phage life cycle	20
Figure 9.	Schematic representation of the endolysin modular structure and catalytic cleavage sites on peptidoglycan	21
Figure 10.	Map of pET SUMO vector	27
Figure 11.	Screening for the endolysin gene in chromosomal DNA of <i>S. aureus</i>	47
Figure 12.	Lytic activity of phages against <i>S. aureus</i> strains using the spot method and the plaque assay method	48
Figure 13.	Transmission Electron Microscopic images of isolated phages	49
Figure 14.	Host range of the seven phages against 60 <i>S. aureus</i> isolates	51
Figure 15.	One-step growth curve of phage Φ trsa10, Φ trsa14, and Φ trsa15	52
Figure 16.	Agarose gel electrophoresis of phage genomic DNA.	53
Figure 17.	Restriction analysis of Φ trsa10, Φ trsa14, and Φ trsa15 DNA	53
Figure 18.	Amplification of endolysin gene from phage DNA	54
Figure 19.	Screening of recombinant plasmids from <i>E. coli</i> OneShot transformed by pET SUMO-endolysin construct	55
Figure 20.	Sequencing of endolysin genes cloned on pET SUMO vector	56
Figure 21.	Phylogenetic position of LysSA10, LysSA14, LysSA15, and LysSA52 endolysin genes derived from phages Φ trsa10, Φ trsa14, Φ trsa15 and phage 52 endolysins, respectively	59
Figure 22.	SDS-PAGE analysis of expressed LysSA10 endolysin at 37° C	61
Figure 23.	SDS-PAGE analysis of expressed LysSA10 endolysin at 20°C	61

Figure 24. SDS-PAGE analysis of supernatant fractions of four endolysins after large-scale expression at 20°C for 20 hours	62
Figure 25. SDS-PAGE analysis of SUMO fused endolysins before and after purification	63
Figure 26. Spot assay showing the ability of endolysins to lyse <i>Staphylococcal</i> species	65
Figure 27. Temperature stability of LysSA10, LysSA14, LysSA15, and LysSA52 endolysins	69
Figure 28. Influence of pH conditions on the bacterial activity of four endolysins	70
Figure 29. Effects of divalent metal ions (Mg ²⁺ , Ca ²⁺ , and Ca ²⁺) on lytic activity of the four endolysins	70
Figure 30. Biofilm degradation capacity of endolysins as determined by 96-well microtitre plate assay	71
Figure 31. Effect of endolysins on biofilm formation by <i>S. aureus</i> and <i>S. epidermidis</i> as determined by 96-well microtitre plate assay	72
Figure 32. The ability of endolysins to degrade 48 h old <i>S. aureus</i> and <i>S. epidermidis</i> biofilms from catheter sections as determined by viable cell count assay method	73
Figure 33. Effect of catheter coating with endolysin on the adherence of <i>S. aureus</i> and <i>S. epidermidis</i> to the catheter surface	74
Figure 34. Scanning electron microscopy showing the effect of treatment with the endolysin cocktail on 48 h old biofilms of <i>S. aureus</i> TRSA8 established on glass coupons	75
Figure 35. Scanning electron microscopy to show the effect of treatment with endolysin cocktail on 48 h old biofilms of <i>S. epidermidis</i> 30 (TRSE30) on coupons	76
Figure 36. Scanning electron microscopy (SEM) images of treated and untreated <i>S. aureus</i> and <i>S. epidermidis</i> biofilms on catheter surfaces	78
Figure 37. Assessment of cytotoxicity of four endolysins (LysSA10, LysSA14, LysSA15, and LysSA52) on human fibroblast cells	79

Figure 38. Amino acid sequence alignment of LysSA10, LysSA14, LysSA15, and LysSA52	80
Figure 39. Neighbor-joining phylogenetic tree showing the relationship between the four endolysin protein sequences isolated from Φ trsa10, Φ trsa14, Φ trsa15, and bacteriophage 52	81
Figure 40. Domain organization of the four endolysins (LysSA10, LysSA14, LysSA15, and LysSA52)	82
Figure 41. The predicted 3-D structures of endolysins	83



LIST OF ABBREVIATIONS

APS	Ammonium persulfate
ATCC	American Type Culture Collection
BLAST	Basic Local Alignment Search Tool
bp	Base pair
CFU	Colony forming units
CHAP	Cysteine and histidine-dependent amino hydrolase
CoNS	Coagulase-negative <i>Staphylococcus</i>
ddH₂O	Double distilled water
°C	Degree Centigrade
DNA	Deoxyribonucleic acid
EDTA	Ethylenediaminetetraacetic acid
h	Hour
His	Histidine
IPTG	Isopropyl β -D-1-thiogalactopyranoside
kDa	kilo Dalton
KCl	Potassium chloride
Km	Kanamycin
LB	Luria Bertani
MgCl₂	Magnesium chloride
μL	Microliter
min	Minute
mL	Millilitre
MRSA	methicillinMethicillin-resistant <i>S. aureus</i>
MTT	3-(4, 5-dimethylthiazol-2-yl)-2,5-diphenyltetrazolium bromide
NaCl	Sodium chloride
NAG	N-acetylglucosamine
NaOH	Sodium hydroxide
Ni-NTA	Nickel-nitrilotriacetic acid
nm	Nanometerre
OD	Optical Density
PAGE	Polyacrylamide gel electrophoresis
NAG	N-acetylmuramic acid

PBS	Phosphate-buffered saline
PCR	Polymerase Chain Reaction
PEG	polyethylene Polyethylene Glycol
PFU	Plaque forming units
SDS	Sodium dodecyl sulfate
SDS-PAGE	Sodium Dodecyl Sulfate-Polyacrelamide Polyacrylamide Gel Electrophoresis
SEM	Scanning Electron Microscopy
SOC	Super Optimal broth with catabolite repression
SUMO	Small ubiquitin-related modifier
TEM	Transmission Electron Microscope
TSA	Tryptone Soya Agar
TSB	Tryptone Soya Broth
V	Voltage

1. ABSTRACT

Recombinant Phage Endolysins Production and Investigation of their Efficacy against Staphylococcal Biofilms

Due to increasing antibiotic resistance among pathogenic bacteria, and inefficient strategies to combat biofilm infections, rigorous search for new alternative antimicrobial and anti-biofilm agents are subjects of many recent studies. Recently, phage endolysins have been investigated as potential antimicrobial agents that kill the cells by disrupting the bacterial cell wall. The present study aimed to isolate bacteriophages that infect *Staphylococcus aureus* and to express their endolysin genes as recombinant enzymes and then test their efficacy in killing and removal of *Staphylococcus* biofilms. Seven lysogenic phages were isolated from clinical isolates of *S. aureus* using the mitomycin C induction. Three phages with widest host range including Φ trsa10, Φ trsa14, and Φ trsa15, were selected and further characterized. From the genomic DNA of these three phages and one commercial phage, *S. aureus* subsp. *aureus* bacteriophage 52, the endolysin genes were amplified and cloned into pET SUMO expression vector. Four cloned endolysins, LysSA10, LysSA14, LysSA15, and LysSA52, with a molecular mass of 66 kDa were over-expressed in *E. coli* BL21 (DE3) and characterized in terms of their anti-staphylococcal and anti-biofilm properties. The therapeutic effects of the four endolysins in combination were significantly superior to that of the individual ones and they showed activity against 78 (88.6 %) of the 88 total planktonic *Staphylococcal* strains including *S. aureus*, *S. epidermidis*, and *S. heamolyticus*. For *S. aureus* and *S. epidermidis* biofilms established on catheters, the addition of endolysin cocktail resulted in up to 2.6 log reduction and coating of catheters with these enzymes resulted in inhibition of biofilm by 1.5 log units. Disruption of biofilms was confirmed further by scanning electron microscope. Overall, the newly identified endolysins exhibited a broad host range, especially in combination, against staphylococcal strains both as planktonic and biofilm forms. Thus, these endolysins are promising antimicrobial agents for combating staphylococcal infections.

Key Words: Bacteriophage, biofilm, cloning, endolysin, *Staphylococcus*

2. ÖZET

Faj Kaynaklı Endolizinin Rekombinant Olarak Üretilmesi ve *Staphylococcus* Biyofilmleri Üzerine Etkisinin Araştırılması

Patojen bakteriler arasında antibiyotik direncinin giderek yayılması ve biyofilm enfeksiyonları ile etkin bir mücadele için günümüzde alternatif antimikrobiyal ve antibiyofilm özellik gösteren ajanların keşfedilmesine yönelik yapılan çalışmalar giderek önem kazanmıştır. Son zamanlarda yapılan çalışmalar, bakteriyofaj kaynaklı endolizinin, bakterilerin hücre duvarı yıkımına neden olmaları ile antibakteriyel ajan olarak kullanılma potansiyellerinin olduğunu göstermiştir. Bu çalışmada, *Staphylococcus aureus*'u enfekte eden bakteriyofajların izole edilmesi ve bunların endolizin genlerinin rekombinant olarak üretilmesi ve daha sonra stafilokokal biofilmlere karşı etkinliklerinin test edilmesi amaçlandı. Klinik *S. aureus* suşlarından mitomisin C indüklemesiyle yedi lizojenik faj izole edildi. Konak spektrum aralığı en geniş olan üç faj (Φ trsa10, Φ trsa14 ve Φ trsa15) seçilerek karakterize edildi. Bu üç faj ve ilave olarak ticari *S. aureus* subsp. *aureus* 52 fajının endolizin kodlayan gen bölgeleri amplifiye edilerek pET SUMO ekspresyon vektörüne klonlandı. Molekül ağırlıkları 66.22 kD olarak tespit edilen bu dört rekombinant enzim LysSA10, LysSA14, LysSA15 ve LysSA52 olarak adlandırıldı ve *E. coli* BL21 (DE3) suşunda ekspresse edilerek anti-stafilokok ve anti-biyofilm özellikleri açısından karakterize edildi. Dört endolizin kombine edildiğinde tedavi edici etkilerinin, tek tek uygulanmasına göre daha fazla olduğu ve bunların *S. aureus*, *S. epidermidis*, *S. heamolyticus* de dahil olmak üzere toplam 88 planktonik stafilokokal suşun 78 ine (% 88,6)' karşı aktivite gösterdiği belirlendi. Kateter üzerinde oluşturulan *S. aureus* ve *S. epidermidis* biyofilmlerine dört endolizin kombinasyonu eklendiğinde biyofilmdeki hücre popülasyonunda 2.6 log değerinde azalma olduğu, katater endolizin kombinasyonu ile kaplandığında biyofilm inhibisyonunun 1.5 log oranında gerçekleştiği tespit edildi. Bu azalma taramalı elektron mikroskobu ile gösterildi. Sonuç olarak yeni tanımlanan endolizinin stafilokokların planktonik ve biyofilm formlarına karşı, özellikle kombine halinde kullanıldıklarında, geniş spektrumda litik aktiviteye sahip oldukları gösterildi. Bu sonuçlar, endolizin enzimlerinin stafilokokal kaynaklı enfeksiyonlarla mücadelede kullanılmak için umut verici bir antibakteriyel ajan olduğunu göstermektedir.

Anahtar Kelimeler: Bakteriyofaj, biyofilm, endolizin, klonlama, *Staphylococcus*

3. INTRODUCTION AND OBJECTIVES

Staphylococcus species are one of the most frequent causes of healthcare-associated infections and mainly responsible for infections related to medical devices (1). Many of the healthcare associated infections, particularly those with *Staphylococcus* species including methicillin-resistant *Staphylococcus aureus* (MRSA), are mainly transmitted either by direct contact with colonized healthcare workers or as a result of invasive medical procedures including surgeries and the introduction of medical implants. Among staphylococcal strains, *S. aureus* and *S. epidermidis* are the most common in biofilm-associated infections (2). These infections usually lead to an increase in hospital stays, as well as hospital-associated mortality and substantial economic burden (3).

Today, as the use of medical devices increases, the rate of staphylococcal biofilm infections also increases. Staphylococcal strains participating in the biofilm structure are much more resistant to antibiotics than their counter free-living strains. While replacing biofilm-covered devices with new ones can provide a partial solution (2), patient discomfort, high cost and some complications are significant disadvantages. To date, most research has focused on coating the material surface with antibiotics. While the results of such studies are promising, the concern has been raised that the use of antibiotic-coated devices may lead to the generation of antibiotic resistance (4). For this reason, there is a need for novel methods to prevent colonization and biofilm formation particularly on biomaterials.

Lytic bacteriophages (phages) have been used by themselves or together with conventional antimicrobial agents in the treatment of infections (5). However, the narrow host range, which is largely due to variability in phage receptor molecules on the host cell surface, limit the application of phage therapy (6). In recent years, researchers have been investigating the therapeutic efficacy of endolysins for Gram-positive bacterial infections including the infections caused by antibiotic-resistant bacteria (7-9). Endolysins are enzymes synthesized in the host cell at the last stage of bacteriophage life cycle for the release of their newly produced phage particles by disrupting the peptidoglycan structure of the host bacteria (10). It has been observed that when recombinant endolysin is added exogenously to the Gram-positive bacterial culture, it results in disintegration of bacteria within a very short period of time without the assistance of holin proteins unlike in their normal life cycle (11-14), and this characteristic made them attractive antibacterial agents.

There are a number of advantages for using phage endolysins over phages and classical antimicrobial agents. This is because they have the ability to kill the cells upon exposure. Phage endolysins are very specific and they do not harm the normal microflora, and it is very rare to develop bacterial resistance (15). These features of phage endolysins allow them to be utilized in various areas such as in medicine, veterinary medicine, agriculture, food industry and biotechnology (10).

The production of recombinant endolysin has been achieved in a number of studies and their antimicrobial potential against clinically relevant pathogens to humans and animals has been described previously (9, 16, 17). However, compared to the estimated global phage population size, which is most abundant and diverse biological entities on the planet, the reported phage endolysins are very limited in numbers (18). Phages can be readily isolated from any environmental samples that can support bacterial growth such as aquatic habitats (18), soil (19), sewage or wastewater (20), or induction of phages from lysogenized host strains (21, 22). Therefore, all these indicate that there are still potential novel phages and their endolysins to be explored.

Formation of biofilm on a range medical device like catheters, orthopedic implants, and others are the main concern of device-related infections (4). In response to these problems, there have been few studies that demonstrated the efficacy of phages in preventing the formation of biofilm by *S. epidermidis*, *Pseudomonas aeruginosa*, *Proteus mirabilis* and *E. coli* on the catheters (23-25). Even though the results of these studies are promising, there are certain disadvantages for using whole phages. Phages are highly host specific, have limited bacterial host range and are ineffective against biofilms of different species in the same genera, even the same species with different serotypes. In addition, there is a risk of transferring antimicrobial resistance and virulence genes between bacteria. For this reason, use of phage endolysins should be considered instead of total phages in order to overcome these problems. The ability of endolysin to remove catheter-associated biofilm remains largely unexplored. To our knowledge, there are few studies that investigated anti-biofilm activities of endolysins. In one of these studies, endolysin was used against *Acinetobacter baumannii* biofilm established on the catheter (26), and no phage endolysin has been reported to disrupt *Staphylococcal* biofilms on the catheters.

The aim of this study was to isolate phages that infect *Staphylococcus aureus* species, clone and produce their endolysins in *E. coli*, and test the efficacy of recombinant

endolysins in inhibition and removal of *Staphylococcus* biofilms including biofilms on catheters. This study was carried out in four parts: i) isolation of temperate phages from clinical strains of staphylococci using induction method, morphological (transmission electron microscopy), genetic and functional (life cycle, host range) characterization of the isolated phages, ii) molecular cloning and expression of endolysin genes from phages (DNA isolation, PCR amplification, cloning and expression of amplified endolysin genes in *E. coli* BL21 (DE3) using pET SUMO expression system), iii) functional evaluation of recombinant endolysins (anti-staphylococcal and anti-biofilm features) using various methods such as spot assay, crystal violet assay, plate count assay, and scanning electron microscope, and iv) evaluation of cytotoxicity of the endolysins on a human fibroblast cell in an *in vitro* conditions.

4. LITERATURE REVIEW

4.1. Overview of *Staphylococcus* Species

Staphylococcus is Gram-positive, non-motile, facultatively anaerobic, with a diameter of 0.5-1.5 μm spherical or cocci cells form a shape that looks like a bunch of grapes. These cocci cause a variety of diseases both in humans and animals (27, 28). The *Staphylococcus* genus comprises more than 30 different species and some of them can cause a variety of infections, but most infections are caused by *S. aureus* and many of them preferentially colonize the human body (29).

Usually, members of the staphylococci are catalase-positive, and this distinguishes them from other Gram-positive cocci such as streptococci, which is catalase-negative (30). Within staphylococci, the most pathogenic strain such as *S. aureus* is differentiated from others (like *S. epidermidis*, *S. haemolyticus*, *S. saprophyticus*, and others) by their ability to produce an enzyme called coagulase, which help them to escape from the immune system of the host by clotting the plasma and which in turn resist to phagocytosis (27).

4.1.1 *Staphylococcus aureus*

Staphylococcus aureus is in clusters or tetrad, Gram-positive, producing buttery yellow colonies on mannitol salt agar due to the phenol red in the media that turns yellow by acidic product formed upon mannitol fermentation by the organism (31). They appear as grape-like cluster when viewed through an electron microscope (Figure 4.1). They are catalase positive, the enzyme which breaks down the hydrogen peroxide into oxygen and water. *S. aureus* displays golden color when grown in certain solid media (32). They produce also coagulase and they are responsible for many diseases such as food poisoning (within 4-6 hours of ingestion of contaminated foods), boils and other skin infections including pimples, impetigo, and cellulitis. It can also cause toxic shock syndrome, septic arthritis, nosocomial or hospital-acquired infections (31, 33). Like *S. epidermidis*, they are common causes of infections associated with medical devices (4). Generally, with the emergence of antibiotic resistance strains, they have become the major health problems for humans (34).

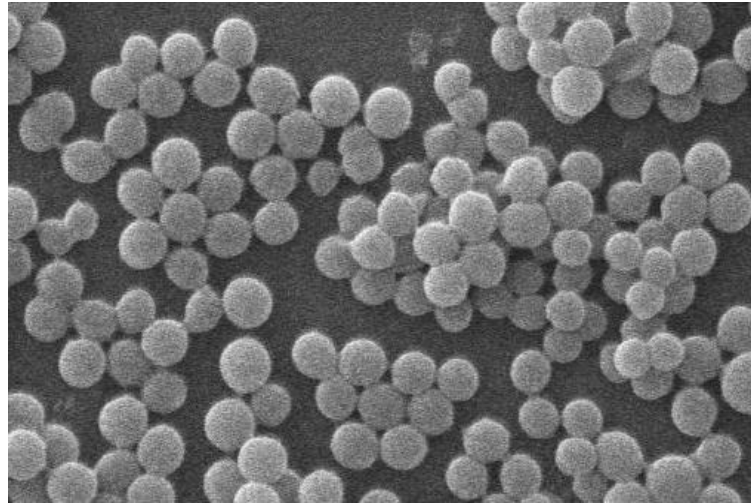


Figure 1. Electron micrograph of *Staphylococcus aureus* (from this study)

4.1.1.1. Cell Wall Structure

The *S. aureus* cells are surrounded by a thick protective cell wall, which provides structural support and prevents cell lysis. Peptidoglycan, teichoic acids, and proteins are the main components of the cell wall (35). Among these, peptidoglycan is a primary component and makes up the majority of the cell wall mass. The backbone of the peptidoglycan is composed of two derivatives of glucose molecules: N-acetylglucosamine (NAG) and N-acetylmuramic acid (NAM) that are cross-linked by a pentaglycine linkage (Figure 2). This maintains the cell shape and is responsible for withstanding the internal osmotic pressure (33, 36). The second largest component of the cell wall is teichoic acid (phosphate-containing polymers) and, it accounts for about 40% of the total cell wall mass. Normally, teichoic acid classified into two; those attached to the membrane (membrane-associated teichoic acid) and those attached to peptidoglycan. Teichoic acids contribute a negative charge to the staphylococcal cell surface and play a role in the acquisition and localization of metal ions, particularly divalent cations, and the activities of autolytic enzymes (37).

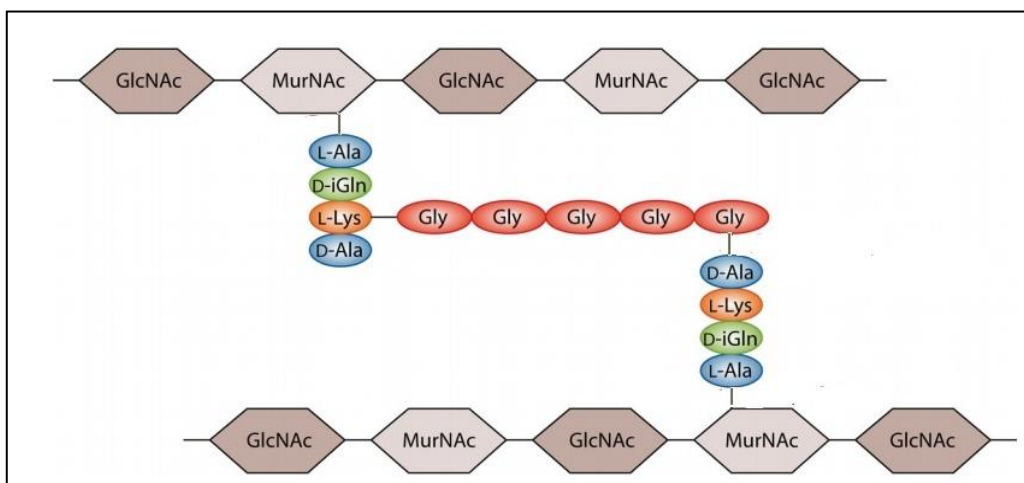


Figure 2. Peptidoglycan units of *S. aureus* cell wall. It is made up of several different units of sugars and amino acids. Penta Gly (Glycin) form a linkage between peptide bonds and branching off the amino sugars (36)

4.1.1.2. Mechanism of *S. aureus* Pathogenicity

Microbes exert their pathogenesis by means of their virulence factors (38). There are numerous virulence factors for *S. aureus* to cause infection (Figure 3). One mechanism is their ability for adhesion and colonization of the host through their teichoic acid structures to the nares and damaged skin (39) or to the surface of implanted medical devices to cause bacteremia (40). Another potential pathogenicity of *S. aureus* involves the evasion of the host immune system by different mechanisms. For example, they produce some chemotaxis inhibitory proteins that can prevent phagocytosis by neutrophils (38). They have also displayed an immunoglobulin binding factor called protein A on their surfaces and as a result, they can prevent opsonophagocytosis. *S. aureus* produces a coagulase (clumping factor) protein that binds to prothrombin and form blood clots to shield themselves from phagocytic cells of the human immune system (41).

Furthermore, the *S. aureus* secretes invasive toxins. Exfoliative toxins cause the sloughing off the body, and the cytolytic toxins disrupt the cytoplasmic membrane of a variety of cells (42). Moreover, staphylococcal superantigens (TSST-1 or toxic shock syndrome toxin1) are important virulence factors in infectious endocarditis, sepsis, as well as toxic shock syndrome (33). The pathophysiology of *S. aureus* also includes biofilm formation. For example, prosthetic device infections are often mediated by the ability of *S. aureus* strains to form biofilms via communicating by using their quorum sensing signals in a cell density-dependent manner (31). The rate of invasion increases with the

compromised immune system, and the presence of damage in the physical integument. The pathogenesis of the majority of the diseases caused by this organism is multifactorial (43).

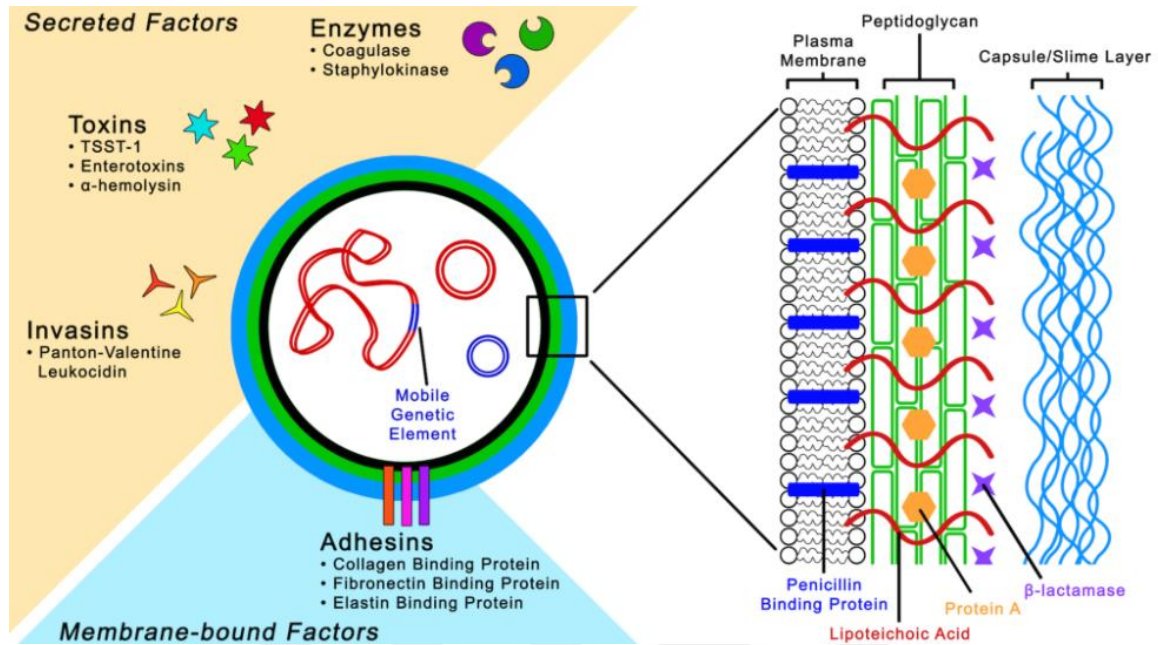


Figure 3. Virulence determination in *S. aureus* (44)

4.1.1.3. Epidemiology of *S. aureus*

The epidemiology of *S. aureus* is dynamic and has changed significantly over the years with distributions worldwide (45). Though it is most often found in hospitals and nursing homes, time to time community setting becomes increasingly contaminated as well (44). It is the most opportunistic pathogen that causes many different clinical manifestations. They are found in the environment and in normal human flora as well. Humans are the major reservoir for this organism and mainly they are located on the skin and mucous membranes. It is estimated that up to half of all adults are colonized, and approximately 20 % of the population persistently harbor *S. aureus* in the anterior part of the nares. Some people tends to have higher rates of *S. aureus* colonization especially healthcare workers, intravenous (IV) drug users, hospitalized patients, and immunocompromised individuals (46). Normally these bacteria do not cause infection on the healthy skin; however, if it is allowed to enter the bloodstream or internal tissues, they may cause a variety of potentially serious infections (45). Nosocomial infections, often associated with *S. aureus* including MRSA, are commonly transmitted either by direct contact with colonized healthcare workers or as a result of invasive medical procedures

including surgeries and the introduction of medical implants. These infections usually lead to an increase in hospital stays as well as hospital-associated mortality, likely due to infection with antibiotic-resistant *S. aureus*, resulting in a substantial economic burden on the medical industry (47).

4.1.2. *S. epidermidis* and other Coagulase Negative Staphylococcus

Historically, coagulase-negative *Staphylococcus* (CoNS) species are categorized as less or non-pathogenic historically but they have become one of the major causes of nosocomial infections, particularly *S. epidermidis* followed by *S. haemolyticus*. Some strains like *S. saprophyticus* are responsible for acute urethritis because they usually colonize the rectum and genitourinary tract (48). They are also associated with infection of implanted foreign bodies and infections in preterm newborns (49). The key source for endogenous infection by CoNS is mainly from colonized strains on various parts of the body including skin and mucosa, where they constitute part of the microbiota of these sites. However, their transmission is mainly through invasive medical procedures. Once inserted, foreign bodies can be colonized by CoNS, and they become a major source of infection, make the treatment unsuccessful and result in considerable medical and economic burden (49).

Among the CoNS strains, *S. epidermidis* is the leading and the most prevalent species that contribute about 60-70 % of the CoNS Staphylococci strains colonized on the skin (48). Pathogenesis of *S. epidermidis* is mostly involved in biofilm formation especially in the foreign body related infections, which begin by attachment on the surface of indwelling or implanted medical devices before proliferation as well as producing an extracellular polysaccharide matrix that help them attach together and form multilayered biofilms matrix (50). This extracellular polysaccharide, also termed as polysaccharide intracellular adhesin, are positively charged homopolymers of β -1,6-linked N-acetylglucosamine (NAG) residues. These are produced by the *ica* gene cluster. The presence of this gene is used as an epidemiological marker for the biofilm infections, since the presence of the *ica* genes responsible for polysaccharide intracellular adhesin production correlate with infections (51).

4.2. Bacterial Biofilms

A biofilm is an assemblage of microbial cells or a surface-attached bacterial community of cells. Biofilms can be formed on various surfaces of living and non- living

materials by surrounding themselves with extracellular polymeric substances (EPS) mainly composed of proteins, polysaccharides, and also extracellular DNA (52). The extracellular polymeric substances provide the ability to attach on surfaces, which is the initial step in the colonization of any surfaces by planktonic cells during biofilm formation, and provide structural support (53, 54). EPS may also provide a protective barrier by giving them resistance to host defenses during infection and confers tolerance to various antibiotics and disinfectants (54).

4.2.1. Stage of Biofilm Formation

Formation of biofilm involves sequential steps (Figure 4), which fall into four main stages: i) bacterial attachment to the surface, ii) microcolony formation, iii) biofilm maturation, and iv) detachment or disassembly of single or cell cluster by various mechanism, which is believed to be crucial for the colonizing of new sites by a process known as biofilm dispersal (50, 52). At each step, the attachment and development of a microbial community makes them highly protected from antimicrobial agents including the actions of cleaners or sanitizers. Commonly, in addition to the interaction between the cells, initial adhesive force is required for the growth and development of biofilm. The attachment of microorganisms to a surface can be facilitated by a number of factors like an increase in shear force, motility of bacteria, and electrostatic interaction between microbes and the surface (55). In addition, the developments of fluid-filled channels are important for nutrient delivery to cells in the biofilm. These channels are also responsible for the three-dimensional structure for the matured biofilm. The disruptive forces also involved in the detachment of cell cluster from the biofilm, which are able to colonize new sites and dissemination of infection within the host (56). For many pathogens, this process plays an important role in the transmission of bacteria from the environmental reservoir to the human host, in horizontal and vertical cross-host transmission, and also increases the severity and spread of infection within the host (57). Since host defense mechanisms and response to antimicrobials are severely reduced against bacteria living in the biofilm, related chronic infections and sepsis represent a major concern in nosocomial infections (58).

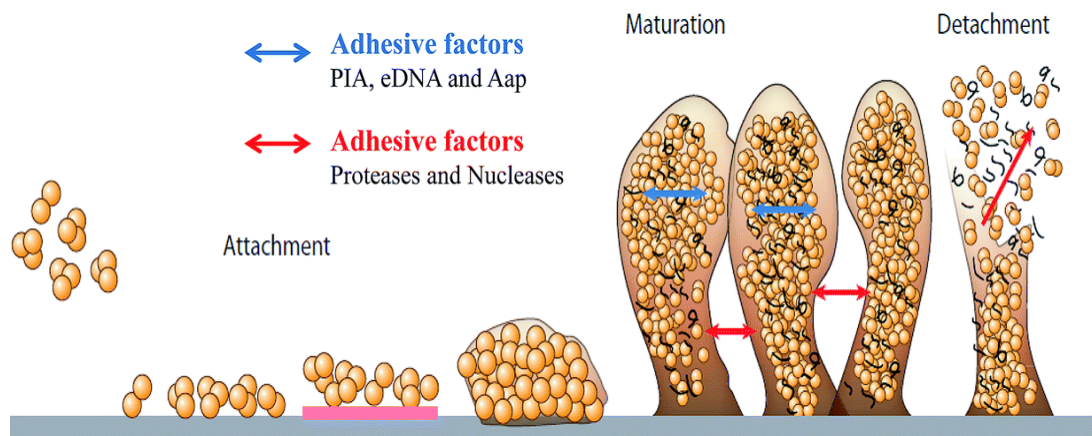


Figure 4. Stages of biofilm formation (52)

4.2.2. Biofilms in Device-Related Infections

Microbial biofilm infection plays a major role in nosocomial infections especially those related to the indwelling devices. To date, there is an increasing use of biomaterial to facilitate management of serious medical and surgical illness. Many types of artificial devices such as catheter (vascular and dialysis), and prosthetic joints heart are among widely used. However, there are increasing evidences that bacterial biofilms are responsible for the failure of these medical devices, leading to device-associated infections (2, 59). From all the hospital-associated infections, about 60 % and over one million cases per year are due to biofilms that have formed on indwelling medical devices (60). The initial contamination of medical devices most likely occurs from patient's skin or from invasive nursing procedures, contaminated water or other external environmental sources (59). This initial contamination is subsequently followed by successive adherence to the devices to form biofilms, which are protected from the antimicrobial agents and host defense mechanisms (56, 60).

Failure of treatment of device-related infections depends on a number of factors such as the type of host, biomaterial, and microbial factors. Even though a number of microorganisms have been involved in medical device-related infections, *S. epidermidis* and *S. aureus* are recognized as a major source of healthcare associated infections, which are widely associated with biofilms on a range of medical devices (59, 61). There are reports regarding the attachment of microorganisms to the biomaterials through cell surface and biomaterial interactions. For instance, staphylococcal species display cell surface proteins, which is known as staphylococcal surface protein-1 and -2 (SSP-1 and

SSP-2), localized on the cell surface on a fimbria-like polymer and linked with the adhesion of *S. epidermidis* to biomaterials (61). Besides, the capsular polysaccharides/adhesins play major role in the adherence of clinical isolates of CoNS to biomaterials (62). The autolysins in *S. epidermidis* also has been linked with the adhesion of this strain to biomaterial surface (63).

4.2.3. Biofilm Control

Currently, many types of research have focused on more refined methods of sterilization and altering biomaterial surfaces to hinder the colonization of microbes (55). Covering of implanted surface with various antimicrobial agents is one strategy, and for instance, silver has been commonly added as antimicrobial agent. This covering or impregnation of antimicrobial to biomaterials like catheters can apply in different ways: it can be attached ionically or it can be added as a thin film on the surface of the device (64). A study conducted by Francolini and his co-workers (4) have reported the anti-biofilm activity of silver ion impregnated into polymeric materials known as polyurethanes, which are polymers used for the manufacturing of medical devices.

The surface alteration of the medical devices with hydrogel, which is a hydrophilic polymer that has an ability to absorb large quantities of water and minimize microbial colonization and provide biocompatibility (64). Moreover, uses of bioactive molecules and enzymes have also been reported as a preventive mechanism of biofilm growth on implanted materials. Based on the study conducted by Ren and co-workers (65), enzymatic detergent treatment removed *E. coli* biofilm from flexible endoscopes.

Currently, antiseptic wound dressings that are widely used in clinical wound infection are the most common ones, but their effectiveness against chronic wound is very limited and still, appropriate agents are highly in need for this infection. One recent study conducted by Gawande and co-workers (66) showed the efficacy of a naturally occurring enzyme-based gel that has both antimicrobial and anti-biofilm activity on chronic wound associated microorganisms including MRSA, *S. epidermidis*, and other coagulase-negative staphylococcal strains, and *A. baumannii*. In their study, they formulated a novel DispersinB® antibiofilm enzyme-based wound gel containing a broad spectrum cationic antimicrobial decapeptide KSL-W. DispersinB is a naturally occurring enzyme (with anti-biofilm activity) produced by an oral Gram-negative bacterium *Actinobacillus actinomycetemcomitans*, which is associated with juvenile periodontitis (67). Different

studies reported the efficacy of phages in preventing various bacterial biofilm formations on the catheter. In the study of *P. aeruginosa* biofilm control (25), use of cocktail phages demonstrated a significant reduction in the number of colony forming unit on the phage-treated catheter, and as a result of this, biofilm formation was reduced.

4.3. Bacteriophages

Bacteriophage or phages are viruses that infect bacterial cells and they are considered the most abundant and diverse biological entities on the planet, which are estimated to be over 10^{31} in the population (18). From these, approximately 5,100 phage types had been isolated and identified by the end of the last century (68). Phages were discovered independently by two scientists; in 1915 by the British bacteriologist Fredrick Twort and in 1917 by a Canadian microbiologist Felix d'Herelle. But before these discoveries, their presence was reported in 1896 by Ernest Hankin (69), after observing that there were filterable entities having antibacterial action (against *Vibrio cholerae*, restrict epidemic at that time) in the water of Ganges and Jumna rivers in India.

In 1915, Twort (69) isolated filterable entities that produced small cleared areas on bacterial lawns (micrococci, intestinal bacilli, and *Staphylococcus aureus*). Following this, d'Herelle (1917) isolated the filterable entities from fecal matter and tested them on agar plates containing *Shigella* strains, and after observing a small clear area called plaque, he proposed a name “bacteriophage” which means in Greek bacteria eating (70).

4.3.1. Phage Structure

A phage has an outer protein shell called the head or capsid, which can vary in size and shape (71). Some are icosahedral and others are filamentous. The head, which is present in every phage, acts as a protective covering and encloses the phage's genetic material. The genetic material of the phage can be either DNA or RNA, which, in turn, can be double or single-stranded, in a linear or a circular form (71). Some phage heads have tails, through which its genomic material passes into the bacterial cell during infection. The tail may be surrounded by a contractile sheath (Figure 5), as in the T4 phage. Some phages have tail fibers and a base plate at their tail terminal that play a role in the attachment of the phage to the bacterial cell.

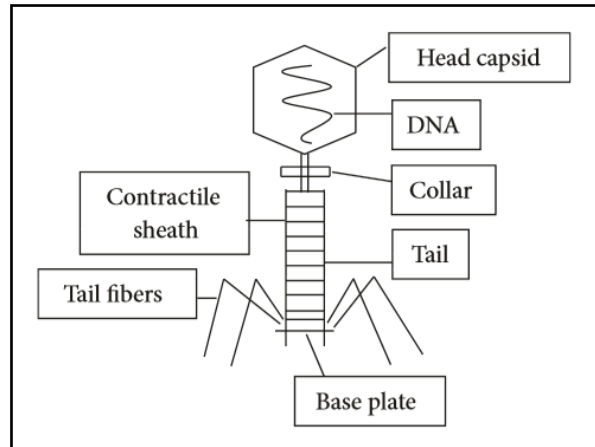


Figure 5. Generalized structure of tailed phage (72)

4.3.2. Phage Life Cycle

Like all viruses bacteriophages require a specific host cell in order to multiply themselves. Basically, they have a lytic and/or lysogenic cycle (Figure 6) (72). In the Lytic cycle, the host bacterial cells are destroyed at the end of the replication cycle. As soon as the cell is destroyed, the newly formed progeny phages can find a new host to continue the cycle. These phages are lytic phages or virulent phages. In contrast, the lysogenic cycle does not result in immediate lysing of the host cell and those phages that are able to undergo lysogeny are known as lysogenic phages or temperate phages. Generally, in the lysogenic cycle, the nucleic acid of the phage integrates into the host genome and replicates when the DNA of the host cell is replicated. The virus is thus transmitted to daughter cells at each subsequent cell division and stays there as prophage until they are forced by the harsh conditions faced by their respective hosts (73).

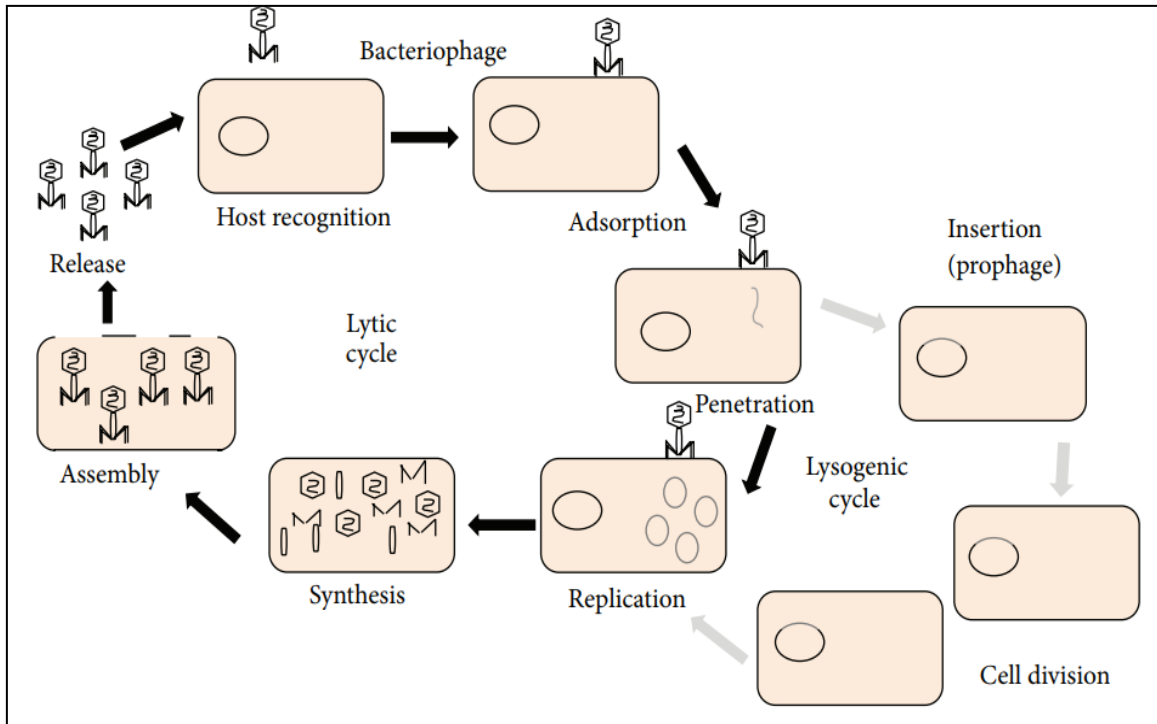


Figure 6. Bacteriophage life cycle (72)

4.3.3. Prevalence, Isolation, and Classification of Phage

Bacteriophages can be found in almost all environments on earth, ranging from soil, sediments, water, and in/on living or dead plants/animals. Essentially, phages can exist on any material that will support bacterial growth; because of this, they are the most abundant ‘life’ forms on earth (69). For instance, it is estimated that aquatic environments have a total phage population above 10^{31} (18). Many terrestrial ecosystems have been shown to harbor 10^7 phages per gram of soil (19); and raw domestic waste is known contain in the range of 10^5 - 10^7 PFU cm^{-3} (20).

Phages can be readily isolated from feces, sewage, soil, water and any water, and in/on living or dead plants/animals. An enrichment method is classical and is still the most common approach for isolating virulent bacteriophages from environments. This method involves growing cultures of the host bacterium with an inoculum which is expected to contain phage, following incubation for a certain period of time, cells are pelleted and the supernatant is evaluated for the presence of phages (75).

Temperate or lysogenic phages can be isolated by induction from bacterial genome using some inducing agents such as UV radiation, hydrogen peroxide, and mitomycin C. Among these, mitomycin C is the most commonly used for isolation of the lysogens.

Mitomycin C is a natural product isolated from *Streptomyces caespitosus* and was discovered by a Japanese microbiologist in the 1950s (76). Its mode of action involves a cross-linking of DNA bases that leads to cell death (76). The DNA damage to the bacterial cell appears to be the trigger that stimulates the production of RecA proteins via the SOS (Save Our Souls) DNA repair system, which induces prophages to switch to the lytic cycle (77). The induction of prophages from various bacterial strains by treatment with mitomycin C has previously been described (26, 78-80). Many of the *S. aureus* phages isolated so far are temperate phages (21).

Over the years, a sophisticated phage classification system has been drawn up by the International Committee for Taxonomy of Viruses (ICTV) to account for the diversity (72). Originally the taxonomy of phages was organized according to their morphological characteristics, type of nucleic acid, and presence of envelope or lipid. Accordingly, the phages were categorized into 14 distinct phage families as shown in Figure 7 and Table 1 adopted from elsewhere (72, 81). Since 1959, over 5,500 bacteriophages have been studied by electron microscopy, and of those studied from the morphological perspective, 96.3% have been reported as “tailed phages”, which are composed of an icosahedral head and a tail, with double-stranded DNA (dsDNA) (82). Based on their tail morphology, these phages were further categorized into three main families. These are i) *Myoviridae* (phages with contractile tail), ii) *Siphoviridae* (phages with long non-contractile tail), and iii) *Podoviridae* (phages with a short tail) (83). The majority of *S. aureus* phages isolated so far are categorized in *Siphoviridae* family and they have double-stranded DNA (21).

Table 1: The phage families based on morphology and genome characteristics. Adopted from Elbreki *et al.* (72)

Family	Morphology	Nucleic acid
Myoviridae	Non-enveloped, contractile tail	Linear dsDNA
Siphoviridae	Non-enveloped, long contractile tail	Linear dsDNA
Podoviridae	Non-enveloped, short contractile tail	Linear dsDNA
Micoviridae	Non-enveloped, isometric	Linear dsDNA
Corticoviridae	Non-enveloped, isometric	Circular dsDNA
Tectiviridae	Non-enveloped, isometric	Linear dsDNA
Leviviridae	Non-enveloped, isometric	Linear ssRNA
Cystoviridae	Enveloped, spherical	Segmented dsDNA
Inoviridae	Non-enveloped, filaments	Circular ssDNA
Lipothrixviridae	Enveloped, rod-shaped (Helical)	Linear dsDNA
Rudiviridae	Non-enveloped, rod-shaped (Helical)	Linear dsDNA
Plasmaviridae	Enveloped, pleomorphic	Circular dsDNA
Fuselloviridae	Enveloped, lemon-shaped	Circular ssDNA

ssDNA = single-stranded DNA; dsDNA = double-stranded DNA

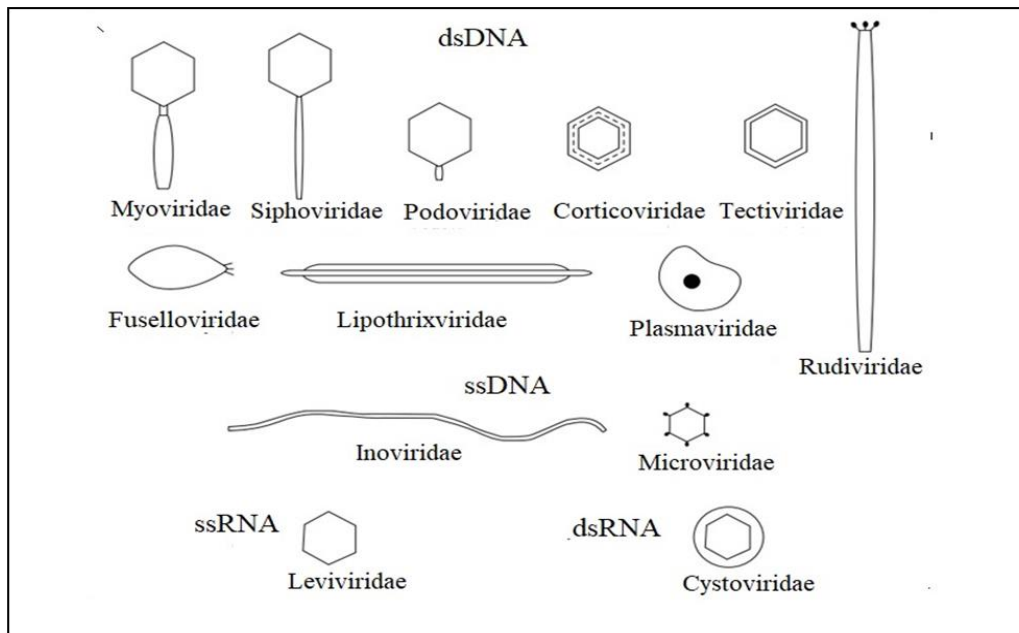


Figure 7. Schematic representation of major phage groups (72)

4.3.4. Bacteriophage Therapy

The killing of bacteria by a bacteriophage is used for the treatment of disease, and this process is known as bacteriophage therapy. This practice was started for almost a century ago but the development of conventional antibiotics surpassed the use of phages. Currently, with the decreasing effectiveness of classical antimicrobial agents and the emergence of antibiotic resistant strains, use of phage therapy is reviving. Historically, the treatment of infection by phages is performed by simply adding naturally existing bacteriophages at the site of infection in order to kill the bacteria. The advancement of biotechnology now expanded the potential applications of phage therapy to include various novel strategies using bioengineered phages and phage derived lytic proteins (72).

In addition to therapeutic use, phages are also used in food preservation. But considerable attention must be given to the lytic phage rather than the lysogenic phages because of the fear of the resistance gene of transferring to the host by these phages (84). Phage therapy has been successfully used both in human and animal treatment either alone or in combination with antibiotics (5, 70, 85). Bacteriophage proteins, including endolysin, have also been investigated for their use in the treatment of bacterial disease of humans and plants. The uses of bacteriophage proteins rather than whole bacteriophages eliminate the possibility of phages entering lysogenic lifecycle in the bacteria thus potentially increasing virulence (72).

4.4. Bacteriophage Endolysins

Endolysins or lysins are essential enzymes encoded by bacteriophages at the last stage of their replication cycle to lyse the infected host cell for releasing of the newly formed phage particles (7). Endolysins acts as molecular scissors by cutting or degrading the peptidoglycan meshwork of the cell wall (7, 9, 10). As displayed in Figure 8, to achieve access to the cell wall, endolysin require a second lysis factor called holin, which is a small membrane protein used for penetrating the plasma membrane (10). Like endolysin, holin protein is produced in the late phase of the phage lytic cycle and accumulates in the cytosol of the host cell. The holin protein forms pores on plasma membranes at a genetically specific time, as a result the endolysin easily goes through this pore to access its target in the peptidoglycan where they cut peptidoglycan meshwork. Consequently, impairing of the peptidoglycan results in an unsustainable internal pressure, which in turn results in osmotic lysis with the concomitant release of mature phage progeny (9).

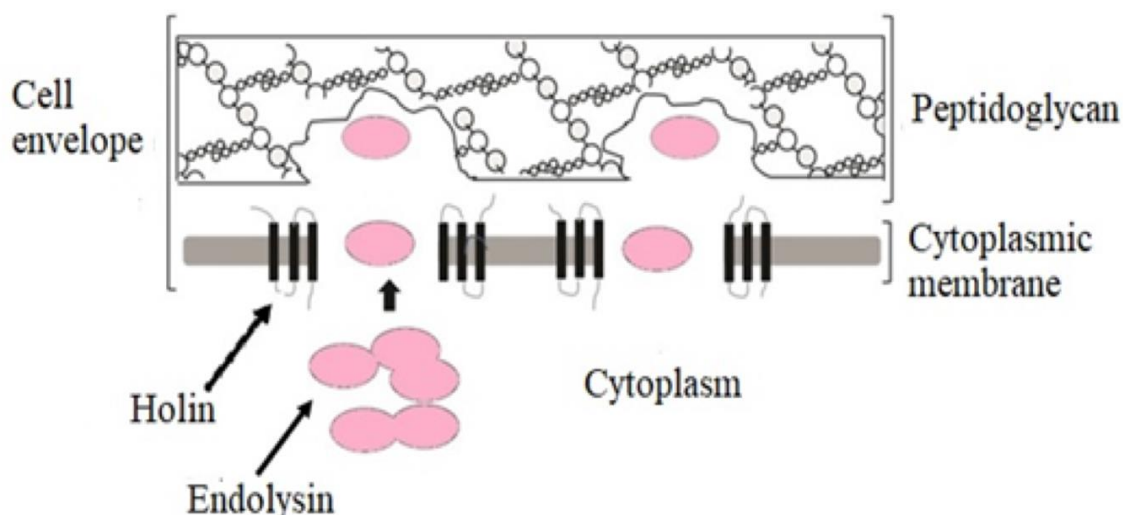


Figure 8. Schematic representation of mode of action of endolysin in the phage life cycle. Image is modified from Elbreki et al. (72)

4.4.1. The Structural and Biochemical Diversity of Endolysins

Structurally the endolysins derived from bacteriophage infecting Gram-positive bacteria generally possess a modular organization with one or two catalytic domain (s) at the N-terminal and one cell wall binding domain at the C-terminal (Figure 9A). Both termini separated from each other by a short flexible interdomain linker (10, 92). The catalytic domain or enzymatically active domains (EAD) show a large diversity depending on the type of chemical bonds of peptidoglycan (PG) they target. Based on the targeted sites on the bonds of peptidoglycan (Figure 9B), endolysin can be classified into five major groups (93). These are: i) N-acetyl-muramidase (generically also termed lysozymes), which cleave the N-acetylmuramoyl- β -1,4-N-acetylglucosamine glycosidic bonds of the sugar strand; ii) N-acetyl- β -D-glucosaminidase, cut the glycosidic bond, N-acetylglucosaminyl- β -1,4-N-acetylmuramamine, in the sugar strand; iii) N-acetyl-muramoyl-L-alanine amidase hydrolyze the amide bond between the sugar and the peptide moieties; iv) L-alanoyl-D-glutamate endopeptidase cleaves within the peptides making up the interconnecting stem portion of the peptidoglycan units; v) Interpeptide bridge-specific endopeptidase.

In contrast to endolysins originated from Gram-positive bacteria, most endolysins derived from bacteriophages infecting Gram-negative bacteria possess a single globular protein having only one catalytic domain with low molecular mass ranging from 15 to 20 KDa. But there are also a few reports that demonstrate phage endolysin with both catalytic

and cell wall binding domains. For example, endolysins KZ144 and EL188 isolated from *Pseudomonas aeruginosa* phage Φ KZ and phage Φ EL respectively, harbor a lytic domain in the C-terminal and cell wall binding or substrate domain at the N-terminal positions, which is opposite to the modular arrangement of endolysin from Gram-positive bacteria infecting phages (94).

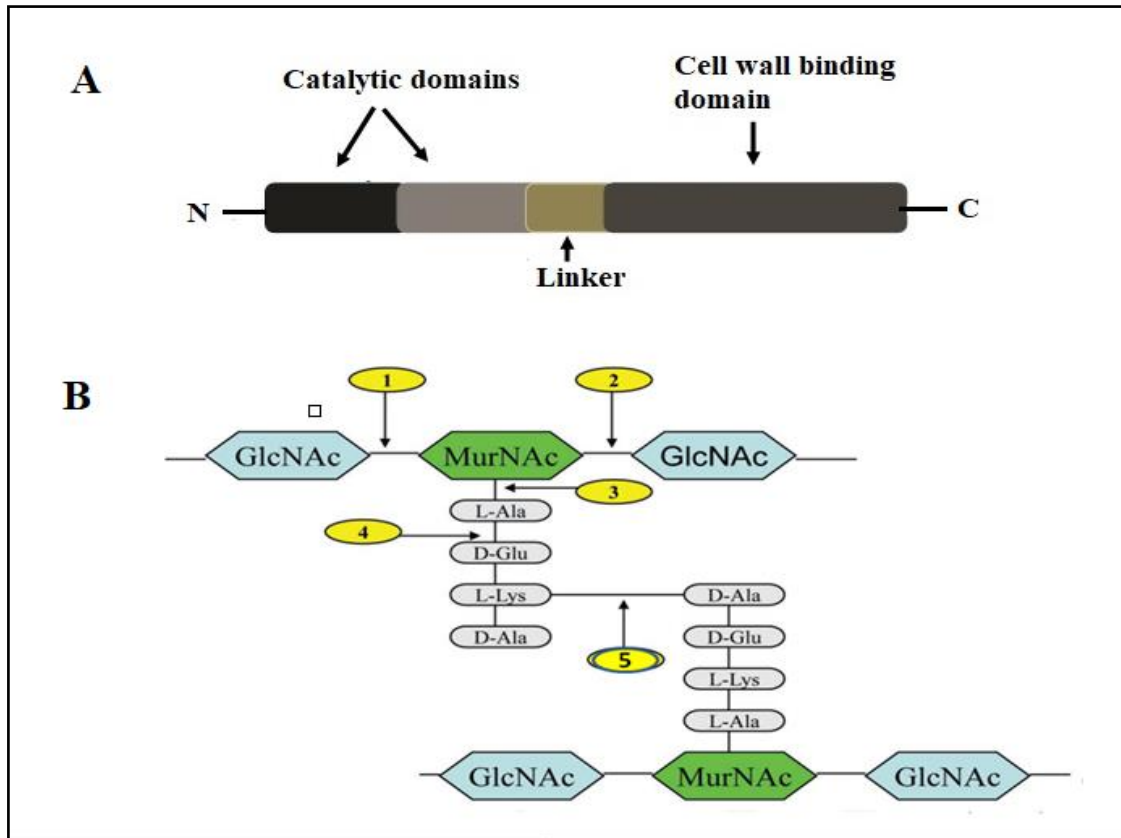


Figure 9. Schematic representation of the modular structure of endolysin (A), and catalytic cleavage sites on peptidoglycan (B). The endolysin target sites: 1) N-acetylmuramidase (lysozymes); 2) N-acetyl- β -D-glucosaminidase; 3) N-acetylmuramoyl-L-alanine amidase; 4) L-alanoyl-D-glutamate endopeptidase; 5) Interpeptide bridge-specific endopeptidase. Image is adopted from Fenton *et al.* (12)

4.4.2. Applications of Endolysins

The increasing interest in endolysins as novel antimicrobial agents is due to its ability to lyse and result in immediate cell death of Gram-positive bacteria when added exogenously even in the absence of holin (7-10). The cell death occurs due to the local degradation of the exposed peptidoglycan and as a result, the cytoplasmic membrane alone cannot withstand the osmotic pressure of the cytoplasm (69). This characteristics of phage endolysin pave the way for the exploitation of phage endolysin as novel antimicrobial agents and having various potential applications in different sectors such as health-care community, food industry, veterinary and agriculture, and other biotechnology sectors (95). In contrast to Gram-positive pathogens, the use of phage endolysins for Gram-negative bacteria is limited due to the presence of outer membrane which hinders the endolysins activity when added exogenously (7).

4.4.2.1. Endolysin as Therapeutic Agents

The therapeutic potential of endolysin against bacterial infections of humans and animals was first reported in 2001 by Nelson and co-workers (96). In their study, they reported the potential application of an endolysin called PlyC (then termed C1 lysin) in controlling colonization of *Streptococcus* species in mice. After this date, studies regarding the therapeutic application of endolysin have been on the increase (97).

As a potential therapeutic method, phage endolysins have many important features such as distinct mode of action. They are also highly specific and rapid in their actions, and they are active against the bacterial cell in spite of their antibiotic resistance properties (92). Furthermore, phage endolysin have an advantage over conventional antibiotics in that they demonstrate a low probability of developing resistance, due the fact that they target only unique and conserved bonds in the peptidoglycan (98). Their specificity allows them to target specific bacterial pathogens without affecting the commensal microflora. For example, endolysin originated from streptococcal phage will specifically target streptococci (92). But in some cases, phage endolysin with broad host range have also been reported. For example, lysine PlyV12, which is isolated from enterococcal bacteriophage Φ 1, is demonstrated lytic activity against *S. aureus* and *Streptococcus* species besides to the *E. faecalis* and *E. faecium* (99).

Many pre-clinical *in-vivo* trials performed using topical, systemic or intravenous routes. The therapeutic effects of endolysins in these trials showed the absence of side

effects in the host (10). Although endolysins are able to stimulate an immune response, it does not neutralize or hinder their activity (100, 101). The organizations of their modular arrangement can be exploited for bioengineering, as the different domains can be shuffled within the protein, or domains from different endolysins can be combined to generate new enzymes that are more potent. For example, chimeric Ply187 endolysin (a fusion protein developed from catalytic domain of Ply187AN endolysin and cell wall binding domain from LysK endolysins) has greater activity than the parental endolysins (102).

Different studies have also demonstrated the synergistic effects of endolysin with antimicrobial agents, resulting in overall increased antibacterial efficacy (100, 103, 104). In general, a number of *in vitro* and *in vivo* tests using different purified endolysins either alone or together with classical antimicrobial agents have been demonstrated to possess therapeutic effects (Table 2). For example, Cpl-1, a pneumococcal phage lytic enzyme, showed synergistic effect with either penicillin or gentamycin in the killing of *Streptococcus pneumonia* (100). The synergy of ClyS, chimeric endolysin obtained from two different *S. aureus* phages (Twort phage and phiNM3) with oxacillin to eradicate MRSA has also been demonstrated and its synergy with oxacillin demonstrated synergic effect in the eradication of MRSA (104).

Table 2. Some examples of recombinant phage endolysins targeting pathogenic bacteria

Endolysin	Origin	References
Cp1-1	<i>Streptococcus pneumoniae</i> ϕ Cp1-1	(101, 105)
Ply700	<i>S. suis</i> ϕ SMP	(106)
PlyC	<i>S. pyogenes</i> Φ C1	(96)
Ply118	<i>Listeria monocytogenes</i> ϕ A118	(91)
Ply511	<i>L. monocytogenes</i> ϕ A511	(91)
CD27 endolysin	<i>Clostridium difficile</i> Φ CD27	(107)
PlyB	<i>B. anthracis</i> Φ Bcp1	(108)
Lys16	<i>S. aureus</i> Φ P68	(109)
LysK	<i>S. aureus</i> Φ K	(8)
Phi11 endolysin	<i>S. aureus</i> Φ 11	(16)
MV-L	<i>S. aureus</i> Φ MR11	(13)
LysGH15	<i>S. aureus</i> Φ GH15	(110)
LysWMY	<i>S. warneri</i> M Φ WMY	(111)
Ply3626	<i>C. perfringens</i> Φ 2626	(112)
EFAL-1	<i>E. faecalis</i> Φ EFAP-1	(113)

4.4.2.2. Application of Endolysin in Biofilm Removal

Many pathogenic bacteria organize in a multispecies community called biofilms and formation of this biofilm usually results in resistance to many antimicrobial agents (60). Biofilm formations are also a problem in food industry (9). In response to this problem, recent studies demonstrated a promising application of endolysins. *Staphylococcus* strains are one of the most recognized causative agents of infections and biofilm formation. Endolysin destroying these biofilms have been reported. Bacteriophage Φ 11 lysin derived from *S. aureus* phage is able to eliminate biofilms of *S. aureus* (16). Another staphylococcal phage endolysin, SAL-2, significantly removed *S. aureus* biofilms compared to its parental phage (84). The destruction of *Streptococcus pneumoniae*, *S. pseudopneumoniae* and *S. oralis* biofilms by pneumococcal phage endolysins (Cp1-1 and Cp1-7) has been reported. A cooperative effect of Cp1-1 with autolysin LytA in the disintegration of *S. pneumoniae* biofilm has also been reported in the same study (114).

4.4.2.3. Endolysin in Veterinary and Food Applications

Endolysins have also potential application in the veterinary sector in preventing the spread of zoonotic disease or transmission of pathogens into food (9). For example, bovine mastitis is one of the most common diseases in adult dairy cows which accounts for most of the morbidity and causes significant economic loss in dairy farm sectors. Mastitis also results in contamination of the raw milk, and this poses a more direct threat to public health (115). In this context, Obeso and his-coworkers demonstrated a possible application of endolysin as an antimicrobial additive for preventing the growth of *S. aureus* in dairy products (115). In their report, the addition of purified endolysin LysH5 was able to kill *S. aureus* growing in pasteurized milk rapidly. The LysH5 also exhibited synergy with the bacteriocin nisin at a low concentration resulting in complete elimination of *S. aureus* in milk (116).

A study conducted by Zhang and his coworkers showed experimental evidence for successful control of *Listeria monocytogenes* in soy milk to an undetectable level by *L. monocytogenes* phage endolysin LysZ5 (117). In the same report, more than 4 log reduction of *L. monocytogenes* growing in soya milk after 3 h of treatments at refrigeration temperature (4°C) was reported. Generating safe surface and enhancing food safety are other approaches for endolysin applications. Solanki and his co-workers demonstrated endolysin-based listericidal nanocomposites in order to control bacterial growth in lettuce (118). They formulated *Listeria* bacteriophage endolysin Ply500 by attaching this enzyme to silica nanoparticles (SNPs) followed by incorporating the conjugate into a thin poly film and binding to edible crosslinked starch nanoparticles via construction of a maltose binding protein fusion. This formulation was demonstrated to be effective in killing of *L. innocua* on lettuce.

4.5. Production of Recombinant Proteins

Currently, recombinant proteins are widely used by various sectors including medical, agricultural and food industries. Higher production efficiencies and, consequently, lower costs of the final active product that can be used for intended applications is of great importance (86). The choice of expression systems (bacteria, yeast, or insect cell), the choice of vector, the size of the protein to be expressed, the type of affinity tag if required, and the most appropriate purification strategy are the main concerns for cloning, expression, and purification of any protein including phage endolysins (87).

As proteins vary in their characteristics including phage endolysins, there is no definitive cloning strategy. Thus, it must be determined empirically and optimized for each individual protein (88).

Recombinant proteins are produced in various hosts including bacteria, yeast, insect and mammalian cells, filamentous fungi, transgenic animals, and plants. Among these, prokaryotic cells are the most widely used expression systems. These systems allow one to obtain large quantities of protein in a short time. A simple and inexpensive bacterial cell culture and well-known mechanisms of transcription and translation facilitate the use of these microorganisms (89). But production of large proteins in bacterial cells may result in aggregation of insoluble proteins, which is a drawback of this system (90). The majority of cloned phage endolysin proteins have been expressed in *E. coli* strains. But there are also few reports in which *Lactococcus lactis* was used as an expression host; as in the case of *S. aureus* endolysin LysK expressed in *L. lactis* NZ9800 and MG1614 (8), and *Listeria monocytogenes* endolysin Ply511 expressed in *L. lactis* MG1363 (91).

5. MATERIALS AND METHODS

5.1. Materials

5.1.1. Bacterial Strains and Plasmids

Clinical isolates of staphylococcal strains including *S. aureus*, MRSA, *S. epidermidis*, and *S. haemolyticus* (Table 6) were used in the current study. All listed strains in Table 6 were used for endolysin activity and phage infectivity tests, and some of them were used for prophage induction. *E. coli* One Shot Mach1™-T1R strain (Invitrogen, USA) was used for stable propagation and maintenance of recombinant plasmids. *E. coli* BL 21 (DE3) cells having a genotype of $F^- ompT hsdS_B (r_B^-, m_B^-) gal dcm$ (Invitrogen, USA) were used as expression host in the production of endolysin proteins.

pET SUMO vector plasmid was used as cloning and expression vector (Invitrogen, USA). This plasmid has cloning and expression features such as TA cloning site for ligating the amplified PCR product, a promoter (T7 lac), IPTG inducible gene, histidine tag for facilitation of purification, SUMO protein fusion at the N-terminus for enhancing solubility of target proteins, and also contain kanamycin resistance gene for selection upon transformation in *E. coli* (Figure 10)

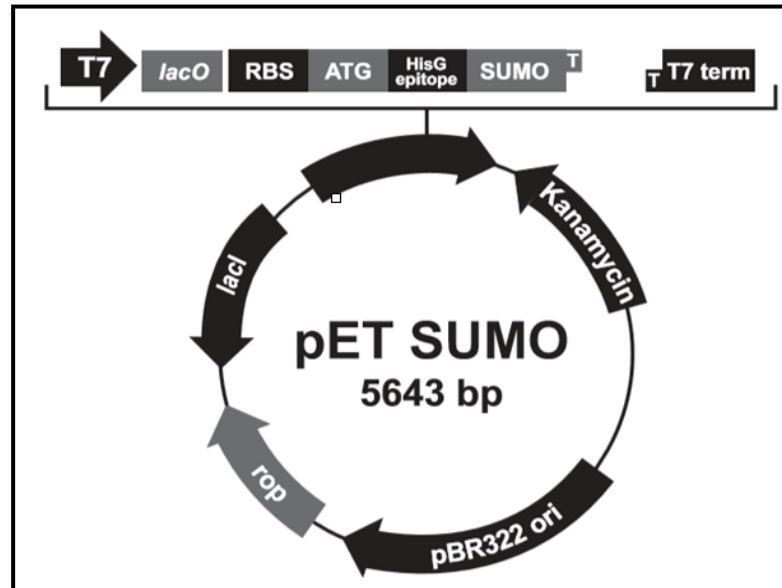


Figure 10. Map of pET SUMO vector

5.1.2. Primers Used in the Study

Primers used in this study are listed in Table 3. Two pairs of primers covering staphylococcal endolysin genes were designed based on the published sequences of DW2, phiMR11, phiSauS-IPLA88, SA12, and SA13 with accession numbers of KJ140076, NC_010147, EU861005, KC677663, and NC_021863 respectively.

Table 3. List of primers used in this study

Name	Primer sequences
PhiDW2-Lys-F1	5'- ATGCAAGCAAACTAACTAAAAAAG -3'
PhiDW2-Lys-R1	5'- TTAAGTGAATTTCTCCCCATAAGTC -3'
PhiDW2-Lys-F2	5'- AATTGGCTAGGCGGTGGCTGGACTG-3'
PhiDW2-Lys-R4	5'-TTGTATTTTCTGTTTGCTGGTAAT-3'
pET SUMO Forward	5'-AGATTCTTGTACGACGGTATTAG-3'
T7 reverse primer	5'-TAGTTATTGCTCAGCGGTGG-3'

5.1.3. Media, Growth Conditions and Storage of Bacteria and Phage

Tryptic Soy Broth (TSB) and Tryptic Soy Agar (TSA) (Lab M, UK) for the growth of staphylococcal strains, Luria Bertani (LB) broth and Luria Bertani (LB) agar (Lab M, UK) for the growth of *E. coli* cells were used. Kanamycin (Km) at a final concentration of 50 µg/mL was included in LB medium. Top agar prepared by mixing 10 g tryptone, 5 g yeast extracts, 5 g sodium chloride (NaCl), and 7 g agar (Acumedia, USA) in 1 L of distilled water was used to resuspend phage and bacterial cells on top of solidified agar plates. Super Optimal Broth (Invitrogen, US) was used as recovery media for transformed cells. All staphylococcal strains were cultured in TSB and TSA at 37°C. *E. coli* strains were cultured in Luria Bertani (LB) medium at 37°C except for protein expression, which was carried out at 20°C. Plasmid selection was accomplished by the addition of kanamycin. All bacterial strains were stored in 20% glycerol containing broth and maintained at -80 °C.

5.1.4 Enzymes, Chemicals and Reagents

PCR amplification kit, DNA molecular weight standards, endonucleases, T4 DNA ligase, Taq DNA polymerases were purchased from Promega (USA). Big Dye® Terminator v3.1 Cycle Sequencing Kit was purchased from Applied Biosystem (USA), Protein K was purchased from New England Biolabs (USA), mitomycin C, kanamycin, sodium dodecyl sulfate (SDS), DL-dithiothreitol, dimethylsulfoxide (DMSO), potassium chloride (KCl), polyethylene glycol, and ammonium persulfate were purchased from Sigma-Aldrich (USA). Methanol, acetic acid (Chromanorm, France), phosphate buffer solution (Oxoid, UK), magnesium sulphate, dipotassium hydrogen phosphate (K₂HPO₄), isoamyl alcohol, potassium dihydrogen phosphate (KH₂PO₄), sodium hydroxide (NaOH), glucose were purchased from Merck (Germany), N, N, N', N'-Tetramethylethylenediamine (TEMED), acrylamide, Precision plus protein ladder were purchased from Bio-Rad (USA), uranyl acetate (PubChem, ?), agarose and EDTA were purchased from Quantum (New Zealand); Isopropyl β-D-1-thiogalactopyranoside (IPTG) was purchased Thermo Fisher (USA).

5.2. Methods

5.2.1. Bacterial Culture Conditions

A total of 88 staphylococcal strains including 60 *S. aureus*, of which 13 are MRSA, 25 *S. epidermidis*, 3 *S. haemolyticus* strains isolated previously from various clinical samples at the Farabi Hospital of the Karadeniz Technical University and maintained at the Department of Medical Microbiology Culture Collection were revived in TSB at 37°C and used in this study.

5.2.2. Bioinformatics Search and Primer Design

Bioinformatics search was performed for retrieving endolysin gene sequences from the NCBI website (www.ncbi.nlm.nih.gov). Among the various available *Staphylococcal* phage endolysin sequences, five different sequences (with the reference number of NC_021801.1, NC_010147, NC_011614.1, NC_024391.1, and NC_021863.1) and encoding single full open reading frame (ORF) were selected. Then, the sequences were aligned using Multiple Sequence Alignment program called ClustalW which is available at <http://www.ebi.ac.uk/Tools/msa/clustalo/> to check the conserved regions. Following this,

PCR forward and reverse primers specific for whole endolysin genes were designed from the conserved regions.

5.2.3. Genomic DNA Extraction from *S. aureus*

Genomic DNA was extracted from clinical isolates of *S. aureus* using a method described by Englen and Kelley (119) with some modifications. Briefly, cells plated on TSA agar media for 12 to 24 h at 37°C. Then single colony was picked and suspended in 50 µL of lysostaphin (150 µg/mL) in an Eppendorf tube and incubated for 20 min in a water bath at 37°C. Then, 50 µL of proteinase K (100 µg/mL) and 150 µL Tris buffer (0.1 M) was added to the samples and mixed by pipetting up and down before incubating the tubes at the 37°C heating block for 20 min. The tubes were then transferred to 97°C heating block for 10 min to inactivate proteinase K. After this, the tubes were centrifuged for 1 min at 5000 rpm to pellet the cell debris. Supernatant was used directly as DNA template for PCR amplification, and remaining supernatants were stored at -80°C until needed.

5.2.4. PCR Screening of Endolysin Genes in Genomic DNA of *S. aureus* Strains

Presence of prophages in the chromosomes of *S. aureus* strains was evaluated by PCR before phage induction. Chromosomal DNA extracted from *S. aureus* strains were used as template for PCR, and conditions described by Biddappa and co-workers (79) were used for amplification. Briefly, the PCR reaction was adjusted into 25 µL reaction volume containing 5µL PCR buffer (Promega 5x), 0.5 µL dNTP (2.5µM), 0.75µL of each forward and reverse primer of phage endolysin gene (10 pmol/ µL), 1.5 µL of MgCl₂ (25mM), 0.15 µL (5U/µL) Taq DNA polymerase (Promega), 5 µL DNA template, and 11.35 µL sterilized distilled water. PCR conditions adjusted to initial denaturation at 94°C for 5 min, followed by 30 cycles of denaturation at 94°C for 1 min, annealing at 51.8°C for 1 min, extension at 72°C for 1 min, and a final extension at 72°C for 7 min. After completion of the PCR amplification, the presence of products was checked by 1 % agarose gel electrophoresis, stained with ethidium bromide, and visualized under UV illuminator (Cleaver Scientific, UK).

5.2.5. Phage Isolation

PCR positive strains for endolysin genes were subsequently exposed to mitomycin C (Sigma-Aldrich, USA) for phage induction as described elsewhere (80) with some modifications. Briefly, *S. aureus* strains were inoculated in 5 mL of TSB media and grown

for overnight at 37°C. The overnight culture samples were then diluted into 1:100 in fresh TSB media and grown at 37°C until the exponential phase was attained ($OD_{600nm} = 0.5$). Subsequently, mitomycin C was added to the culture at a final concentration of 1 µg/mL and incubation at 37°C with shaking at 200 rpm was continued for 4 hours to release phage particles. Then, 1 ml culture samples were centrifuged at 4500 rpm for 20 min and supernatants were sterilized using 0.22 µm pore size filter. This clear supernatant (5 µL) were then spotted into plates with agar overlay lawns of the staphylococcal strains and incubated for 12 to 24 h at 37°C. Presence of phage plaques or clear zone on the plates was confirmed using single plaque assay.

5.2.6. Plaque Assay and Phage Purification

Positive phage lysates for spot test were further examined for the presence of a single type of phage using the plaque assay method as previously described by Carey-Smith and co-workers (120) with some modifications. Briefly, a 100 µL of diluted phage lysate, 100 µL of logarithmic phase *S. aureus* cultures and 2 µL of 1M CaCl₂ were mixed thoroughly in an Eppendorf tube and incubated at room temperature for about 30 min to facilitate bacteriophages to adsorb to their host. After the incubation period, the mixture was transferred to a tube containing 4 mL of TSA soft agar (0.6 %) at 49°C and mixed thoroughly before pouring it to the TSA plate and incubated for 12-24 hours. Phage plaque were picked and resuspended in a 50-100 µL SM buffer for further purification by infecting logarithmic phase culture of *S. aureus* as described before.

5.2.7. Phage Propagation and Concentrations

For propagation, each single plaque solution was poured into 8-10 TSA plates using the same procedure mentioned previously. Plates covered with plaques were used to harvest the phage particles. Briefly, 2 to 4 mL of SM buffer (50 mM Tris-Cl, pH 7.5; 8 mM MgSO₄.H₂O; 100 mM NaCl) was added on each plate and incubated on a shaker at room temperature for about 1 h. Then top agar containing plaques was collected in a falcon tube, gently vortexed, and centrifuged at 10,000 rpm for 20 min. The supernatant was transferred to a new tube and filtered through 0.2µm filter (Sartorius Stedim Biotech GmbH, Germany). The resulting filtered lysate concentrated further by polyethylene glycol (PEG) solution as described elsewhere (121). Briefly, to 40 mL of phage lysate in a sterile conical flask containing 1M NaCl and 1 µl/mL DNase was added and incubated for 1 h at room temperature. After the incubation, 10 ml of PEG (20 %) solution was added,

thoroughly mixed, and left overnight at 4°C. The solution was then centrifuged at 10,000xg for 40 min (Eppendorf Centrifuge 5804 R, Germany) to pellet the phage particles. After pouring of the supernatant, pellets were re-suspended in 2 mL of SM buffer and filtered through 0.22 mm filter and stored at 4°C for short term and at -80 °C in SM buffer containing 50 % glycerol for long term.

5.2.8. Imaging of Phages by Transmission Electron Microscopy (TEM)

Purified and concentrated phage particles were used to examine the phage morphology by Transmission Electron Microscopy after staining with 2 % uranyl acetate (pH 4.0) using a method described elsewhere (122) with some modifications. Briefly, 10 µL of phage suspension (with a minimum concentration of 10¹⁰ PFU/mL) was placed on the top of formvar carbon-coated grid (Electron Microscopy Science, USA) and allowed to absorb for about 4 min. Excess lysate was removed with filter paper from the copper-grids. Then the grid was rinsed with 5 µL of sterile water. After 1 min incubation, the excess water was completely removed with filter paper. Following this, the phage lysate was stained for 3 min by adding 10 µL of 2 % uranyl acetate. The excessive stain was also removed by touching the side of the grid using Whatman paper. The grids were then allowed to air dry for overnight. Finally, the copper grids were examined using JEOL JEM-1010 Transmission Electron Microscope operating at 75 kV.

5.2.9. Determination of Phage Host Range

The host range of each phage was investigated against different staphylococcal strains using the spot test method described previously (122) with little modification. Briefly, 100 µL exponential phase *S. aureus* cultures were mixed with 0.6 % top agar before overlaying on TSA plates. After solidifying for about 10 min, 5 µL of each phage lysate was dropped on the lawns and incubated at 37°C overnight. Results were analyzed based on detection of lysis of host bacteria with clear or turbid phage plaques. Those phages having broad lytic spectrum were selected for further characterization including endolysin gene extraction.

5.2.10. One-step Growth Curve

To understand the phages growth cycle, one-step growth curve was conducted as previously described (123) with some modifications. Briefly, the phage lysate and exponential phase of *S. aureus* cells were mixed at a multiplicity of infection of 0.01, and then allowed to adsorb for 30 min by incubating at 37°C. After the incubation period, samples were centrifuged at 10,000 rpm for 1 min and the pellet containing infected cells was resuspended in 3 mL of prewarmed TSB medium and incubated at 37°C with shaking at 160 rpm. At 10 min intervals for 2 h, 100 µL of the sample was taken and serial dilution was performed immediately followed by double-layer agar plate method for enumerating the plaque forming unit per milliliter (PFU/mL) after 12 to 24 h of incubation at 37°C. Phage growth parameters such as latent period (the time between adsorption of phage by the host and the beginning of lysis), burst size (the ratio of the final phage particles liberated to the inoculum) were calculated.

5.2.11. Phage DNA Isolation

The phenol-chloroform extraction method was used for DNA isolation. Briefly, 468 µL purified phage samples (approximately 1×10^{12} PFU/mL) was treated with lysis buffer (100 mM Tris-HCl, pH7.5; 300 mM MgCl₂; 10 mg/mL DNaseI and 20 mg/mL RNase A) for 30 min at 37°C. The samples were centrifuged at 10,000 rpm for 5 min and supernatants were transferred to new Eppendorf tubes followed by addition of phenol in one to one ratio with supernatant. The tube contents were mixed by gentle inverting for 5 min in order to digest phage structural proteins before centrifugation at 10,000 rpm for 5 min. The supernatant was transferred to new tube for chloroform:isoamyl alcohol (24:1) extraction for 5 min at room temperature. Following centrifugation at 4°C, supernatants were mixed with 2 volumes of 95% ethyl alcohol and incubated at 20°C overnight. DNA was precipitated by centrifugation for 5 min at 10,000 rpm, and DNA washed with 70% ethanol and dried at 65°C for 15 min. DNA was resuspended in TE buffer and run on 1 % agarose gel electrophoresis to examine its quality.

5.2.12. Restriction Enzyme Analysis of Phage DNA

Restriction endonuclease analysis was performed in order to estimate the genome size of the phages. Phage DNA was digested with *Bam*H I, *Hind* III, *Pst* I, *Xba* I (Promega, USA) according to the manufacturer's recommendations. The digested DNA fragments

were then analyzed by 0.8 % agarose gel electrophoresis along with 1 kb DNA ladder (Promega, USA) to compare and calculate the sizes of the phage genome.

5.2.13. Amplification of Endolysin Gene from Phage DNA by PCR

PCR primers for endolysin gene amplification were designed in accordance with appropriate TA cloning site of pET SUMO expression vector (Table 3). The PCR amplification was undertaken in 25 μL reaction volume containing the following compositions: 5 μL PCR buffer (Promega 5x), 0.5 μL dNTP (2.5 μM), 0.75 μL of each primer (10 pmol/ μL), 1.5 μL of MgCl_2 (25 mM), 0.15 μL (5U/ μL) Taq DNA polymerase (Promega), 1 μL of phage DNA, and 15.35 μL of sterilized distilled water. Then PCR conditions adjusted to 5 min of initial denaturation at 94°C, followed by 30 consecutive cycles of denaturation at 94°C for 1 min, annealing at 51.8°C for 1 min, extension at 72°C for 1 min, and a final extension at 72°C for 7 min. PCR products were analyzed by agarose gel electrophoresis.

5.2.14. Agarose Gel Electrophoresis for Separation of DNA Fragments

The agarose gel was prepared by melting 1 % (w/v) agarose in 100 ml of 1xTris-borate EDTA (TBE) using a microwave oven. The gel was then loaded with 3-5 μL volume of amplified PCR product in loading buffer and subjected to electrophoresis for 45 min at 100 volts. The gel was visualized under UV illuminator. The size of the amplified PCR product was determined by comparison with DNA marker.

5.2.15. Purification of PCR Products

The amplified PCR product were purified before ligating into pET SUMO expression vector using High Pure PCR Product Purification Kit (Sigma-Aldrich, USA) according to the manufacturer's instructions. Briefly, 500 μL of binding buffer was added to each of the 100 μL PCR tube before mixing the samples well. Then the samples were transferred into the upper reservoir High Pure Filter Tube connected to collection tube and centrifuged a maximum speed for 1 min in a standard table top centrifuge at room temperature. The flow through solution was discarded and the Filter Tube was reconnected to same collection tube prior to adding 500 μL wash buffer to the upper reservoir tube and centrifugation for 1 min at a maximum speed. The flow through was discarded and the same washing step was repeated using 200 μL washing buffer. Following this, the flow-through and collection tube were discarded and the Filter Tube was reconnected to a clean 1.5 mL of

microcentrifuge tube. Finally, 10-50 μL elution buffer was added to the upper reservoir of the Filter Tube and centrifuged at a maximum speed for 1 min. The quality of the purified DNA was checked by gel electrophoresis.

5.2.16. Cloning and Transformation of Endolysin Genes

5.2.16.1 Preparation of Competent Cells

E. coli OneShot competent cells were prepared according to the method described by Chung and Miller (124). Briefly, a single colony was inoculated into 5 mL LB media and grown overnight at 37°C with shaking at 200 rpm. Then, the culture was diluted to 1:100 in a flask containing 100 mL of LB media and grown until the OD₆₀₀ reached 0.4-0.5. Cells were then centrifuged at 10,000 rpm for 10 min at 4°C. The supernatant was discarded while the tube was retained on ice. The pellets were re-suspended in 0.5 to 1 mL of TSS buffer (1 % Bacto-Tryptone, 5 % Yeast extract, 0.5 % NaCl, 10 % (w/v) PEG 3350, and 5 % (v/v) dimethyl sulfoxide). Then aliquots of 100 μL were made and used immediately for transformation. Remaining competent cells were stored at -80°C up to 3 months.

5.2.16.2. Cloning of PCR Products

PCR amplified and purified endolysin genes were cloned into commercially available linearized pET SUMO expression vector according to the manufacturer's recommendations. Briefly, 1 μL of 10 x ligation buffers, 2 μL pET SUMO vector, 4 μL of PCR purified DNA fragments, and 2 μL of double-distilled water (ddH₂O) and 1 μL of T4 DNA ligase (5U) were mixed and incubated at room temperature for 30 min to get recombinant plasmids (designated as pET SUMO-LySA10, pET SUMO-LySA14, pET SUMO-LySA15 and pET SUMO-LySA52).

5.2.16.3 Transformation of Recombinant Plasmids into *E. coli*

Each ligation mixture was added to 100 μL of thawed competent *E. coli* OneShot cells and kept on ice for 30 min before heat shocked for 2 min at 42°C. Following the heat shock, tubes transferred back to on the ice for 3-5 min. Cells then transferred to a tube containing 900 μL of SOC medium (Super Optimal Broth, Invitrogen, USA) for expression at 37°C for 1 h with shaking at 220 rpm. Following incubation, cells were transferred to 1.5 mL Eppendorf tubes and centrifuged at 10,000 rpm for 1 min. About 800 μL of supernatant was discarded and pellets were resuspended in the remaining liquid.

From each homogenized pellet, 10 μL , and 90 μL were spread on pre-warmed agar plates containing 50 $\mu\text{g}/\text{mL}$ kanamycin, and plates were incubated at 37°C for 12 to 24 h.

5.2.17. Plasmid DNA Isolation

From each plate containing transformed cells, colonies were picked and inoculated into LB media with kanamycin (50 $\mu\text{g}/\text{mL}$) and grown at 37°C with shaking at 220 rpm overnight. From this culture, plasmids isolation was performed using QIAprep Miniprep kit (Quiagen, Germany) based on the manufacturer's instructions. The plasmid DNA was eluted in 30 to 40 μL of elution buffer. Plasmid DNAs were checked for insert by gel electrophoresis. Plasmids with heavier bands considered as having the insert were selected for further confirmation by sequencing.

5.2.18. Sequencing of Plasmid DNA

Selected purified plasmids were sequenced to confirm both presence and correct orientation of insert within the vector. To perform sequencing, Applied Biosystem ABI 373x1 DNA Analyzer with BigDye® v3.1 Cycle sequencing kit (Applied Biosystem®, USA) and vector specific sumo forward and T7 reverse primer were used. The sequence reaction was carried out in a total of 10 μL reaction volume consisting of 2 μL of plasmid DNA, 1.5 μL of 5x sequencing buffer, 1 μL of BigDye v 3.1; 0.32 μL of each forward/reverse primer (10 pmol/ μL) and 5.18 μL of sterile ddH₂O. After the reagents were mixed, PCR was run with the following PCR conditions: 3 min of initial denaturation at 96°C, followed by 25 cycles of denaturation at 96°C for 10 sec, annealing at 50°C for 5 sec, extension at 60°C for 4 min, and a final extension at 4°C. The resulting PCR products were purified by passing through a spin column containing polymerized Sephadex G-25®. The purified product was loaded onto microtiter plate of the DNA sequence Analyzer and the results of the sequencing were analyzed. Plasmids with correct sequence orientation were selected for protein expression in *E. coli* BL21 (DE3).

5.2.19. Transformation of Recombinant plasmids into Expression Host

Competent *E. coli* BL 21 (DE3) cells were prepared and transformed with 1-2 μL of each recombinant plasmid with correct orientation of the insert as described earlier.

5.2.20. Expression of Endolysins

Before performing a large-scale protein expression, a small-scale expression analysis was performed to evaluate the expression conditions, such as solubility of the proteins and optimum expression time in *E. coli*. For this, the standard procedure provided by the manufacturer was used. Briefly, single colony from each plate containing transformed *E. coli* BL21 (DE3) cell with recombinant plasmids was inoculated into 5 mL LB media containing 50 $\mu\text{g}/\text{mL}$ kanamycin and grown overnight at 37°C shaking. From overnight culture, 500 μL of the samples were transferred into 20 mL of fresh LB medium containing 1% glucose and kanamycin and were grown further at 37°C shaking until the optical density at 600 nm reached 0.4-0.6. The culture was then divided into two sets, each containing two cultures. One set of the cultures were induced with IPTG (Isopropyl- β -D-thiogalactopyranoside) at a final concentration of 1 mM and the second set left uninduced. Then the cultures were incubated at two different temperatures, 37°C and 20°C, for the expression. At different time points, 1 mL of sample was collected from each tube and centrifuged at full speed for 1 min, the supernatant was removed and the pellet was kept at -20°C until protein expression analysis was conducted using sodium dodecyl sulfate-polyacrylamide gel electrophoresis (SDS-PAGE).

5.2.21. Preparation of Samples for SDS SDS-PAGE Analysis

Frozen cell pellets were thawed on ice and lysed in 150 μL Lysis buffer (50 mM Potassium Phosphate pH 7.8, 400 mM NaCl, 100 mM KCl, 10 % glycerol, 0.5 % Triton X-100, 10 mM imidazole), followed by three cycles of freeze-thawing with alternating -20°C and 42°C. Maintaining the samples on ice, cells were further disrupted by sonication for 10 sec sonication followed by 10 sec rest over 3 min (Vibra Cell™ Sonics, USA)). The lysate was centrifuged at maximum 12,000 rpm for 10 min at 4°C to remove the cell debris. The supernatant was transferred to new Eppendorf tube and 30 μL was taken and mixed with 7 μL of 2x SDS loading buffer. The pellet was resuspended in 300 μL of 1x SDS-PAGE loading buffer. Both pellet and supernatant samples were incubated at 99°C for 5 min in a heating block before analyzed by SDS-PAGE.

5.2.22. Analysis of Expressed Endolysins by SDS-PAGE

SDS-PAGE was carried out using the Mini-PROTEAN 4 apparatus (Bio-Rad, USA) according to the manufacturer's instructions. Briefly, a 12% v/v resolving gel was prepared by combining 3 mL of 40 % w/v acrylamide, 4.35 mL of ddH₂O, 2.5 mL of 1.5 M Tris-HCl (pH 8.8), 0.1 mL of 10 % w/v SDS, 5 µL of TEMED and 50 µL of 0.1 % fresh ammonium persulfate. The solution was carefully mixed and immediately poured into the glass plate cassette. About 500 µL 2-propanol or alternatively ddH₂O was added over the top of resolving gel to prevent the gel from drying and then left to polymerize for 40 min. The 2-propanol or water on top of the gel was carefully removed and a 4 % v/v spacer gel was prepared by combining the following components; 1 mL of 40 % w/v acrylamide, 6.4 mL of ddH₂O, 2.5 mL of 0.5 M Tris-HCl (pH 6.5), 0.05 mL of 10 % w/v SDS, 3 µL of TEMED and 0.05 mL of 0.1 % fresh ammonium persulfate. The solution was carefully mixed and immediately poured on top of the resolving gel before inserting a comb. After about 40 min, the comb was removed and the gel cassette placed in electrophoresis tank. The tank was filled with 1X electrode buffer, and protein samples were loaded into wells using capillary pipette tips (20 µl from the supernatants and 10 µl from the plates). The gel was run first at 75 V for 15 min then run at 100 V for about 1.5 h until the dye reached the bottom of the resolving gel. Following this, the gel was removed from the cassette and rinsed in distilled water. The gel was placed in fixing solution (46 % methanol and 7% acetic acid) for 30 min to immobilize proteins. Gels were then washed 2 times with distilled water and stained for 30 min with coomassie blue. Finally, the gel was destained with destaining solution (5 % methanol, and 7.5 % acetic acid) for overnight. The gel image was captured using ChemiDOC™ MP imaging system (Bio-Rad, USA). The Precision Plus Protein Ladder was used as molecular weight marker. The gel image was analyzed and the conditions for best expression were selected for the large-scale production.

5.2.23. Large-scale Expression of Recombinant Endolysin Production

The expression parameters such as temperature and incubation time were selected based on the result obtained from pilot expression assay. Then large-scale production carried out as follows: 10 ml of LB containing kanamycin was inoculated with *E. coli* BL 21 (DE3) carrying the recombinant plasmids and grown overnight at 37°C shaking. The next day, 100 mL of LB containing kanamycin and 1 % glucose was inoculated with 2 mL

of the overnight culture and grown at 37°C shaking. When the optical density at 600 nm reached 0.4-0.5, the culture was induced with IPTG at a final concentration of 1 mM and incubated for additional 18-20 h by shifting the temperature from 37 to 20°C shaking. The cell pellet was collected by centrifugation at 8,000 rpm for 10 min at 4°C and resuspended in 4 mL of lysis buffer (50 mM potassium phosphate pH 7.8, 400 mM NaCl, 100 mM KCl, 10 % glycerol, 0.5 % Triton X-100, 10 mM imidazole) and kept at room temperature for 1 h on a rocking platform. The resulted cell lysate was then subjected to three freeze-thaw cycles (-80°C/42°C) maintaining the samples in ice, cells were further disrupted by sonication (18 cycles, 10 s pulse, 10 s rest, amplitude set at 40 %). The homogenized suspension was centrifuged at a maximum speed of 12,000 rpm for 15 min at 4°C to remove the cell debris. The protein lysates were then filtered through Minisart® Syringe Filters with 0.2 µm pore size (Sartorius Stedim Biotech GmbH, Germany) and aliquots were made for storing at -20°C until needed.

5.2.24. Purification of Recombinant Endolysins

Filtered protein lysates were used for purification using Nickel-Nitrilotriacetic Acid (Ni-NTA) affinity chromatography system (Qiagen, USA). In brief, 3 mL of Ni-Binding buffer was added to Ni-NTA gravity column and allowed to drain by gravity. Then, 1 mL of cleared supernatant protein lysate was mixed with 2 mL of Ni-washing buffer and passed through the column. After this, the column was washed with 3 mL of Ni-washing buffer to remove unbound protein from the column. At this stage, the flow through of the column was collected for analysis. Following washing, 1 to 3 mL of elution buffer was added to the column to elute the protein bound in nickel column. Finally, eluted protein fractions, crude lysate, and flow through were run alongside with protein ladder on 12% (w/v) SDS-PAGE gels for analysis as described before.

5.2.25. Biological Activity of Recombinant Endolysins

The lytic activity of each expressed endolysin was determined by the spot test method as described elsewhere (125) with some modification. Briefly, 100 µL of exponential phase *S. aureus* culture was spread on TSA agar plate and allowed to dry for about 10 min. Then 10 µL of filtered cleared lysate from induced *E. coli* cells harboring plasmids containing LysSA10, LysSA14, LysSA15, and LysSA52 were dropped on TSA agar plates and incubated at 37°C overnight. As a negative control cleared lysate from *E.*

coli cells without insert DNA was used. After incubation overnight visualization of inhibition zone on agar plates indicated the presence of endolysin activity.

5.2.26. Biochemical Characterization of Recombinant Endolysins

5.2.26.1. Heat Sensitivity Test for Endolysins

The sensitivity of lysSA10, lysSA14, lysSA15 and lysSA52 to heat was evaluated as previously reported (126). Briefly, each endolysin was incubated at different temperatures (30°C, 40°C, 50°C, 60°C, 70°C, 80°C, and 90°C) for 30 min followed by a 20 min cooling step on ice, after which the activity was checked by spotting 10 µL each of the treated endolysin on *S. aureus* strain and incubating at 37°C for 24 to 48 h. Endolysin enzyme solution without preheating was used as a control. Inhibition zone diameters were measured for each treatment and compared with the control, and the relative activities were presented in percentage compared to the control, assuming that the activity for control is 100 %.

5.2.26.2. Influence of pH on Endolysin Activity

To evaluate the effect of pH on endolysin activity the following experiment was carried out. First, 10 µL of phosphate buffered saline (PBS; 137 mM NaCl, 2.7 mM KCl, 10 mM Na₂HPO₄, 2 mM KH₂PO₄) with pH values of 4, 5, 6, 7, 8, 9, and 10 was added to separate tubes containing 45 µL endolysin and 10 µL from each mixture was dropped on TSA agar preinoculated with *S. aureus*. Following 24 to 48 h incubation, presence of clear zone was checked and pH range for each endolysin was determined based on their lysis efficiency and diameter of the inhibition zones.

5.2.26.3. The Effect of Divalent Metal Ions on Activity of Endolysins

To evaluate the effects of divalent metal ions on the activity of each endolysin, a previously described method (126) was employed with some modifications. In brief, each endolysin was treated with EDTA at a final concentration of 50 mM for 30 min at room temperature to chelate metal ions and remove any residual metal ions attached to the endolysin, thereby inhibiting its catalytic function. Subsequently, enzymes were dialyzed against 50 mM phosphate buffer (pH 8.0) using mini dialysis column (Slide-A-Lyzer™ MINI Dialysis Devices, ThermoFisher, USA) to remove the EDTA. Following this, suspension of metal ions such as CaCl₂, MgCl₂, and ZnCl₂ buffers at 0.5 mM and 1mM concentrations were added to the EDTA treated endolysin separately and mixed gently by

pipetting before incubating for 15 min at room temperature. After the end of incubation period, 10 μ L from each mixture was dropped on TSA agar containing *S. aureus* and incubated for 24 to 48 h. Non-EDTA treated endolysin and EDTA treated but no divalent ions endolysin were also dropped as controls. Zone of inhibitions (clear zones) were measured for each treatment and expressed as an average of three replicates. From this measurement, the relative activities were presented in percentage by comparing with the control, in which the activity for the control was assumed 100 %.

5.2.27. Host Range Determination of Endolysins

The spot test method described before was used to test the lytic range for each endolysin proteins against 88 clinical staphylococcal strains including *S. aureus*, MRSA, *S. epidermidis*, and *S. haemolyticus* strains.

5.2.28. In Vitro Anti-biofilm Properties of Endolysin

The effect of LysSA10, LysSA14, LysSA15, and LysSA52 endolysins on biofilms were evaluated before and after the establishment of *S. aureus* and *S. epidermidis* biofilms in 96 well microtiter plates and on catheter sections.

5.2.28.1. Biofilm Disruption Test in Microtiter Plates

Biofilm removal or disruption assay was evaluated using microtiter plate assay as previously described (127), with some modifications. Briefly, an overnight culture of *S. aureus* or *S. epidermidis* strains were diluted with 0.25 % w/v D-(+)-glucose to attain an initial inoculum level of 10^6 CFU/mL. From each strain, 200 μ L of prepared inoculums was poured into 96 wells flat-bottomed microtiter plate and 200 μ L TSB was added in separate wells as negative control. Microtiter plates were then incubated at 37°C without agitation for 48 h to allow biofilm formation. After incubation period, the contents of the wells were removed and wells were washed 2 times with PBS. Following washing, 100 μ L of each recombinant endolysin at three different concentrations 0. 20 mg/mL, 0. 30 mg/mL, and 0. 50 mg/mL were added to each well. For each treatment and control four wells were used. Plates were incubated for 12 h at 37°C before discarding the contents and washing with PBS. To quantify the remaining biofilm the wells were stained by adding 200 μ L of 1 % (w/v) crystal violet solution. The unbound crystal violet was removed by washing with PBS, and then 200 μ L ethanol-acetone (80:20) was added in each well to solubilize the bound crystal violet from the stained *S. aureus* and *S. epidermidis* biofilms.

The the solubilized samples were measured using plate reader at OD₅₉₅ nm to quantify the remaining biofilms. The results were presented in percent remained biofilms. The mean of four wells used and the experiments were repeated three times.

5.2.28.2. Biofilm Inhibition Assay in Microtiter Plates

To investigate the ability of each endolysin in preventing the formation of *S. aureus* and *S. epidermidis* biofilms, crystal violet staining assay was used except that endolysins were added before biofilm establishment. Simply, an overnight culture of *S. aureus* and *S. epidermidis* strains were diluted with 0.25 % w/v D-(+)-glucose to attain an initial inoculum level of 10⁶ CFU/mL. From each strain, 180 µL culture was transferred into 96 wells flat-bottomed microtiter plate and 20 µL (0.50 mg/mL) endolysin was added immediately to each well before incubating at 37°C for 48 h. In a control set, the same amount of PBS was used instead of endolysins. After incubation period, the planktonic bacteria were removed and the wells were washed, stained and quantified as described in earlier section.

5.2.28.3. Biofilm Removal Assay from Catheters

For determining the biofilm removal capacity of endolysins, previously reported method (26) was used. Briefly, Foley catheter was cut into 3 cm pieces with a sterile scalpel and placed in test tubes. Overnight culture of *S. aureus* and *S. epidermidis* strains were diluted with 0.25 % w/v D-(+)-glucose to attain an initial inoculum level of 10⁶ CFU/mL from which 900 µL culture was added to each tube and incubated at 37°C for 48 h to allow biofilm formation. Catheter sections were removed from the tubes and washed 2 times with PBS, and then placed in new sterile test tube where treated with 300 µL of endolysin (0.50 mg/mL). For the control sets, PBS was used instead of endolysins. Both controls and treatment tubes were incubated at 37°C for 12 h. After treatment, the remaining biofilm was removed from the catheter sections mechanically by thoroughly resuspending in 50 mM sodium phosphate buffer (pH 7.5), which was vortexed for 2 min and scrapped with sterile pipette tip. The samples were then serially diluted and plated on TSB agar plates to enumerate the colony forming unit. Results were presented in log of CFU and log reduction unit was also determined as compared to control.

5.2.28.4. Prevention of Biofilm Formation on Catheters

To quantify the extent of biofilm formation on endolysin coated catheter sections, the modified method of a previous report was used (128). Briefly, Foley catheter pieces were placed in test tubes containing 300 μ L endolysin solutions (0.5 mg/mL) and incubated at 4°C for 1 h. After the end of incubation, catheter sections were removed from the tube and air dried in the hood under sterile conditions. Subsequently, the coated and dried catheters sections were submerged in a tube containing 900 μ L of *S. aureus* or *S. epidermidis* diluted overnight culture and incubated at 37°C for 48 h to allow biofilm formation. Sterile PBS was used as control. After incubation period, catheter sections were removed from the tubes, washed with PBS; biofilms were removed mechanically and enumerated as described in previous section. Results were presented in log reduction of CFU as compared to control.

5.2.29. Scanning Electron Microscopy of Biofilms

Biofilm of *S. aureus* and *S. epidermidis* were established on glass coupons (10 mm diameter x 1 mm height) and catheter sections for 48 h followed by washing and treatment with endolysin for 12 h. Then, both treated and untreated biofilm samples were prepared for scanning electron microscopy (SEM, ZEISS EVO LS 10, Germany) examination as previously described (129) with slight modification. In brief, biofilm samples were fixed in 4 % phosphate-buffered glutaraldehyde for 1 h at 4°C, then washed with PBS. Following washing, the biofilm samples were dehydrated with serially increasing concentration of ethanol (50%, 70%, 80%, 90%, 95%, and 100%) for 10 min at 4°C and then were placed in a fume hood for about 2 h to remove any remaining liquid. Specimens were mounted on stubs with silver paint and coated with gold using sputter coater (Quorum Technologies, UK) for 1.5 min. Coated samples were visualized at 15 kV SEM at a magnification of X 5000, X 10,000 and X 20, 000.

5.2.30. *In vitro* Cytotoxic Effects of Endolysins Assay

The cytotoxic effects of each endolysin were evaluated on growing human fibroblast cell derived from kid foreskin, which was kindly provided by the Department of Medical Biology of Karadeniz Technical University (Trabzon, Turkey). Fibroblast cells were thawed and mixed with 10 mL DMEM with 10 % FBS, and 4 % streptomycin (Invitrogen, USA) and grown to the desired level of confluency in a T75 flask by incubating at 37°C incubator under 5% CO₂ air. After the desired confluence was attained, the growth medium in the flask was decanted and flasks were rinsed with a small amount of fresh growth medium to remove the entire old medium. About 1 mL of trypsin solution was added to loosen cells from the flask at 37°C for 1-2 min. Once the cells started lifting up from the surface, the trypsin reaction quickly was quenched by adding 10 mL of cell culture medium. The cell suspension was transferred into sterile 15 mL of falcon tube and centrifuged at 1200 rpm for 5 min. The supernatant was discarded and the pellet was resuspended in 1 mL of cell growth medium. The number of cells in the cell suspension was counted by using hemocytometer stained with Trypan Blue (dilution factor = 2) under an inverted microscope using x20 magnification before they were used in cytotoxicity assay.

5.2.30.1. Cytotoxicity Assay

Fibroblast cells were seeded at 5000 cells per well of 96 well microtiter plate and incubated until 85% cell confluence has been reached. Confluent fibroblast cells were then treated with four endolysins (LysSA10, LysSA14, LysSA15, and LysSA52) at a final concentration of 10 mg/mL and endolysin buffer (20 mM NaHPO₄, 0.5M NaCl, 20mM imidazole) as well as untreated fibroblasts were included as controls and for 24 h. Following the incubation period, MTT cell viability assay [3-(4, 5-dimethylthiazol-2-yl) - 2,5-diphenyltetrazolium bromide (Thermo-Fisher, USA)] was performed as described previously (130) with slight modifications. Briefly, 10 µL of MTT, which is reduced by metabolically active cells due to the action of dehydrogenase enzymes that results in intracellular purple colored formazan crystals, was added to the contents of each well and cover the plates with aluminum foil to prevent the effect of light on MTT. Following incubation of the plate at 37°C for 3 h, the contents of the wells were aspirated and 100 µL DMSO a solvent that can dissolve the crystals formed already as result of MTT, was added to each well and incubated for another 30 min at 37°C. The plates were then analyzed

spectrophotometrically by reading the absorbance at 570 nm. The viability of fibroblast cells was expressed in percentage relative to the untreated control cells.

5.2.31. Statistical Analysis

All experimental results were expressed as the mean \pm standard deviation (SD) for analysis performed in duplicate at least three times. Statistical analysis of the data was performed by Analysis of Variance (ANOVA) and mean comparison using Student's *t*-test, using SPSS software version 22. P-values < 0.05 were considered statistically significant.

5.2.32. Phylogenetic Analysis

The nucleotide sequence of each endolysin was analyzed using the Basic Local Alignment Search Tool (BLASTn) to identify the homologous regions with the sequences deposited in the NCBI database (<https://blast.ncbi.nlm.nih.gov>). Various staphylococcal phage endolysins were first retrieved from NCBI database. Then, multiple sequence alignments were performed using ClustalW2 which is available at <https://www.ebi.ac.uk/Tools/msa/clustalw2/> or MEGA (Molecular Evolutionary Genetic Analysis) 7.0. The phylogenetic tree was then constructed using the neighbor-joining method via MEGA 7.0.

5.2.33. Sequence Variation Analysis

The nucleotide sequences of endolysins were translated into their corresponding protein sequences using Bioinformatics Tools for Sequence translation available at https://www.ebi.ac.uk/Tools/st/emboss_transeq/. The translated amino acid sequences were aligned using ClustalW2. The prediction of protein functional domains was performed by SMART (Simple Modular Architecture Research Tool) available at <http://smart.embl-heidelberg.de/>.

5.2.34. Structural Modeling

The SWISS-MODEL available at <https://www.swissmodel.expasy.org/> was used for structural modeling of the amidase-2 domain of each endolysin. Briefly, PDB database was searched for endolysin proteins homology by using our sequences as a query. The 3-D structure of the amidase-2 domain of LysGH15 with PDB Id: 4ols was selected as it is the best hit with a sequence identity of 53.42 % and 2.3-angstrom resolution among the listed templates for homology modeling. After the selection of the best template, a 3-D model

(Three-dimensional model) was generated using the same web-server (SWISS-MODEL), and then visualized using the UCSF Chimera molecular analysis program (131).



6. RESULTS

6.1. Screening Endolysin Gene in Genomic DNA of *S. aureus*

General primer, which is specific for *S. aureus* bacteriophage endolysin was designed after retrieving endolysin gene sequences from NCBI database and aligned using ClustalW program. From the alignment result, one forward primer having the start codon “ATG” at the beginning and one reverse primer having stop codon “TAA” at the end terminal was designed (Table 3). Using these primers, endolysin gene sequences were screened by PCR in the chromosomal DNA of 60 clinical *S. aureus* isolates. Of these, 17 of them were found to be positive for the endolysin gene, and all of them have almost the same size that is approximately 1500 bp (Figure 11). These positive strains were then selected for phage induction.

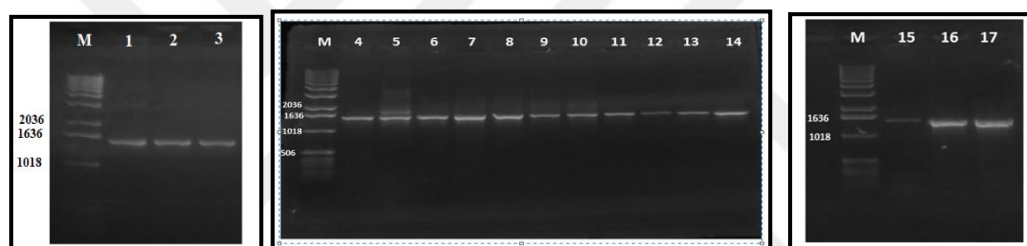


Figure 11. Screening for the endolysin gene in chromosomal DNA of *S. aureus*. M, Molecular Weight Marker; 1-17, endolysin positive *S. aureus* strains: TRSA10, 14, 15, 196, 197, 201, 202, 204, 205, 207, 216, 220, 222, 249, 261, 262, 264, respectively.

6.2. Phage Isolation

Phages were isolated by induction with mitomycin C. Among the 17 PCR positive strains for endolysin genes, 7 of them were induced by mitomycin C and confirmed for the presence of functional phages by spot and plaque assay methods (Figure 12 A, B, C and D) on the lawn of *S. aureus* strains. The seven phages were designated as Φ trsa10, Φ trsa14, Φ trsa15, Φ trsa205, Φ trsa207, Φ trsa220 and Φ trsa222 based on the code given for their respective host in which they were isolated.

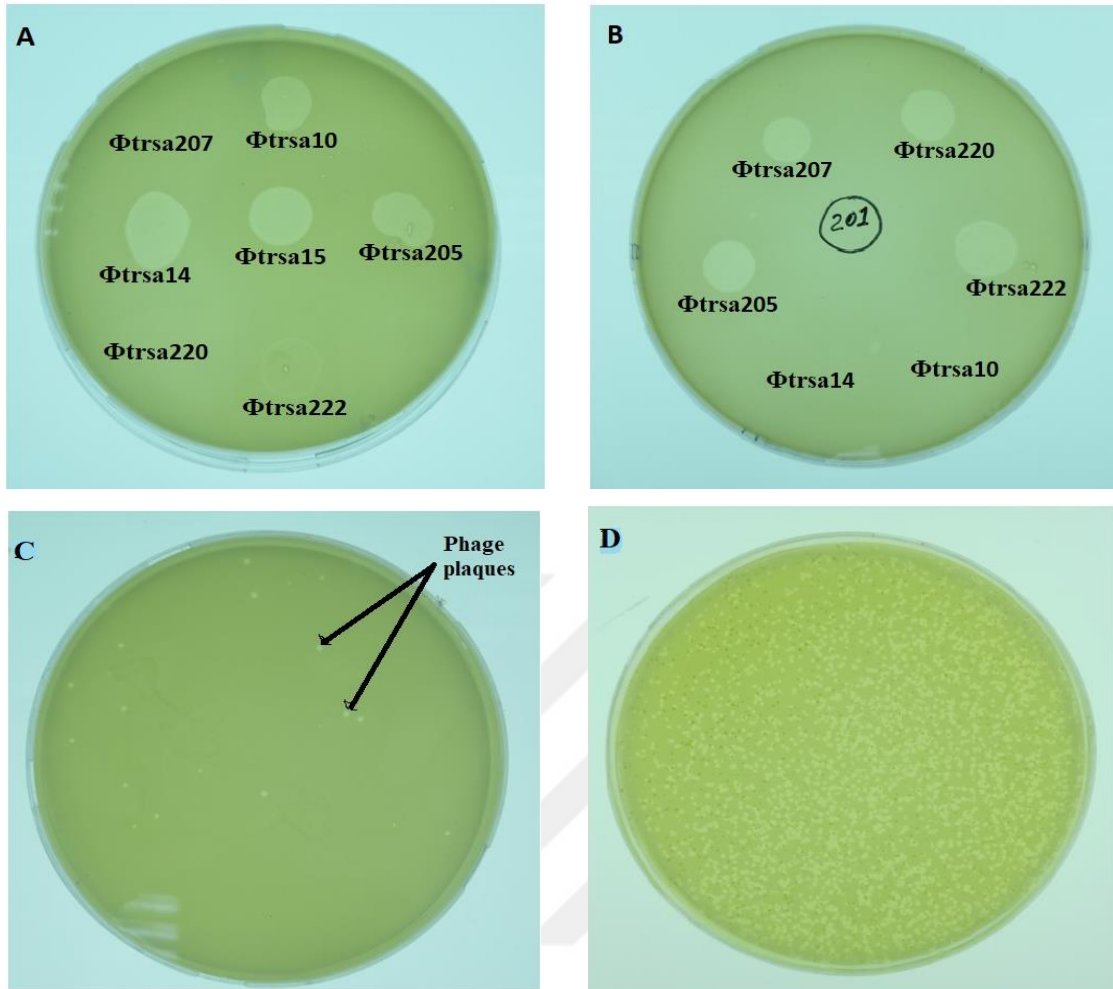


Figure 12. Lytic activity of phages against *S. aureus* strains using the spot method (A and B) and the plaque assay method (C and D)

6.3. Transmission Electron Microscopy of phage

Morphological characterization of phages Φ trsa10, Φ trsa14, Φ trsa15, Φ trsa205, Φ trsa207, Φ trsa220 and Φ trsa222 were made by Transmission Electron Microscopy (TEM). The results of the TEM revealed that all seven phages shared features like an isometric head measuring about 40 – 62 nm and long non-contractile tails of approximately between 90 – 210 nm in length (Table 4). Based on the TEM micrographs, all seven phages belong to the *Siphoviridae* family, which is characterized by phages with a long non-contractile tail (Figure 13).

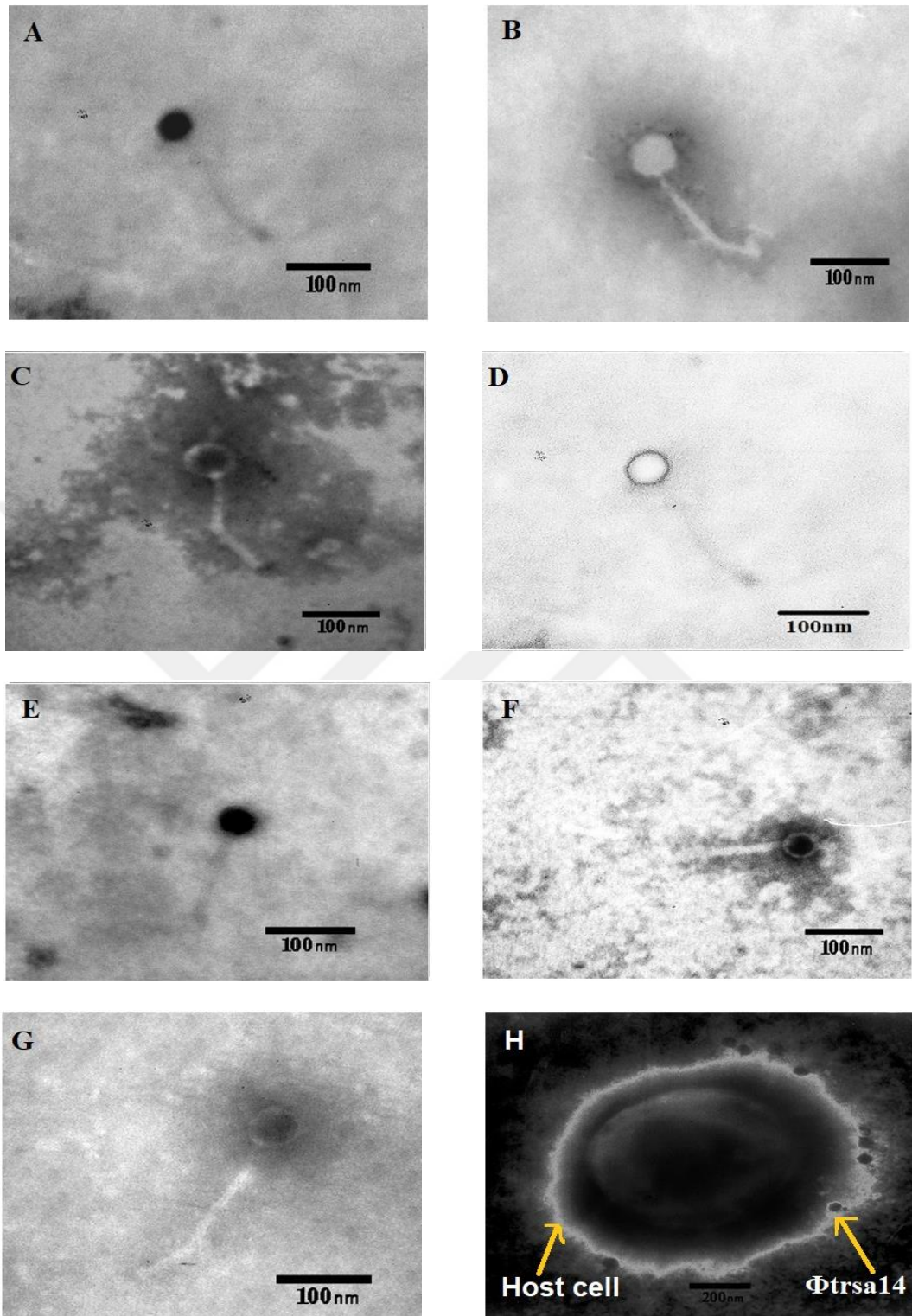


Figure 13. Transmission Electron Microscopic images of isolated phages: A, Φ trsa10; B, Φ trsa15; C, Φ trsa205; D, Φ trsa207; E, Φ trsa220; F, Φ trsa222; G, Φ trsa14; H, Φ trsa14 attached to its host (*S. aureus* 35). The scale bar denotes 100 nm.

Table 4. Morphological characteristics of the seven phages isolated from clinical isolates

Phage	Capsids or head diameter (nm)	Capsids or head length (nm)	Tail width (nm)	Tail length (nm)
Φtrsa10	44.3 ± 1.0	44.3 ± 1.0	8.2 ± 0.6	171.0 ± 2.8
Φtrsa14	43.1 ± 2.3	54.4 ± 2.0	9.7 ± 0.3	213.9 ± 1.0
Φtrsa15	59.3 ± 0.3	59.3 ± 0.3	10.3 ± 1.0	156.2 ± 1.6
Φtrsa205	62.3 ± 1.3	62.3 ± 1.0	14.2 ± 0.3	143.4 ± 1.3
Φtrsa207	46.4 ± 2.0	46.4 ± 2.0	10.7 ± 2.1	165.0 ± 2.8
Φtrsa220	48.6 ± 1.0	48.6 ± 1.0	10.3 ± 0.8	128.3 ± 0.3
Φtrsa222	41.8 ± 0.8	45.1 ± 1.5	12.5 ± 1.3	96.2 ± 2.0

6.4. Host Range Determination and Selection of Virulent Phages

Spot assay method was applied for the determination of the lytic spectrum of each phage and to select phages with the broader host range for further characterization. For this, each phage was challenged with a total of 88 staphylococcal strains (including 60 *S. aureus*, 25 *S. epidermidis*, and 3 *S. haemolyticus*). Results of the spot test showed that phages Φtrsa10 showed effectiveness against 28 (46.6 %) out of 60 *S. aureus* isolates tested, while Φtrsa14, Φtrsa15, Φtrsa205, Φtrsa207, Φtrsa220 and Φtrsa222 were effective against 27 (45 %), 26 (43.3 %), 21 (35%), 15 (25 %), 12 (20 %), and 11 (18.3 out of 60 *S. aureus* tested, respectively (Figure 14). None of them showed effectiveness against any of the *S. epidermidis*, and *S. haemolyticus* isolates. Based on this host range determination result, three most efficient phages namely Φtrsa10, Φtrsa14, and Φtrsa15 were selected for further characterization including cloning, expression, and functional analysis of their respective endolysin genes.

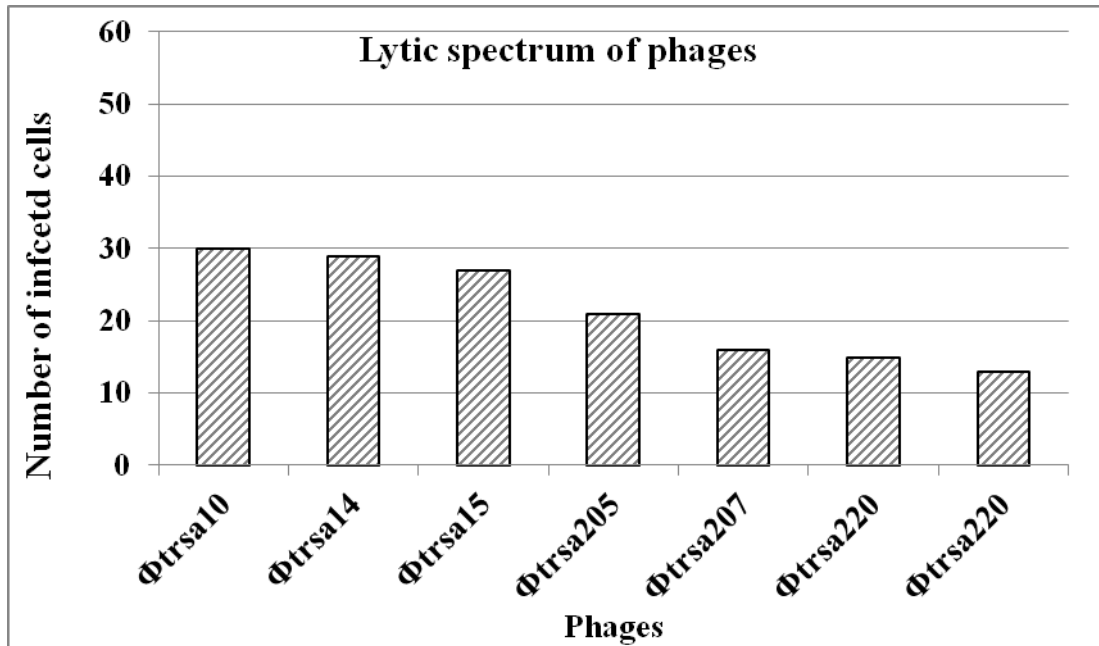


Figure 14. Host range of the seven phages against 60 *S. aureus* isolates

6.5. One-step Growth Curve

One-step growth curve experiments were performed to analyze the life cycle of three phages, Φtrsa10, Φtrsa14, and Φtrsa15. The latent period and burst size of the phages in the phage infection process were estimated from the curve. According to the results obtained from the growth curves, the latent periods for Φtrsa10 and Φtrsa14 were about 20 min which is followed by a raise period of 30 min that results in a burst size of about 30 and 40 PFU per infected cell, respectively (Figure 15 A and B). Phage Φtrsa15 showed a latent period of about 25 min and a raise period of 30 min that resulted in a burst size of about 20 PFU per infected cell (Figure 15 C).

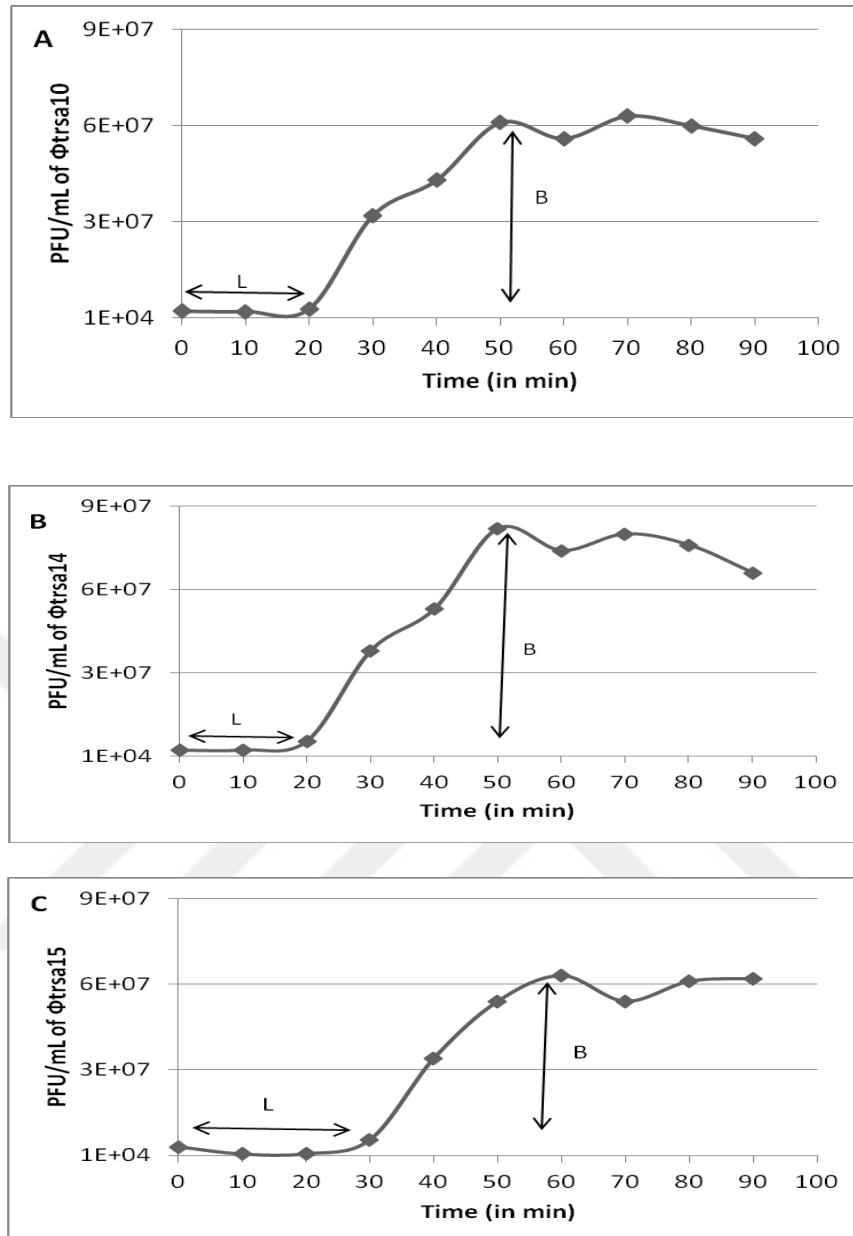


Figure 15. One-step growth curves of phages; Φ trsa10 (A), Φ trsa14 (B), and Φ trsa15 (C). The curves shown here is the PFU/infected cell at several time points over 90 min. L, latent periods; B, burst size.

6.6. Analysis of Phage DNA

DNA extraction was carried out from Φ trsa10, Φ trsa14, and Φ trsa15 using phenol-chloroform methods and visualized by ethidium bromide gel electrophoresis (Figure 16). The purified DNAs were digested with *EcoRI*, *HindIII*, *BamHI*, *BSP*, and *XbaI* restriction enzymes (Figure 17). Based on the restriction endonuclease digestion genomic DNA of the three phages were estimated and the sum of the fragments resulted in the approximate genomic size of 37, 36 and 38 kb for Φ trsa10, Φ trsa14 and Φ trsa15, respectively.

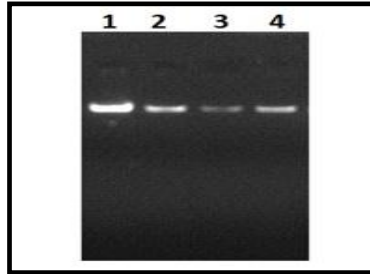


Figure 16. Agarose gel electrophoresis of phage genomic DNA. 1, Φ trsa10; 2, Φ trsa14; 3, Φ 52; 4, Φ trsa15.

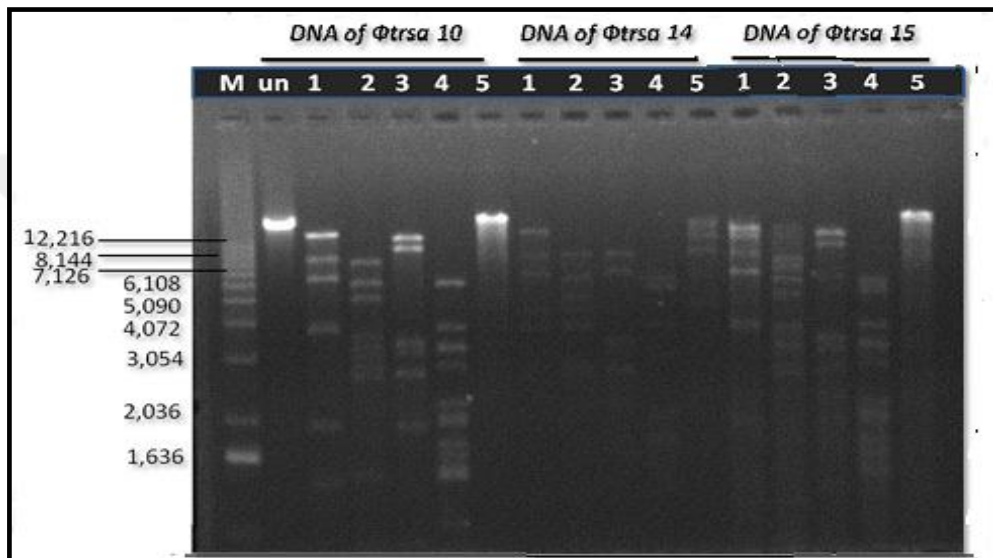


Figure 17. Restriction analysis of Φ trsa10, Φ trsa14, and Φ trsa15 DNA. M, Molecular Weight Marker; un, undigested DNA (as control); and 1-5 indicated each phage DNA digested with *Bam*H I, *Bsp*106 I, *Eco*RI, *Hind* III, and *Xba*I, respectively.

6.7. PCR Amplification of Endolysin Genes from Phage DNA

The endolysin genes were amplified from three phages, Φ trsa10, Φ trsa14, and Φ trsa15, isolated in this study, and an additional phage, *S. aureus subsp. aureus* bacteriophage 52 (ATCC[®]27692-B1[™]) obtained from ATCC using one pair of designed endolysin primers. As shown in Figure 18, single PCR products of approximately 1500 bp in length was successfully amplified using genomic DNA as template from each phage. Accordingly, endolysin from Φ trsa10 was named as LysSA10, and endolysins from Φ trsa14, Φ trsa15 and *S. aureus subsp. aureus* bacteriophage 52 were designated as LysSA14, LysSA15, and LysSA52, respectively.

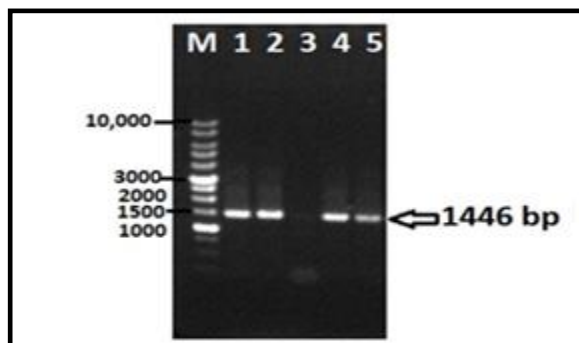


Figure 18. Amplification of endolysin genes from phages DNA. M, Molecular Weight Marker; 1, LysSA10 gene of Φ trsa10; 2 and 3, LysSA14 gene of Φ trsa14; 4, LysSA15 gene of Φ trsa15; 5, LysSA52 gene of Φ 52,

6.8. Molecular Cloning of Endolysin Genes

Purified LysSA10, LysSA14, LysSA15 and LysSA52 endolysin gene fragments were cloned into linearized pET SUMO expression vector (Invitrogen) using TA cloning methods. The ligated products such as pET SUMO- LysSA10, pET SUMO- LysSA14, pET SUMO- LysSA15 and pET SUMO- LysSA52 were first transformed into One Shot®Mach 1™-T1R component *E. coli cells*. To identify the cells that contain the desired insert, plasmid DNA was isolated from resultant colonies and selected based on band size on gel electrophoresis (Figure 19). Accordingly, one plasmid from pET SUMO- LysSA10 construct (Figure 19 I), six plasmids from pET SUMO- LysSA14 (Figure 19 II), 2 plasmids from pET SUMO- LysSA15 (Figure 19 III) and four plasmids from pET SUMO- LysSA52 construct (Figure 19 IV) were obtained by the preliminary criteria (i.e. band size). With sequence analysis, at least one plasmid with the right insert orientation was identified from each construct. The correct orientation from each construct was labeled by a circle in the figure 19 I-IV.

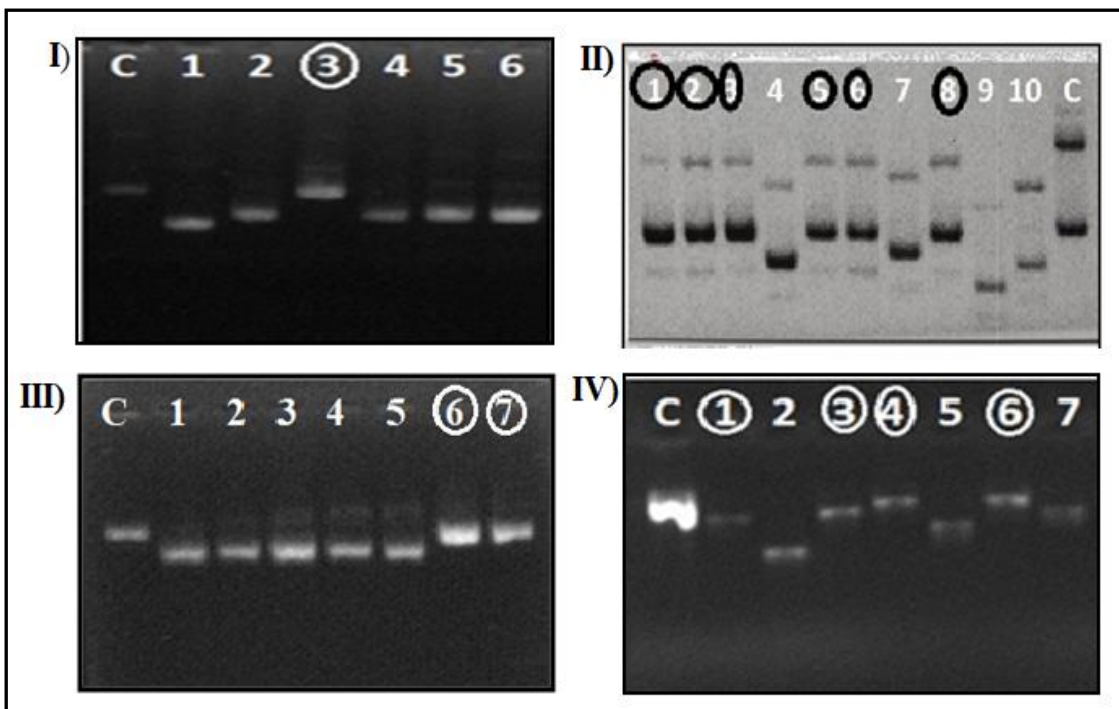


Figure 19. Screening of recombinant plasmids from *E. coli* OneShot transformed by pET SUMO-endolysin construct. I, potential pET SUMO-LysSA10 clones; II, potential pET SUMO-LysSA14 clones; III, potential pET SUMO-LysSA15 clones; IV, potential pET SUMO-LysSA52 clones. Circled numbers are selected plasmids for analysis. C, control, a plasmid harboring known insert.

6.9. Plasmid Sequencing

After positive clones were selected according to plasmid-size based criteria, the presence and orientation of insert were verified by sequencing. From each of the four plasmid constructs, pET SUMO-LysSA10, pET SUMO-LysSA14, pET SUMO-LysSA15, and pET SUMO-LysSA52 were sequenced. With the sequence, an insert size of 1446 bp with correct orientation was obtained and named as LysSA10, LysSA14, LysSA5, and LysSA52 genes. Each of them showed the presence of a 1446 bp encoding single open reading frame that begins with the ATG start codon and ends with the TAA stop codon (Figure 20 A-D). The sequence data were submitted to the GenBank database (National Center for Biotechnology Information, USA) and assigned the accession numbers MH025825, MH025826, MH025827, and MH104949 for LysSA10, LysSA14, LysSA15, and LysSA52 respectively.

A

ATGCAAGCAAACTAACTAAAAAAGAGTTTATAGAGTGGTTGAAAACCTTCTGAGGGAAAACAATTCAATG
TGGACTTATGGTATGGATTTCAATGCCTTGATTATGCCAATGCTGGTTGGAAAGTTTTGTTGGATTACTTCT
AAAAGGTTTAGGTGCAAAAGATATACCATTTGCAAACAATTTTGATGGACTAGCTACTGTATACAAAATA
CGCCGGACTTTTTGGCAAACCCGGCGATATGGTTGTGTTCCGGTAGCAATTACGGTGCAGGATACGGACAC
GTAGCATGGGTAATTGAAGCAACTTTAGATTATATCATTGTATATGAGCAGAATTGGCTAGGCGGTGGCTG
GACTGACAGAATCGAACAACCCGGCTGGGGTTGGGAAAAAGTTACAAGACGACAACATGCCTTACGATTT
CCCTATGTGGTTTATCCGTCTATCCAAAAGCGAAACAGCTCCACGATCAATACAATCTCCTACGCAAGC
ATCTAAAAAGGAAACAGCTAAGCCACAACCTAAAGCGGTAGAACTTAAAATTATCAAGGATGTGGTAAA
GGTTATGACCTTCCTAAACGTGGTGGTAATCCTAAAGGTATTGTCATTCATAATGACGCAGGAAGCAAAGG
GGCGACAGCGGAAGCTTATCGCAACGGATTAGTTAACGCGCCTTTATCGAGATTAGAGGCAGGTATTGCAC
ATAGTTATGTATCAGGTAACACAGTGTGGCAAGCTTTAGATGAATCACAAGTAGGTTGGCATACTGCTAAC
CAATTAGGCAATAAATATTATTACGGTATTGAAGTGTGTCAATCAATGGGCGCAGATAACGCGACATTCTT
AAAAAATGAACAGGCAACTTTCCAAGAATGTGCTAGGTTATTAAAAAAGTGGGGATTACCAGCAAACAGA
AATACAATCAGATTGCACAATGAATTTACTTCAACATCATGCCCTCATAGAAGTTCGGTTTTACACACTGGT
TTTGACCCAGTAACTCGCGTCTATTGCCAGAAGACAAGCGGTTGCAACTTAAAGACTACTTTATCAAGCA
GATTAGGGCGTACATGGATGGTAAAATACCGGTTGCCACTGTCTCTAATGAGTCAAGCGCTTCAAGTAATA
CAGTTAAACCAGTTGCGAGTGCATGGAAACGTAATAAATATGGTACTTACTACATGGAAGAAAGTGCTAG
ATTCACAAACGGCAATCAACCAATCACAGTAAGAAAAGTGGGGCCATTCTTATCTTGTCCAGTGGGTTATC
AGTTCCAACCTGGTGGGTATTGTGATTATACAGAAGTGATGTTACAAGATGGTTCATGTTTGGGTAGGATAT
ACATGGGAGGGGCAACGTTATTACTTGCCTATTAGAACATGGAATGGTTCTGCCCCACCTAATCAGATATT
AGGTGACTTATGGGGAGAAATCAGTTAA

B

ATGCAAGCAAAACAACTAAAAAAGAGTTTATAGAGTGGTTGAAAACCTTCTGAGGGAAAACAATTCAATG
TGGACTTATGGTATGGATTTCAATGCCTTGATTATGCCAATGCTGGTTGGAAAGTTTTGTTGGATTACTTCT
AAAAGGTTTAGGTGCAAAAGATATACCATTTGCAAACAATTTTGATGGACTAGCTACTGTATACAAAATA
CGCCGGACTTTTTGGCAAACCCGGCGATATGGTTGTGTTCCGGTAGCAATTACGGTGCAGGATACGGACAC
GTAGCATGGGTAATTGAAGCAACTTTAGATTATATCATTGTATATGAGCAGAATTGGCTAGGCGGTGGCTG
GACTGACAGAATCGAACAACCCGGCTGGGGTTGGGAAAAAGTTACAAGACGACAACATGCATACGATTTCT
CCTATGTGGTTTATCCGTCTAACTTCAAAAAGCGAAACAGCTCCACGATCAATACAATCTCCTACGCAAGC
ATCTAAAAAGGAAACAGCTAAGCCACAACCTAAAGCGGTAGAACTTAAAATTATCAAGGATGTGGTAAA
GGTTATGACCTTCCTAAACGTGGTGGTAATCCTAAAGGTATTGTCATTCATAATGACGCAGGAAGCAAAGG
GGCGACAGCGGAAGCTTATCGCAACGGATTAGTTAACGCGCCTTTATCGAGATTAGAGGCAGGTATTGCAC
ATAGTTATGTATCAGGTAACACAGTGTGGCAAGCTTTAGATGAATCACAAGTAGGTTGGCATACTGCTAAC
CAATTAGGCAATAAATATTATTACGGTATTGAAGTGTGTCAATCAATGGGCGCAGATAACGCGACATTCTT
AAAAAATGAACAGGCAACTTTCCAAGAATGTGCTAGGTTATTAAAAAAGTGGGGATTACCAGCAAACAGA
AATACAATCAGATTGCACAATGAATTTACTTCAACATCATGCCCTCATAGAAGTTCGGTTTTACACACTGGT
TTTGACCCAGTAACTCGCGTCTATTGCCAGAAGACAAGCGGTTGCAACTTAAAGACTACTTTATCAAGCA
GATTAGGGCGTACATGGATGGTAAAATACCGGTTGCCACTGTCTCTAATGAGTCAAGCGCTTCAAGTAATA
CAGTTAAACCAGTTGCGAGTGCATGGAAACGTAATAAATATGGTACTTACTACATGGAAGAAAGTGCTAG
ATTCACAAACGGCAATCAACCAATCACAGTAAGAAAAGTGGGGCCATTCTTATCTTGTCCAGTGGGTTATC
AGTTCCAACCTGGTGGGTATTGTGATTATACAGAAGTGATGTTACAAGATGGTTCATGTTTGGGTAGGATAT
ACATGGGAGGGGCAACGTTATTACTTGCCTATTAGAACATGGAATGGTTCTGCCCCACCTAATCAGATATT
AGGTGACTTATGGGGAGAAATCAGTTAA

Figure 20. Sequencing of endolysin genes cloned on pET SUMO vector. A, pET SUMO-LysSA10; B, pET SUMO-LysSA14.

C

ATGCAAGCCACCCTAACTAAAAAAGAGTTTATAGAGTGGTTGAAAACCTTCTGAGGGAAAACAATTCAATGT
GGACTTATGGTATGGATTTCAATGCTTTGATTATGCCAATGCTGGTTGGAAGTTTTGTTTGGATTACTTCTA
AAAGGTTTAGGTGCAAAAGATATACCATTTGCAAACAATTTTGATGGACTAGCTACTGTATACCAAAAATAC
GCCGGACTTTTTGGCAAAACCCGGCGATATGGTTGTGTTCCGGTAGCAATTACGGTGCAGGATACGGACACG
TAGCATGGGTAATTGAAGCAACTTCAGATTATATCATTGTATATGAGCAGAATTGGCTAGGCGGTGGCTGG
ACTGACAGAATCGAACAACCCGGCTGGGGTTGGGAAAAAGTTACAAGACGACAACATGCTTACGATTTCC
CTATGTGGTTTATCCGTCCTAACTTCAAAAAGCGAAACAGCTCCACGATCAATACAATCTCCTACGCAAGCA
TCTAAAAAGGAAACAGCTAAGCCACAACCTAAAGCGGTAGAACTTAAAATTATCAAGGATGTGGTTAAAG
GTTATGACCTTCTAAACGTGGTGGTAATCCTAAAGGTATTGTCATTCATAATGACGCAGGAAGCAAAGGG
GCGACAGCGGAAGCTTATCGCAACGGATTAGTTAACGCGCCTTTATCGAGATTAGAGGCAGGTATTGCACA
TAGTTATGTATCAGGTAACACAGTGTGGCAAGCTTTAGATGAATCACAAGTAGGTTGGCATACTGCTAACC
AATTAGGCAATAAATATTATTACGGTATTGAAGTGTGTCAATCAATGGGCGCAGATAACGCGACATTCTTA
AAAAATGAACAGGCAACTTTCCAAGAATGTGCTAGGTTATAAAAAAGTGGGGATTACCAGCAAACAGAA
ATACAATCAGATTGCACAATGAATTTACTTCAACATCATGCCCTCATAGAAGTTCGGTTTTACACACTGGTT
TTGACCCAGTAACTCGCGGTCTATTGCCAGAAGACAAGCGGTTGCAACTTAAAGACTACTTTATCAAGCAG
ATTAGGGCGTACATGGATGGTAAAATACCGGTTGCCACTGTCTCTAATGAGTCAAGCGCTTCAAGTAATAC
AGTAAAACAGTTGCGAGTGCATGGAAACGTAATAAATATGGTACTTACTACATGGAAGAAAAGTGTCTAGA
TTCACAAACGGCAATCAACCAATCACAGTAAGAAAAGTGGGGCCATTCTTATCTTGTCCAGTGGGTTATCA
GTTCCAACCTGGTGGGTATTGTGATTATACAGAAGTGATGTTACAAGATGGTCATGTTTGGGTAGGATATA
CATGGGAGGGGCAACGTTATTACTTGCCTATTAGAACATGGAATGGTTCTGCCCCACCTAATCAGATATTA
GGTGACTTATGGGGAGAAATCAGTTAA

D

ATGCAAGCAAACTAACTAAAAAAGAGTTTATAGAGTGGTTGAAAACCTTCTGAGGGAAAACAATTCAATG
CGGACTTATGGTATGGATTTCAATGCTTTGATTATGCCAATGCTGCTTGGAAAAGTTTTGTTTGGATTACTTCT
AAAAGGTTTAGGTGCAAAAGATATACCATTTGCAAACAATTTGATGGACTAGCTACTGTATACCAAAAATA
CACCGGACTTTTTGGCACAACCCGGCGACATGGTTGTGTTCCGGTAGTAATTACGGTGCAGGATACGGACAC
GTAGCATGGGTAATTGAAGCAACTTTAATTATATCATTGTATATGAGCAGAATTGGCCAGGCGGTGGCTGG
ACTGACGGAATCGAACAACCCGGCTGGGGTTGGGAAAAAGTTACAGACGACAACCTTGCTTACGATTTCCCT
ATGTGGTTTATCCGCCCCGAACTTCAAAAAGCGAAATAGCACCCACGATTCAGTTCAATCTCCTACACAAGCA
CCTAAAAAGGAAACAGCTAAGCCACAACCTAAAGCAGTAGAACTTAAAATCATCAAAGATGTGGTTAAAG
GTTATGACCTACCTAAGCGTGGTAGTAACCCTAAAGGTATAGTTATTTCATAACGACGCAGGAAGCAAAGGG
GCGACAGCAGAAGCGTATCGAAACGGATTAGTTAACGCGCCTTTATCGAGATTAGAGGCAGGTATTGCAC
ATAGTTATGTATCAGGTAACACAGTGTGGCAAGCTTTAGATGAATCACAAGTAGGTTGGCATACTGCTAACC
CAATTAGGCAATAAATATTATTACGGTATTGAAGTGTGTCAATCAATGGGCGCAGATAACGCGACATTCTT
AAAAAATGAACAGGCAACTTTCCAAGAATGTGCTAGGTTATAAAAAAGTGGGGATTACCAGCAAACAGAA
AATACAATCAGATTGCACAATGAATTTACTTCAACATCATGCCCTCATAGAAGTTCGGTTTTACACACTGGT
TTTGACCCAGTAACTCGCGGTCTATTGCCAGAAGACAAGCGGTTGCAACTTAAAGACTACTTTATCAAGCA
GATTAGGGCGTACATGGATGGTAAAATACCGGTTGCTACTGTCTCAAATGATTCAAGCGCTTCAAGTAATA
CAGTTAAACCAGTTGCGAGTGCATGGAAACGTAATAAATATGGTACTTACTACATGGAAGAAAAGTGTCTAG
ATTACAAACGGCAATCAACCAATCACAGTAAGAAAAGTGGGGCCATTCTTATATTGTCCAGTGGGTTATC
AGTTCCAACCTGGTGGATATTGTGATTATACAGAAGTGATGTTACAAGATGGTCATGTTTGGGTAGGATAT
ACATGGGAGGGGCAACGTTATTACTTGCCTATTAGAACATGGAATGGTTCTGCCCCACCTAATCAGATATT
AGGTGACTTATGGGGAGAAATCAGTTAA

Figure 20. (Continued)

All of the four endolysins were then aligned with other *S. aureus* phage endolysin genes found in the databases using the Multiple Sequence Alignment program ClustalW2 to determine the degree of similarity between the endolysins. The neighbor-joining phylogenetic tree showing the relationship between the endolysins was constructed based

on multiple alignments using the DNA sequences generated from ClustalW2 (Figure 21). As can be seen in this figure, all of the four endolysins are closely related to each other. They had an identity between 88 to 99 % with endolysins genes derived from various *S. aureus* phages such as PhiSA13, PhiDW2, PhiSA12, phiSaus-IPLA88, PhiMR11, phi005, and Staphylococcal phage 80 (Table 4). In contrast, they are very divergent from endolysins derived from various *S. aureus* phages such as phiP68, phi44AHJD, phi GRCS, phiH5, Staphylococcal phage SA4, and Staphylococcal phage 812 (Figure 21).

Table 5. Percent identity matrix of each endolysin with some other *S. aureus* phage endolysin genes found in the databases

		1	2	3	4	5	6	7	8	9	10	11
1	PhiSA13	100	93.22	100	96.40	91.45	91.76	91.77	91.56	89.28	91.76	92.18
2	PhiDW2	93.22	100	93.22	91.08	87.76	88.65	88.66	88.45	86.93	88.57	88.86
3	PhiSA12	100	93.22	100	96.40	91.15	91.76	91.77	91.56	89.28	91.76	92.18
4	ΦSauS-IPLA88	96.40	91.08	96.40	100	91.42	91.49	91.49	91.29	89.14	91.90	92.18
5	ΦMR11	91.15	87.76	91.15	91.42	100	95.57	95.57	95.37	95.23	94.60	95.16
6	Φtrsa10*	91.76	88.65	91.76	91.49	95.57	100	99.72	99.52	93.22	97.09	97.37
7	Φtrsa14*	91.77	86.66	91.77	91.49	95.57	99.72	100.00	99.52	93.22	97.09	97.37
8	Φtrsa15*	91.56	88.45	91.56	91.29	95.37	99.52	99.52	100	93.02	96.88	97.16
9	Phi005	92.18	86.93	88.28	89.14	95.23	93.22	93.22	93.02	100	93.35	93.91
10	Φ52**	91.76	88.86	91.76	92.18	94.60	97.09	97.09	96.88	93.35	100	99.52
11	<i>S. aureus</i> phage 80	92.18	88.76	92.18	92.18	95.16	97.37	97.37	97.16	93.91	99.52	93.91

*, Endolysin genes purified from phages obtained during this study;

**, Endolysin genes purified from phage obtained commercially.

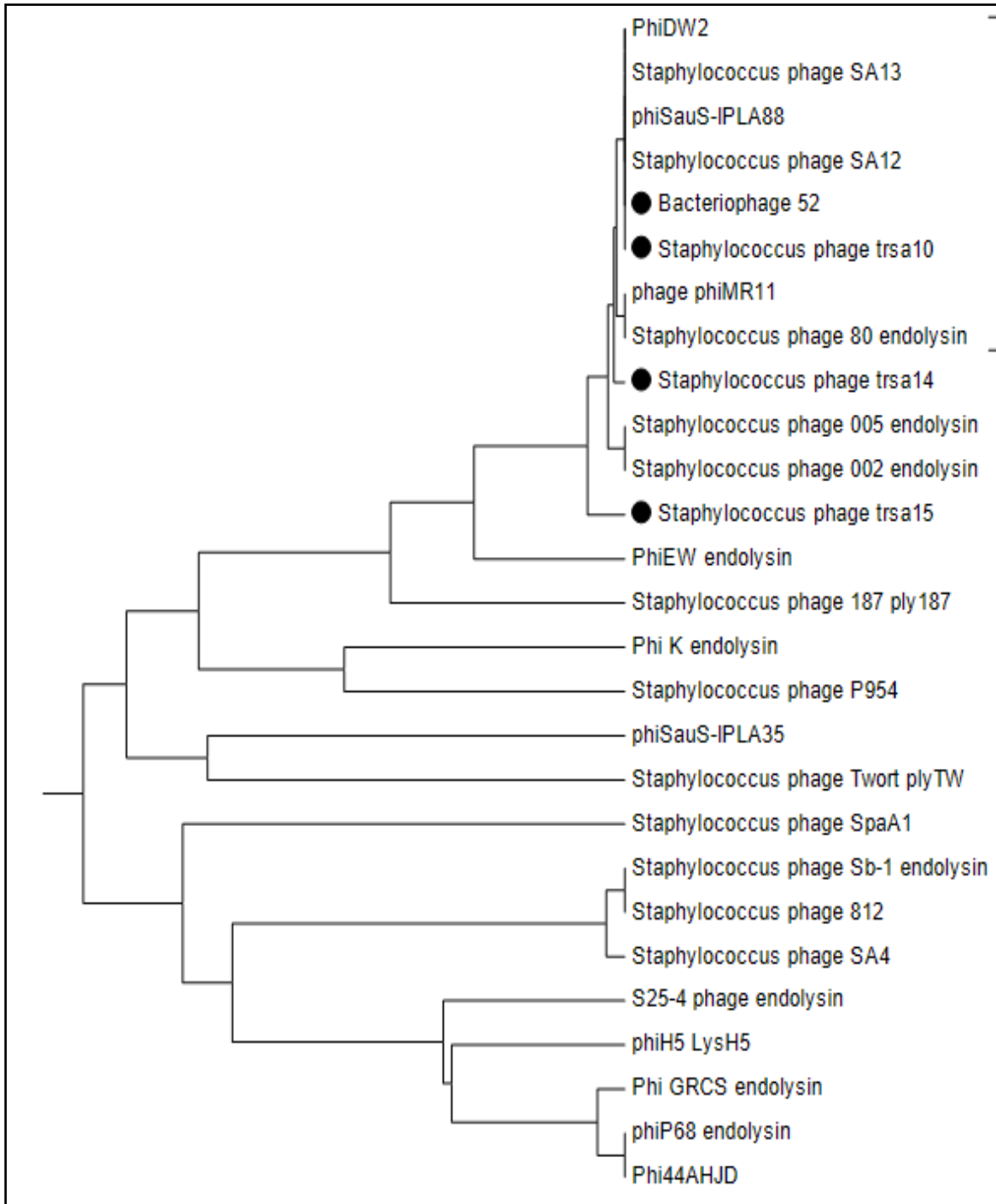


Figure 21. Phylogenetic position of LysSA10, LysSA14, LysSA15, and LysSA52 endolysin genes derived from phages Φ trsa10, Φ trsa14, Φ trsa15 and phage 52 endolysins, respectively. The phylogenetic tree was constructed using the neighbor-joining method.

6.10. Pilot Expression of Endolysin Proteins

Plasmids harboring endolysin genes with the right orientation were successfully transformed into *E. coli* BL 21 (DE3) cells for expression. But before made large-scale purification, small-scale expression analysis was performed by using an *E. coli* BL21 (DE3) transformed with pET SUMO-LysSA10. After induction with IPTG (1mM) at 37°C and 20°C at different times, both pellet and supernatant fractions were analyzed by 12% SDS-PAGE (Figure 22 A and B). As seen in the in the figure 21 A, the desired bands that we are looking for in the lane 2, 4, and 5 of supernatant fractions at about 66 kDa are not distinct and cannot be distinguished from other bands in the lanes. This finding indicated that LysSA10 may not have been present in the soluble fraction at 37°C. In contrast, the protein of interest (LysSA10) is produced quite well in the pellet fractions as shown in the lanes 2, 4, and 6 of Figure 22B. The bands in these lanes are very distinct as compared to non-IPTG induced. This indicates that the LysSA10 is well expressed in *E. coil* BL 21, but was produced in the insoluble fraction at 37°C. The comparison of the molecular weight of the band with protein ladder suggests that the weight of the LysSA10 with SUMO fusion is produced at expected size, which is about 66 kDa (53 kDa for LysSA10 plus 13 kDa for the SUMO fusion protein) (Figure 22B).

However, when the temperature of induction was shifted from 37°C to 20°C the fusion protein (His tag-SUMO-LysSA10) was efficiently over-expressed in its soluble form in the host following induction with 1 mM IPTG at 20°C for 20 h (Figure 23). The band in the lane 3 is very distinct as compared to non-IPTG induced in lane 1 of Figure 23. This indicates that the LysSA10 is well expressed in *E. coil* BL 21, in the soluble fraction at 20°C. Of course, there is also a distinct band in lane 2, which indicate that there is still insolubilized protein remained in the pellet fractions. The comparison of the molecular weight of the band with protein ladder suggests that the weight of the LysSA10 with SUMO fusion is produced both in pellet and supernatant fractions at expected size, which is about 66 kDa (Figure 23).

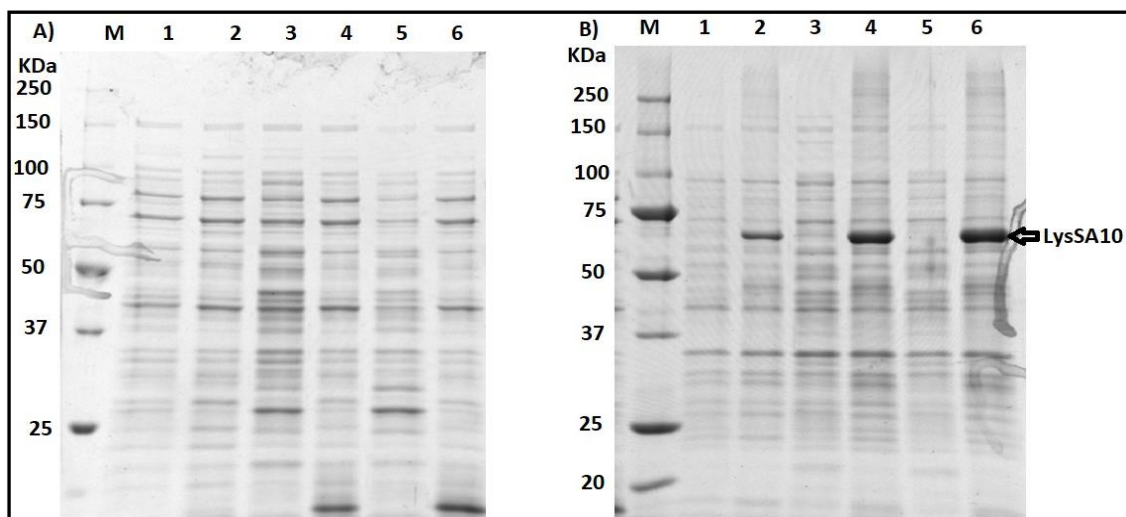


Figure 22. SDS-PAGE analysis of expressed LysSA10 endolysin at 37° C. A, supernatant fractions of LysSA10 endolysin expressed for 3, 6 and 12 hours, respectively; and B, pellet fractions of LysSA10 endolysin expressed for 3, 6 and 12 hours, respectively. Lanes M, protein ladder; 1, uninduced LysSA10 at 3rd h; 2, IPTG Induced LysSA10 at the 3rd h; 3, uninduced LysSA10 at the 6th h; 4, IPTG induced LysSA10 at 6th h; 5, uninduced LysSA10 at 12th h; 6: IPTG induced LysSA10 at the 12th h.

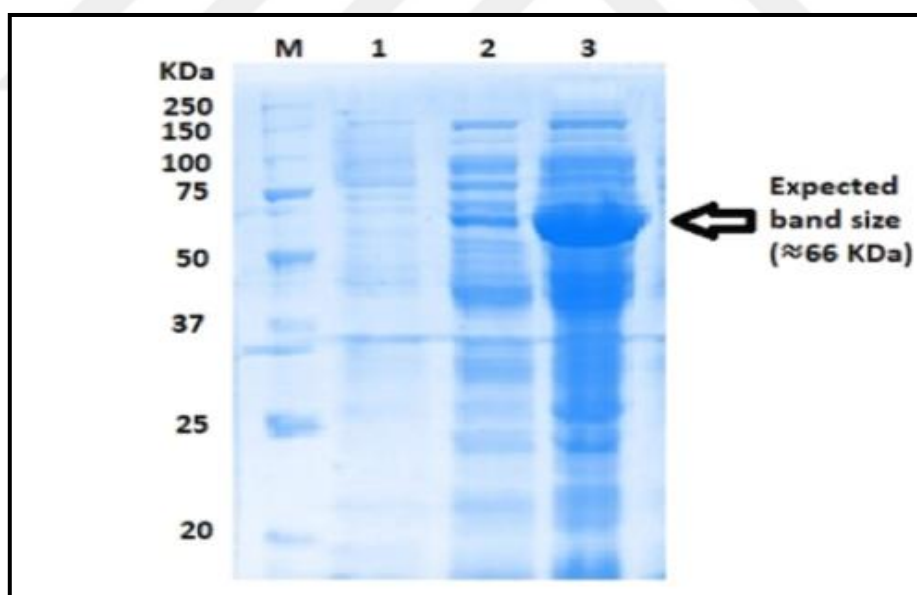


Figure 23. SDS-PAGE analysis of expressed LysSA10 endolysin at 20°C. Lanes M, protein ladder; 1, uninduced LysSA10 for 20 h; 2, IPTG induced LysSA10 (pellet fraction); 3, IPTG induced LysSA10 (supernatant fraction).

6.11. Large Scale Expression of Endolysins

The expression parameters such as temperature and duration of induction time obtained from the pilot study (Figure 22 and 23) assays were used for expressing the endolysins in large scale. Following induction of the culture by IPTG at a final concentration of 1 mM at a temperature of 20°C for 20 h, the cells were harvested, lysed and SDS-PAGE analysis was performed. All the four endolysins (LysSA10, LysSA14, LysSA15, and LysSA52) were produced with SUMO fusion at expected size of 66 kDa (Figure 24). The crude lysates were filter sterilized for biological activity testing and further purifications.

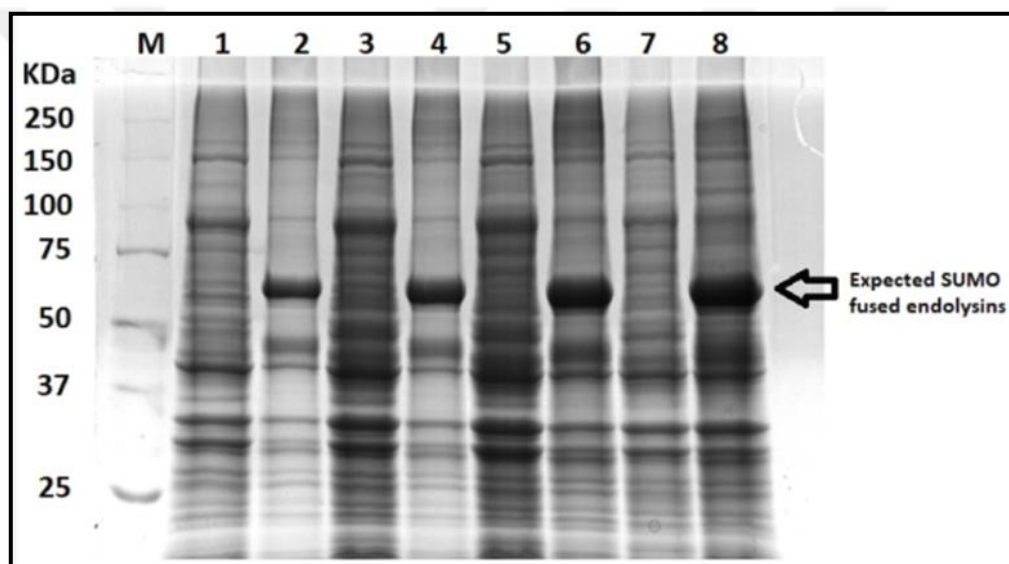


Figure 24. SDS-PAGE analysis of supernatant fractions of four endolysins after large-scale expression at 20°C for 20 hours. Lanes M, protein ladder; 1, uninduced LysSA10; 2, IPTG induced LysSA10; 3, uninduced LysSA14; 4, IPTG induced LysSA14; 5, uninduced LysSA15; 6, IPTG induced LysSA15; 7, uninduced LysSA52; 8: IPTG induced LysSA52.

6.12. Purification and SDS-PAGE Analysis of Expressed Endolysins

As described earlier in section 3, expression cultures were grown in LB broth to an OD_{600nm} of 0.4-0.6 before induction. Following 20 h of incubation, cultures were harvested and the recombinant proteins were purified under native conditions using Nickel-nitrilotriacetic acid (Ni-NTA) affinity chromatography. The targeted proteins were eluted with the elution buffer and visualized in SDS-PAGE gels stained with Coomassie blue stain (Figure 25 A-C). Results of purification in SDS-PAGE for His-SUMO-LysSA10

demonstrated high purity in the first purification attempt, but with the low yield (Figure 25 A). In the rest of the endolysins, partial purifications were achieved, since nonspecific bands were observed in the gel (Figure 25 B and C).

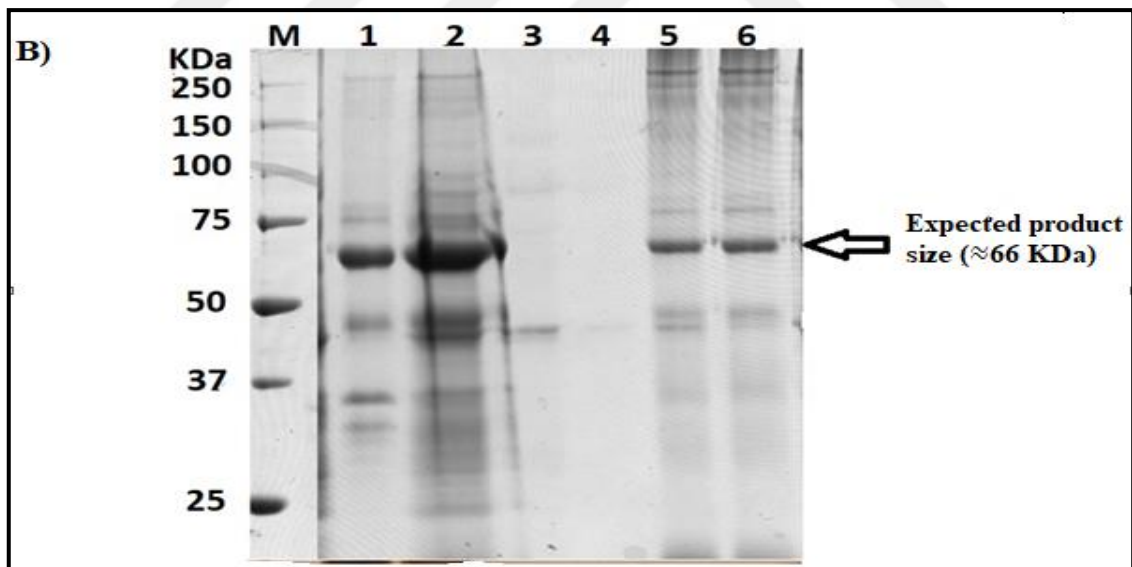
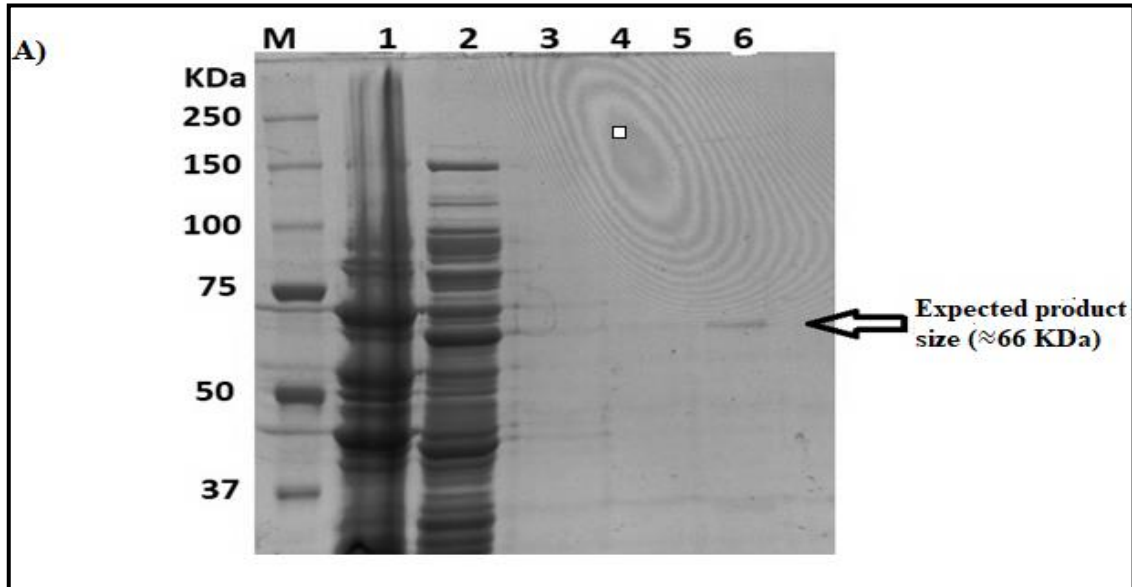


Figure 25. SDS-PAGE analysis of SUMO fused endolysins before and after purifications. A, 6xHis tag-SUMO-LysSA10 fusion protein; B, 6xHis tag-SUMO-LysSA14 fusion protein. Lanes M, protein marker; 1 and 2 total protein before purification; 3 and 4, the flow through from nickel column (wash fraction), and 5 and 6 are eluted fractions.

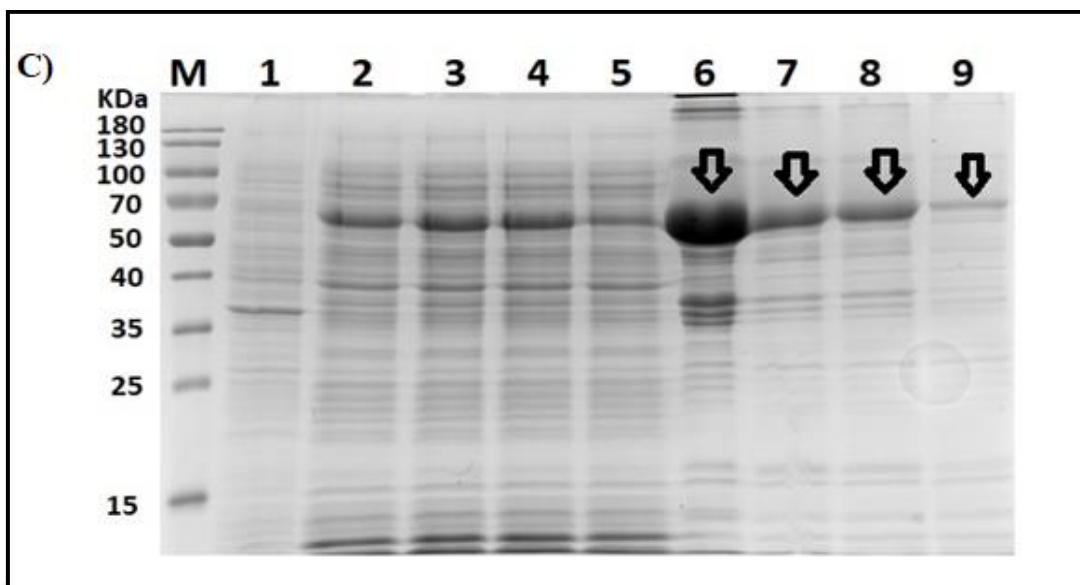


Figure 25. (Continued) SDS SDS-PAGE analysis of SUMO fused endolysins before and after purifications. Lanes M, protein marker; lanes 1, uninduced culture (control); 2, 3, 4, and 5, LysSA10, LysSA14, LysSA15 and LysSA52 before purification; 6, 7, 8, and 9, LysSA10, LysSA14, LysSA15 & LysSA52 after purification. The arrows indicated the predicted size of bands.

6.13. Lytic Activity and Host Range Determination of Endolysins

In the spot test method, drops of filtered crude lysates from induced *E. coli* cultures harboring recombinant endolysins (LysSA10, LysSA14, LysSA15, and LysSA52) were applied on agar plates inoculated with indicator bacteria, *S. aureus*, *S. epidermidis*, and *S. haemolyticus*, and incubated at 37°C for overnight. Cleared lysis zones indicated functional endolysins (Figure 26). No lytic activity was observed in the control extracts. Each phage endolysin was assayed by spot test on 88 staphylococcal strains including 60 *S. aureus*, of which 12 were MRSA, 25 *S. epidermidis*, and 3 *S. haemolyticus*, isolated from clinical samples (Table 6). The results showed that LysSA10, LysSA14, LysSA15, and LysSA52 were active against 59 (64.8%), 67 (76%), 51 (58.9%), and 49 (55.7%) of the strains tested, respectively. A combination of the four endolysins showed activity against 77 (87.5%) of the total strains tested.

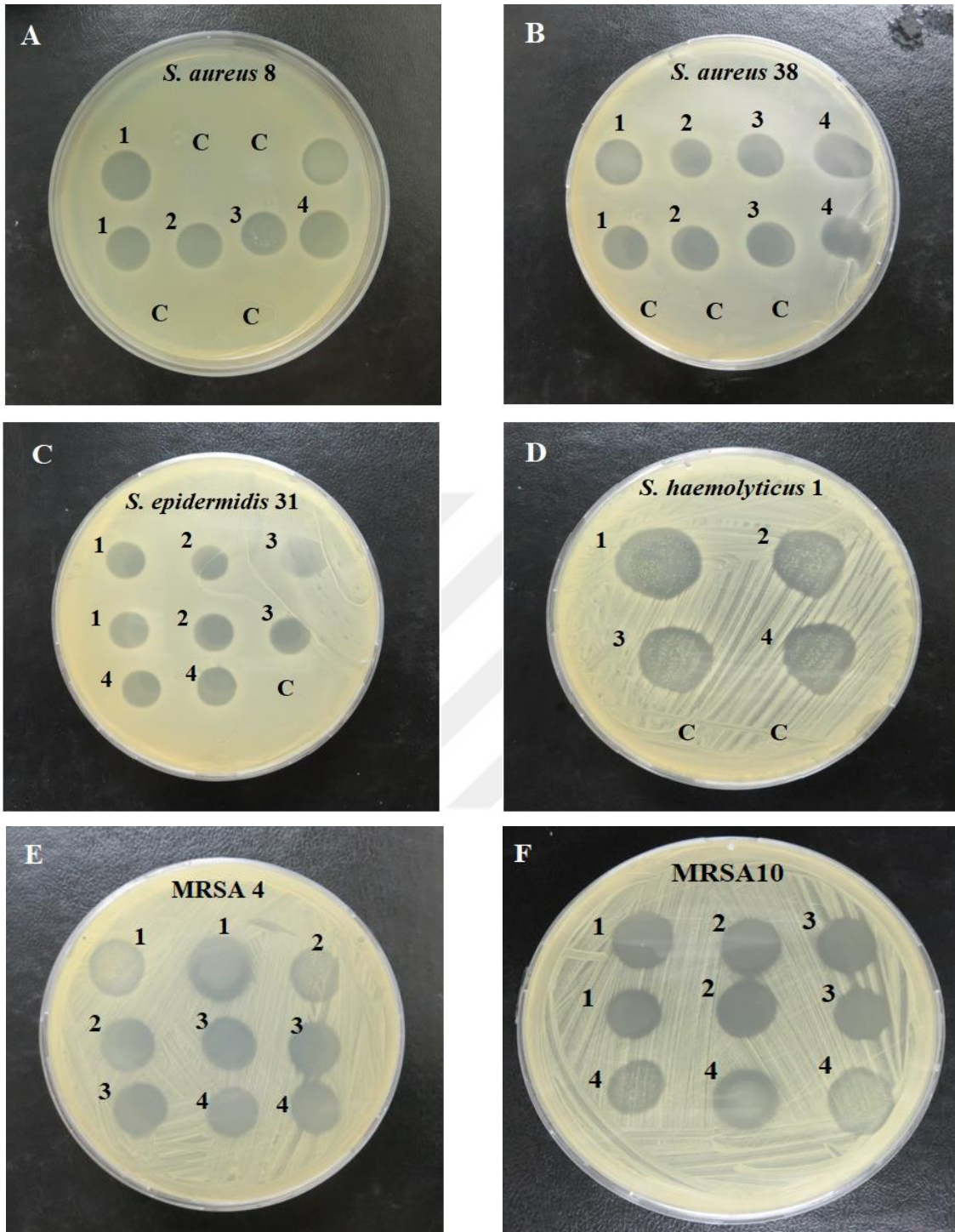


Figure 26. Spot assay showing the ability of endolysins to lyse *S. aureus* (A and B), *S. epidermidis* (C), *S. haemolyticus* (D), and MRSA (E and F). Numbers 1, LysSA10; 2, LysSA14; 3, LysSA15; 4, LysSA52; C, control (lysate prepared from *E. coli* harboring plasmid without insert).

Table 6. In vitro lytic efficacy of phages and its derived recombinant endolysin against *staphylococcus* strains isolates originated from various clinical samples

No.	Isolate code	Strains name	Strains origin	Φtrsa 10	LysSA10	Φtrsa14	LysSA14	Φtrsa 15	LysSA15	LysSA52	Mixed Lysin*
1	TRSA1	<i>S. aureus</i>	Pus	-	-	-	+	-	-	-	-
2	TRSA2	<i>S. aureus</i>	Wound	+++	++	+++	++	+++	++	++	+++
3	TRSA3	<i>S. aureus</i>	Blood	+	++	+	+	+	++	++	++
4	TRSA4	<i>S. aureus</i>	Tr.As	+	+	+	+	+	+	+	++
5	TRSA5	<i>S. aureus</i>	Tr.As	-	-	-	+	-	-	-	+
6	TRSA6	<i>S. aureus</i>	Tr.As	+	+	+	+	+	+	+	++
7	TRSA7	<i>S. aureus</i>	Wound	+	+	+	+	+	+	+	+
8	TRSA8	<i>S. aureus</i>	Tr.As	+++	+++	+++	+++	+++	+++	+++	+++
9	TRSA9	<i>S. aureus</i>	Ear	-	+	-	+	-	+	+	+
10	TRSA10	<i>S. aureus</i>	Wound	-	+	-	+	-	+	+	++
11	TRSA11	<i>S. aureus</i>	Ear	-	-	-	++	-	-	-	++
12	TRSA12	<i>S. aureus</i>	Wound	-	+	-	+	-	+	+	++
13	MRSA1	<i>S. aureus</i>	Tr.As	-	+	-	+	-	+	+	+
14	TRSA14	<i>S. aureus</i>	Wound	+	+	+	+	+	+	+	+
15	MRSA2	<i>S. aureus</i>	Tr.As	-	+	-	+	-	+	+	+
16	TRSA16	<i>S. aureus</i>	Wound	-	-	-	+	-	-	-	+
17	MRSA3	<i>S. aureus</i>	Sputum	-	++	-	++	-	-	-	++
18	TRSA18	<i>S. aureus</i>	Urine	-	-	-	+	-	-	-	+
19	TRSA19	<i>S. aureus</i>	Tr.asp	-	-	-	+	-	-	-	+
20	TRSA20	<i>S. aureus</i>	Wound	-	-	-	+	-	-	-	+
21	TRSA21	<i>S. aureus</i>	Pus	-	-	-	+	-	-	-	+
22	MRSA4	<i>S. aureus</i>	Wound	+	+++	+	+++	+	+++	++	+++
23	MRSA5	<i>S. aureus</i>	Wound	+	+	+	+	+	+	+	++
24	TRSA24	<i>S. aureus</i>	Tr.asp	+	+	+	+	+	+	+	++
25	MRSA6	<i>S. aureus</i>	Tr.asp	-	+	-	+	-	-	-	+
26	TRSA26	<i>S. aureus</i>	Wound	-	-	-	+	-	-	-	+
27	TRSA27	<i>S. aureus</i>	Nose	-	-	-	+	-	-	-	+
28	TRSA28	<i>S. aureus</i>	Wound	+	+	+	+	-	+	+	+
29	TRSA29	<i>S. aureus</i>	Wound	-	-	-	+	-	-	-	+
30	TRSA30	<i>S. aureus</i>	Pus	-	+	-	+	-	+	+	++
31	TRSA31	<i>S. aureus</i>	Tr.asp	-	-	-	+	-	-	-	+
32	TRSA32	<i>S. aureus</i>	Wound	++	++	++	+	++	++	++	+++
33	TRSA33	<i>S. aureus</i>	Tr.asp	-	++	-	+	-	++	++	++

Table 6. (Continued)

No.	Isolate code	Strains name	Strains origin	Φtrsa 10	LysSA10	Φtrsa14	LysSA14	Φtrsa 15	LysSA15	LysSA52	Mixd Lvsins*
34	TRSA34	<i>S. aureus</i>	Wound	+	+	+	+	+	+	+	++
35	TRSA35	<i>S. aureus</i>	Wound	+	+	+	+	+	+	+	++
36	TRSA36	<i>S. aureus</i>	Blood	++	++	++	+	++	++	++	+++
37	TRSA37	<i>S. aureus</i>	Tissue	+	+	+	+	+	+	+	+
38	TRSA38	<i>S. aureus</i>	Blood	+	++	+	+	+	++	++	++
39	TRSA39	<i>S. aureus</i>	Wound	+	+	+	+	+	+	+	+
40	MRSA7	<i>S. aureus</i>	Wound	-	++	-	++	-	++	++	++
41	MRSA8	<i>S. aureus</i>	Tr.As	-	+	-	+	-	+	+	+
42	TRSA42	<i>S. aureus</i>	Wound	+	+	+	+	+	+	+	+
43	TRSA43	<i>S. aureus</i>	Pus	+	++	+	+	+	++	++	++
44	TRSA44	<i>S. aureus</i>	Blood	+	+	+	+	+	+	+	+
45	TRSA45	<i>S. aureus</i>	Wound	++	++	++	++	++	++	++	+++
46	TRSA46	<i>S. aureus</i>	Wound	++	++	++	++	++	++	++	++
47	MRSA9	<i>S. aureus</i>	Wound	-	+	-	+	-	+	+	+
48	TRSA48	<i>S. aureus</i>	Blood	+	+	+	+	+	+	+	+
49	TRSA49	<i>S. aureus</i>	Ear	+	+	+	+	+	+	+	+
50	MRSA10	<i>S. aureus</i>	Tr. asp	-	+++	-	+++	-	+++	++	+++
51	TRSA51	<i>S. aureus</i>	Wound	+	+	+	+	+	+	+	+
52	TRSA52	<i>S. aureus</i>	Blood	-	-	-	-	-	-	-	-
53	TRSA53	<i>S. aureus</i>	Wound	-	+	-	-	-	-	-	+
54	TRSA54	<i>S. aureus</i>	Wound	-	+	-	-	-	-	-	+
55	MRSA12	<i>S. aureus</i>	Blood	-	-	-	-	-	-	-	-
56	MRSA13	<i>S. aureus</i>	Wound	+	++	++	++	-	++	-	++
57	TRSA57	<i>S. aureus</i>	Wound	-	+	-	+	-	+	+	+
58	MRSA14	<i>S. aureus</i>	Blood	+	+	-	+	+	+	+	+
59	TRSA59	<i>S. aureus</i>	Wound	-	-	-	-	-	-	-	-
60	TRSA60	<i>S. aureus</i>	Wound	-	-	-	-	-	-	-	-
61	TRSE1	<i>S. epidermidis</i>	Blood	-	+	-	-	-	+	+	+
62	TRSE2	<i>S. epidermidis</i>	Blood	-	-	-	-	-	-	-	-
63	TRSE3	<i>S. epidermidis</i>	Urine	-	-	-	+++	-	-	-	+++
64	TRSE4	<i>S. epidermidis</i>	Wound	-	-	-	++	-	-	-	++
65	TRSE5	<i>S. epidermidis</i>	Blood	-	-	-	+++	-	-	-	+++
66	TRSE6	<i>S. epidermidis</i>	Urine	-	+++	-	+	-	+++	+++	+++
67	TRSE7	<i>S. epidermidis</i>	Urine	-	++	-	+++	-	++	++	+++

Table 6. (Continued)

No.	Isolate code	Strains name	Strains origin	Φtrsa 10	LysSA10	Φtrsa14	LysSA14	Φtrsa 15	LysSA15	LysSA52	Mixed I _{lysine} *
68	TRSE8	<i>S. epidermidis</i>	Wound	-	-	-	+	-	-	-	+
69	TRSE9	<i>S. epidermidis</i>	Wound	-	+	-	+	-	+	+	+
70	TRSE10	<i>S. epidermidis</i>	Urine	-	-	-	+	-	-	-	+
71	TRSE11	<i>S. epidermidis</i>	Urine	-	+	-	+	-	-	-	+
72	TRSE12	<i>S. epidermidis</i>	Blood	-	+	-	+	-	-	-	+
73	TRSE13	<i>S. epidermidis</i>	Blood	-	-	-	-	-	-	-	-
74	TRSE14	<i>S. epidermidis</i>	wound	-	-	-	-	-	-	-	-
75	TRSE15	<i>S. epidermidis</i>	Wound	-	+	-	-	-	+	+	+
76	TRSE16	<i>S. epidermidis</i>	Blood	-	-	-	-	-	-	-	-
77	TRSE17	<i>S. epidermidis</i>	Wound	-	-	-	+	-	-	-	+
78	TRSE18	<i>S. epidermidis</i>	Wound	-	+	-	+	-	+	+	+
79	TRSE19	<i>S. epidermidis</i>	Urine	-	-	-	+	-	-	-	+
80	TRSE20	<i>S. epidermidis</i>	Wound	-	-	-	+	-	-	-	+
81	TRSE21	<i>S. epidermidis</i>	Blood	-	+	-	-	-	+	+	+
82	TRSE22	<i>S. epidermidis</i>	Urine	-	++	-	-	-	++	-	+++
83	TRSE23	<i>S. epidermidis</i>	Wound	-	+	-	-	-	+	+	++
84	TRSE24	<i>S. epidermidis</i>	Wound	-	-	-	++	-	-	-	++
85	TRSE25	<i>S. epidermidis</i>	Urine	-	-	-	-	-	-	-	-
86	TRSH1	<i>S. haemolyticus</i>	Blood	-	+++	-	+++	-	+++	+++	+++
87	TRSH2	<i>S. haemolyticus</i>	Blood	-	-	-	-	-	-	-	-
88	TRSH3	<i>S. haemolyticus</i>	Blood	-	++	-	++	-	++	++	+++
Total number of positive out of 88				28	57	27	67	26	51	49	77

“+++”, very clear zone; “++”, moderate; “+”, Turbid; “-”, no clear zone at all, Tr.asp, Tracheal Aspirate; MRSA, Methicillin Resistance *S. aureus*

6.14. Biochemical Characterization of Endolysins

In the biochemical characterization of endolysin, the optimal conditions for each endolysin activity such as pH, temperature, and effects of divalent metal ions were evaluated. Among these, the temperature was one of the key factors affecting the bactericidal activity of endolysins. As shown in Figure 27, all of the four endolysins (LysSA10, LysSA14, LysSA15, and LysSA52) displayed high antibacterial activity at temperatures that ranged from 35 to 50°C. At these range of temperatures, they maintained

more than 80 % of their activity. However, their activities sharply decreased at or above 60°C (Figure 27).

Regarding the pH conditions, all the four endolysins works best at alkaline pH range with a maximum activity at pH 8.0 for LysSA10, LysSA14, and LysSA15. For LysSA52, the maximum activity was observed at a pH of 7.0. However, the activities of the four endolysins were markedly decreased at acidic pH (below 6.0) (Figure 28). The effects of addition of divalent metal cations was assessed by three different buffers containing calcium, magnesium, and zinc ions, which were added individually to each endolysin before quantifying their activity. The results showed that the addition of 1 mM of calcium and magnesium ions increased enzymatic activity by 2 to 10 % as compared to the control (Figure 29).

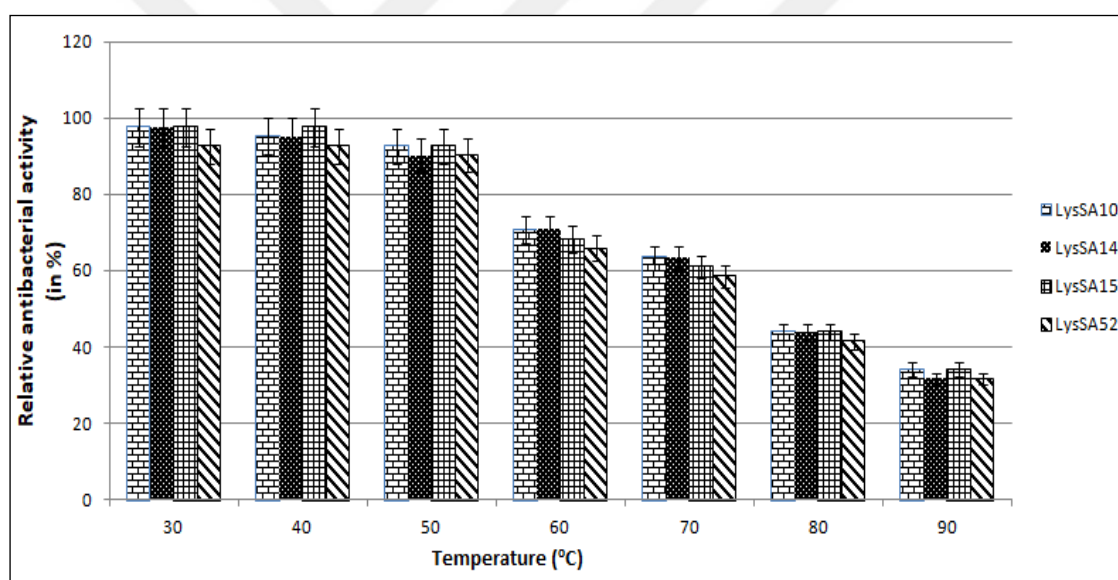


Figure 27. Temperature stability of LysSA10, LysSA14, LysSA15, and LysSA52 endolysins. The activity was determined by measuring of inhibition zones and expressing the results in percentage relative to control (non-heat treatment endolysin). Each column represents the mean of triplicate assays, and error bars indicate the standard deviation.

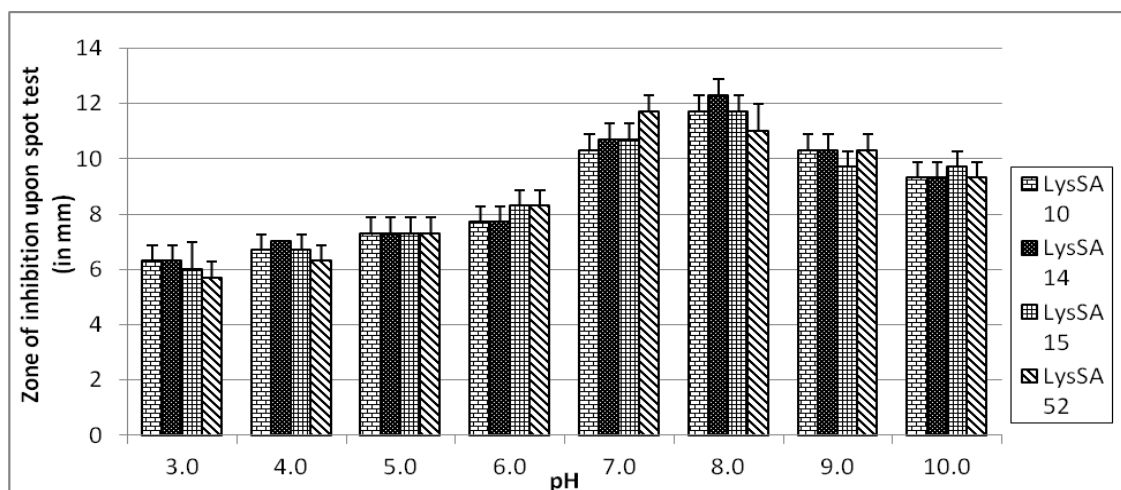


Figure 28. Influence of pH conditions on the bacterial activity of four endolysins (LysSA10, LysSA14, LysSA15, and LysSA52). The activity was determined by measuring of inhibition zones. Each column represents the mean of triplicate assays, and error bars indicate the standard deviation.

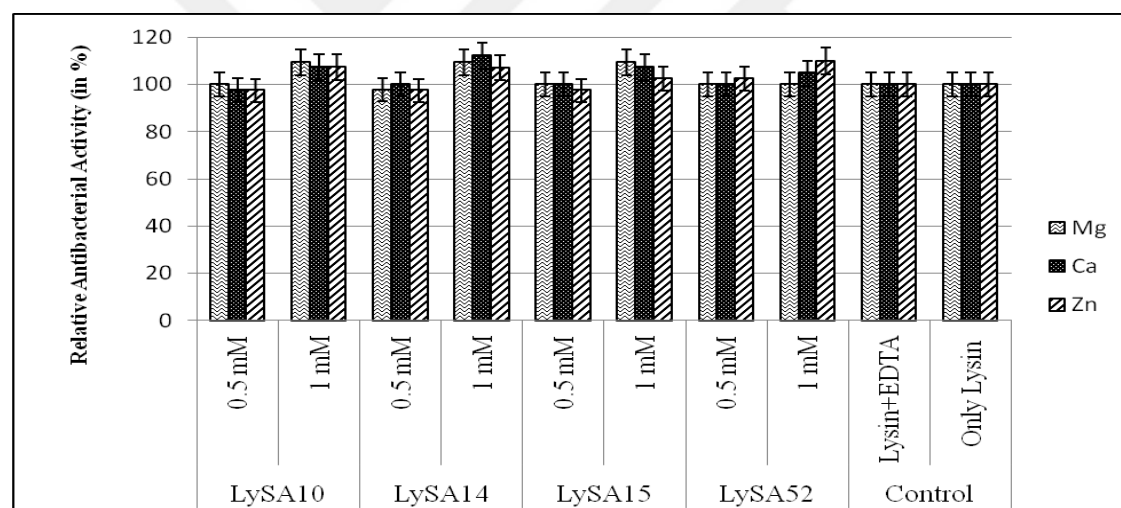


Figure 29. Effects of divalent metal cations (Mg^{2+} , Ca^{2+} , Zn^{2+}) on the lytic activity of the four endolysins. Each column represents the mean of results from triplicate assays, and error bars indicated the standard deviation.

6.15. Biofilm Removal and Inhibition Capacity of Endolysin

6.15.1. Biofilm Removal Assay Using Plate Staining Method

To see the biofilm removal capacity of endolysin using crystal violet assay, 48 h mature biofilms of *S. aureus* and *S. epidermidis* established in microtiter plates were treated with each endolysin and endolysin cocktail at three different concentrations (0.20 mg/mL, 0.30 mg/mL, and 0.50 mg/mL) for 12 h. Solubilization of crystal violet stain and subsequent measurement of OD_{595nm} allowed to obtain the quantitative information

between control and endolysin treated well. The data demonstrated that all endolysins treatment reduced biofilms of both *S. aureus* and *S. epidermidis* relative to the control group at all concentration tested as shown in Figure 30 A and B. In these graphs, it is a clear that the reduction was displayed in a dose-dependent response for each endolysin and was markedly sensitive to 0.50mg/mL concentration of each endolysin. At this particular concentration, a reduction of 61%, 57%, 56 %, 54%, and 47% of *S. aureus* biofilm after treatment with mixed lysins, LysSA10, LysSA14, LysSA15, and LysSA52, respectively was observed (Figure 27). In the *S. epidermidis* biofilm removal test, almost comparable results with *S. aureus* biofilm were identified (Figure 28). A one-way ANOVA indicated that LysSA10 and endolysin cocktail (mixed lysins) treatment showed a statistically significant change in biofilm disruptions in both strains (P-value < 0.05).

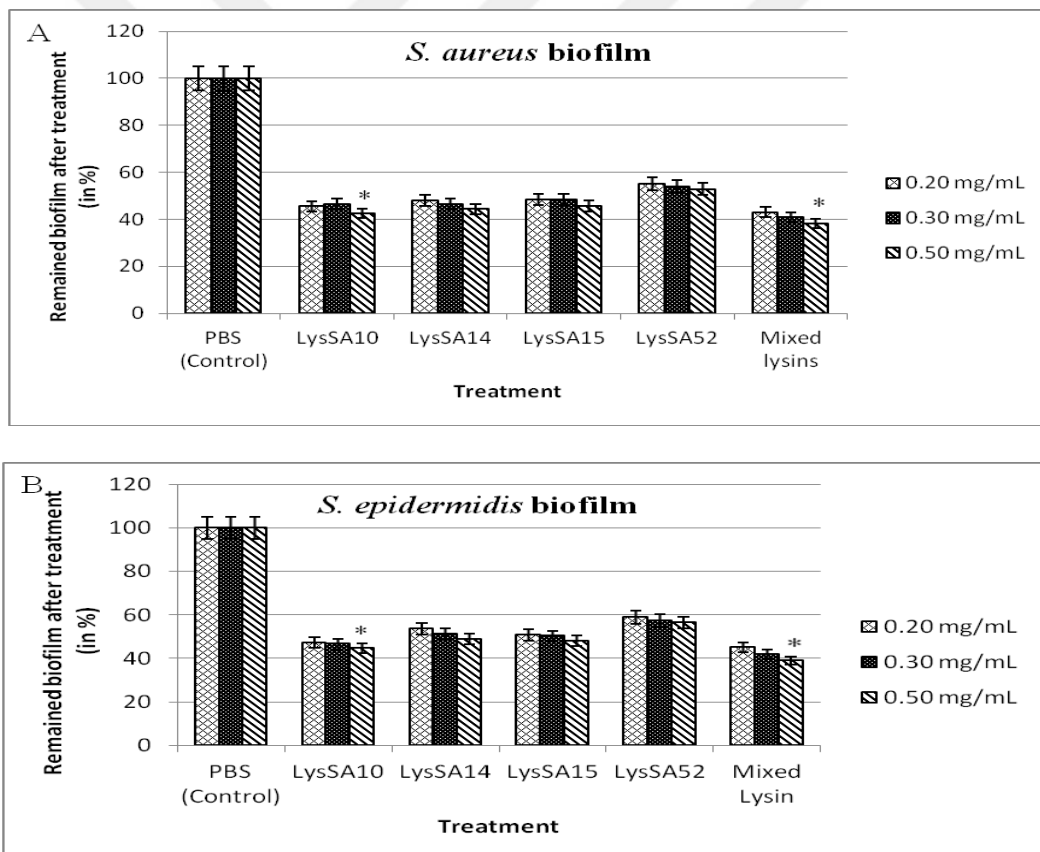


Figure 30. Biofilm degradation capacity of endolysins as determined by 96-well microtiter plate assay. A, mean percentage of *S. aureus* biofilm; B, mean percentage of *S. epidermidis* biofilm. Error bars represent the SD of three independent experiments. Significant differences marked by an asterisk (*) (two-tailed t-test, P < 0.05).

6.15.2 Prevention of Biofilm Formation Using Plate Staining Method

While all four endolysins can be shown to remove the established *S. aureus* and *S. epidermidis* as shown in Figure 30 A and B above, we tested if they could also prevent the initial formation of biofilms. For this, a microtiter plate containing a combination of 0.50 mg/mL of each endolysin and planktonic *S. aureus* or *S. epidermidis* in each well was incubated at 37°C for 48 h to determine if the bacterial attachment and subsequent biofilm formation would be prevented. Biofilms grown individually in the presence of all the four endolysins tested individually or in cocktail forms showed biofilm inhibition compared to the control group both in *S. aureus* and *S. epidermidis* (Figure 31). The maximum inhibition, which is about 57 %, was observed in wells containing mixed lysin. While the lysSA10, lysSA14, lysSA15, and lysSA52 were showed inhibition capacity of *S. aureus* biofilms formation by 54 %, 53 %, 53.5 %, and 48 % respectively (Figure 31). As clearly seen in the same graph of Figure 31 below, almost comparable *S. epidermidis* biofilms inhibitions were detected by all the four endolysins tested.

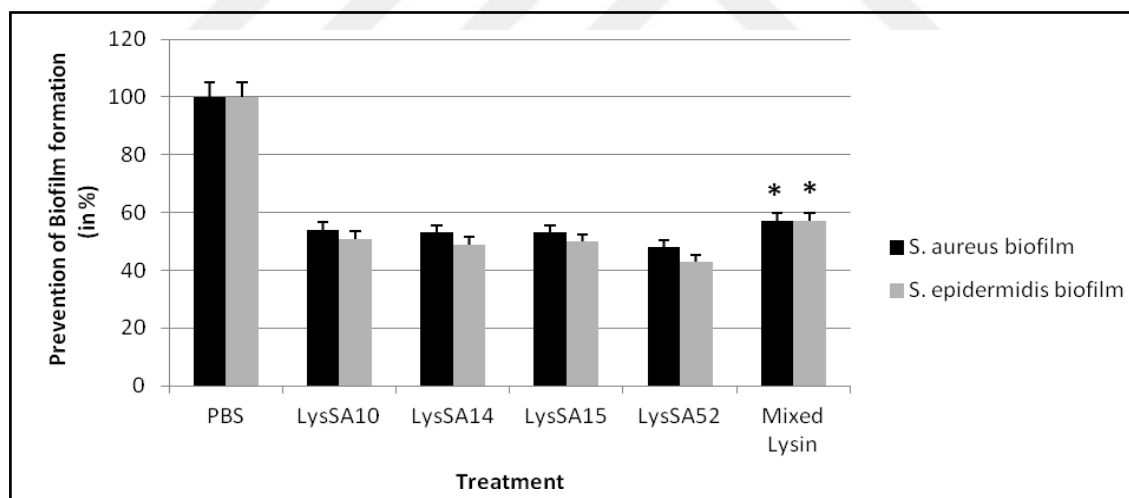


Figure 31. Effect of endolysins on biofilm formation by *S. aureus* and *S. epidermidis* as determined by 96-well microtiter plate assay. Bars represent mean percentage of biofilm. Error bars represent the SD of three independent experiments. Significant differences in values compared with control are marked by an asterisk (*) (two-tailed t-test, $P < 0.05$).

6.15.3. Biofilm Removal Assay from Catheter

S. aureus and *S. epidermidis* are among the most common microorganisms associated with biofilm formation on biomaterials including catheters. Therefore, we investigated

whether the endolysins produced in this study had anti-biofilm activity on catheter sections. For this, 0.50 mg/mL of each endolysin was used to treat 48 h old *S. aureus* and *S. epidermidis* biofilms. Following treatment for 12 h, a plate count assay was performed in order to evaluate the biofilm removal capacity. The results of viable cell counts are summarized in the bar chart in Figure 32. The maximum log reduction was observed in the endolysin cocktail, which was about 2.6 for *S. aureus* (Figure 32 A), and 2.5 for *S. epidermidis* (Figure 32 B). On the other hand, treatment with LysSA10, LysSA14, LysSA15, and LysSA52 resulted in 2.2, 1.9, 2.0, and 1.4 log reduction in *S. aureus* cell numbers, respectively. In the biofilm of *S. epidermidis*, about 1.9 log reduction was achieved after treated with LysSA10, LysSA14, and LysSA15 endolysins individually. LysSA52, on the other hand, decreased the cell number by 1.5 log units (Figure 32 B).

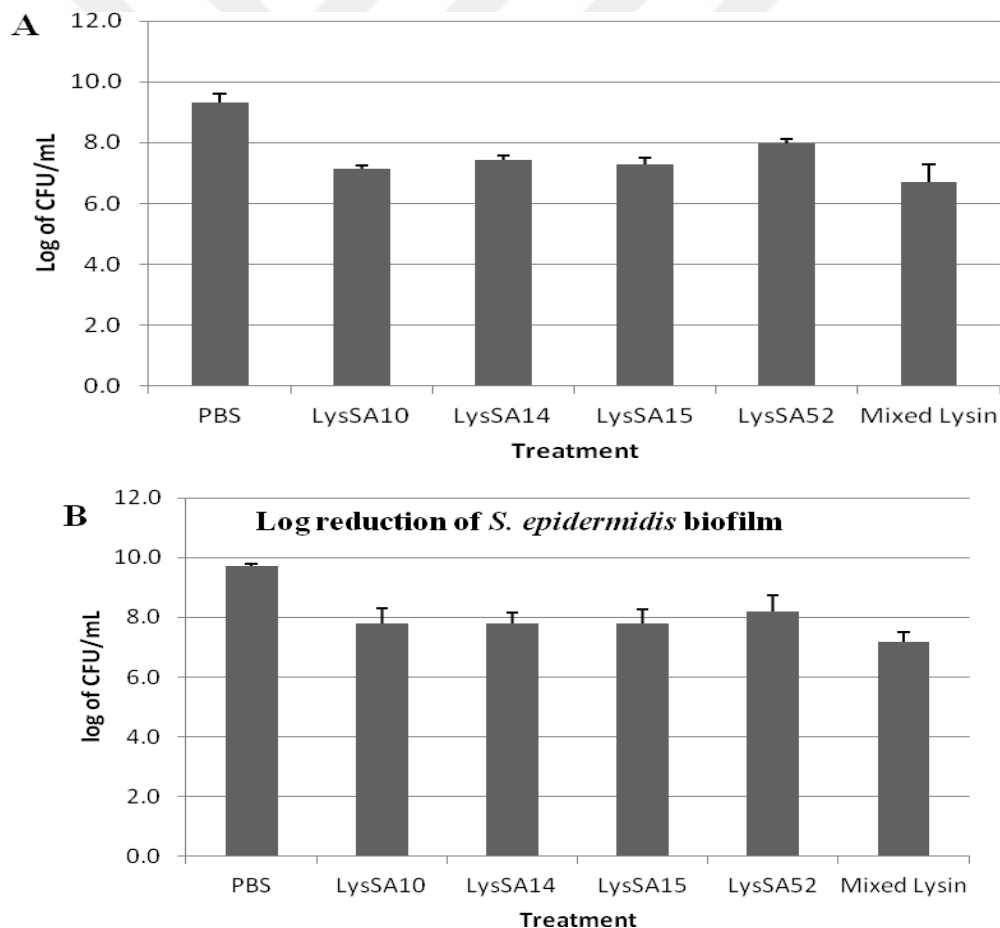


Figure 32. The ability of endolysins to remove 48 h old *S. aureus* (A) and *S. epidermidis* (B) from catheter sections as determined by viable cell count assay method. Error bars represent the SD of three independent experiments.

6.15.4. Prevention of Biofilm Formation on Foley Catheter

To examine whether the expressed endolysins are able to prevent biofilm formation on the catheter, a section of catheter was coated with 0.50 mg/mL of each endolysin for 1 h prior to the establishment of *S. aureus* and *S. epidermidis* biofilms. Following 48 h of incubations, catheter sections were washed with PBS and then biofilm inhibition capacity was enumerated using plate count assay and presented as log reduction in Figure 33 A and B. The growth of *S. aureus* on catheter sections coated with mixed lysin caused a 1.3-log cell number drop in biofilms, while LysSA14, LysSA15, and LysSA52 showed an approximate biofilm inhibition capacity of 1.1 log units (Figure 33 A). Similar results were observed for *S. epidermidis* biofilm inhibition (Figure 33 B).

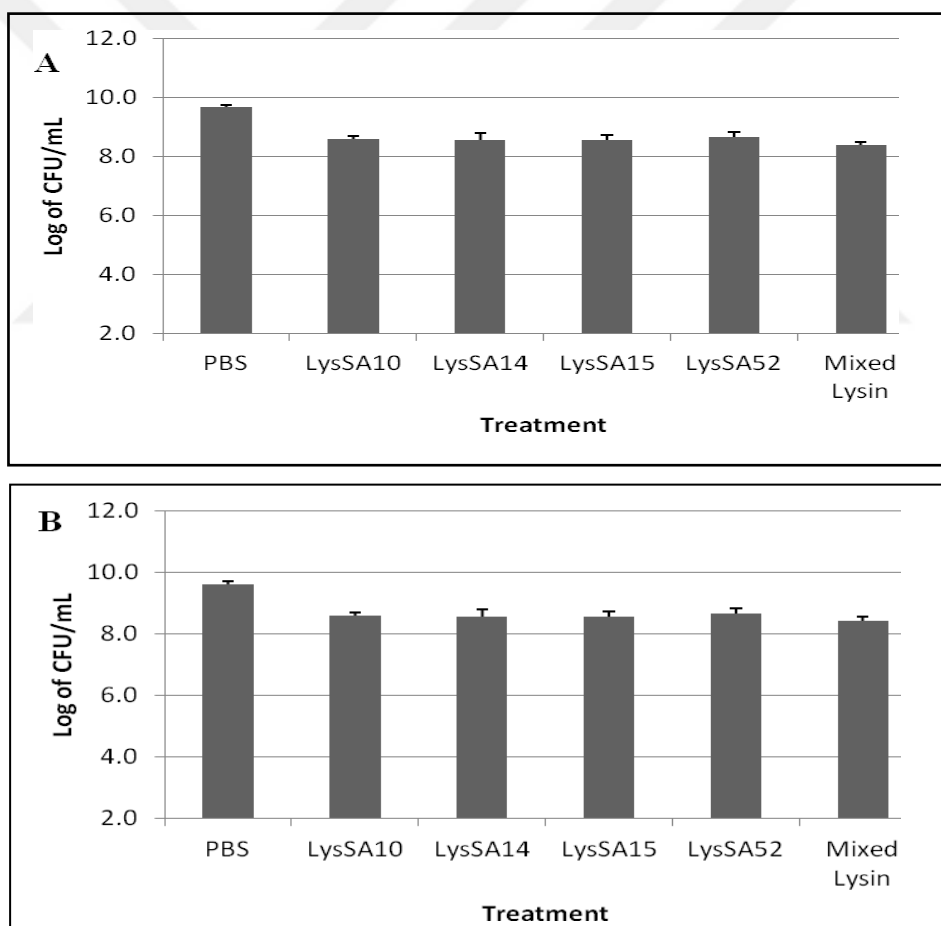


Figure 33. Effect of catheter coating with endolysin on the adherence of *S. aureus* (A) and *S. epidermidis* (B) to the catheter surface. The extent of prevention of biofilm formation was determined by enumerating CFU of treatment and control groups. Error bars represent the SD of three independent experiments.

6.16. Analysis of Biofilm Disruption Capacity of Endolysins by Scanning Electron Microscopy (SEM)

Endolysin treated and untreated *S. aureus* and *S. epidermidis* biofilms established on catheter sections and glass coupons were examined by SEM. The examination of the SEM images revealed that the endolysin treatment disrupted the biofilms of both *S. aureus* and *S. epidermidis* strains formed on glass coupons (Figure 34 and 35) and on the surfaces of catheter sections (Figure 36). Morphologically, the bacterial morphology was distorted, and only cell debris was observed after treatment.

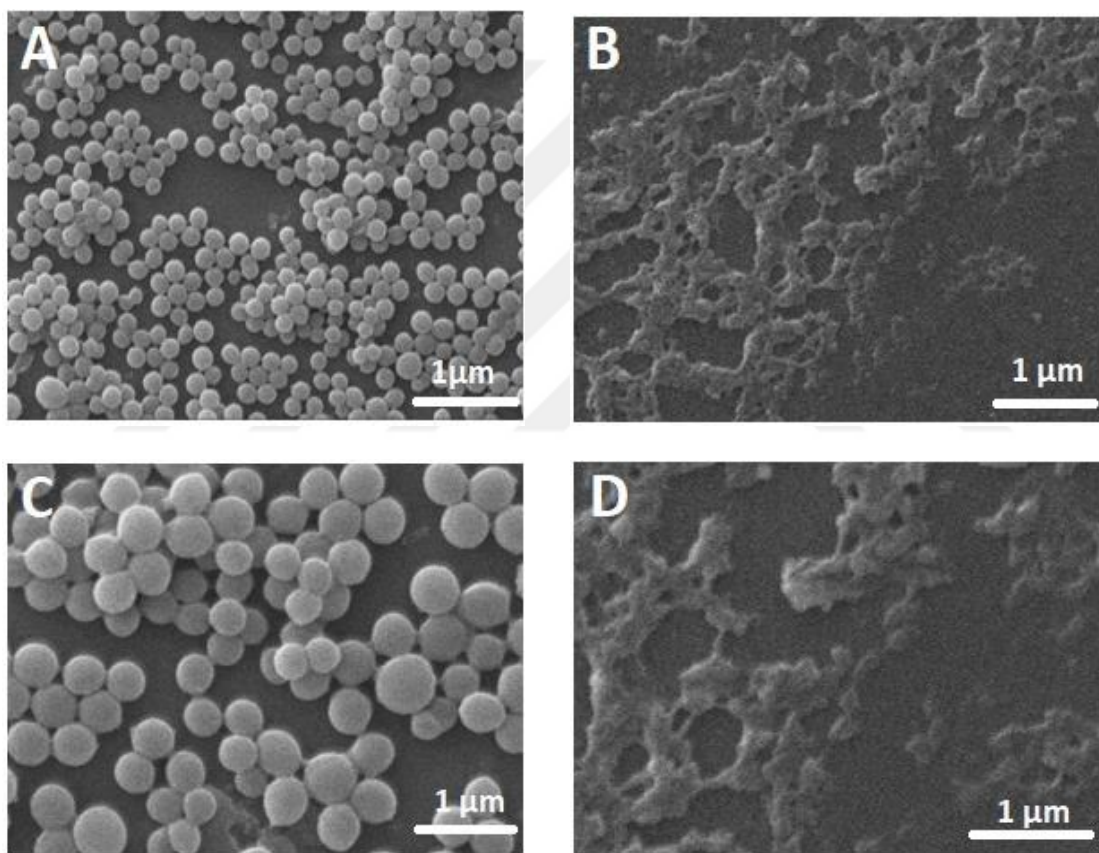


Figure 34. Scanning electron microscopy showing the effect of treatment with the endolysin cocktail on 48 h old biofilms of *S. aureus* TRSA8 established on glass coupons. The pictures on the left column are untreated biofilm imaged at different magnification (A = 10,000x; and C = 20,000x). The pictures on the right column (B and D) are post-treatment with endolysin (0.50 mg/mL), which were imaged at different magnifications (B, 10,000x; and D, 20,000x).

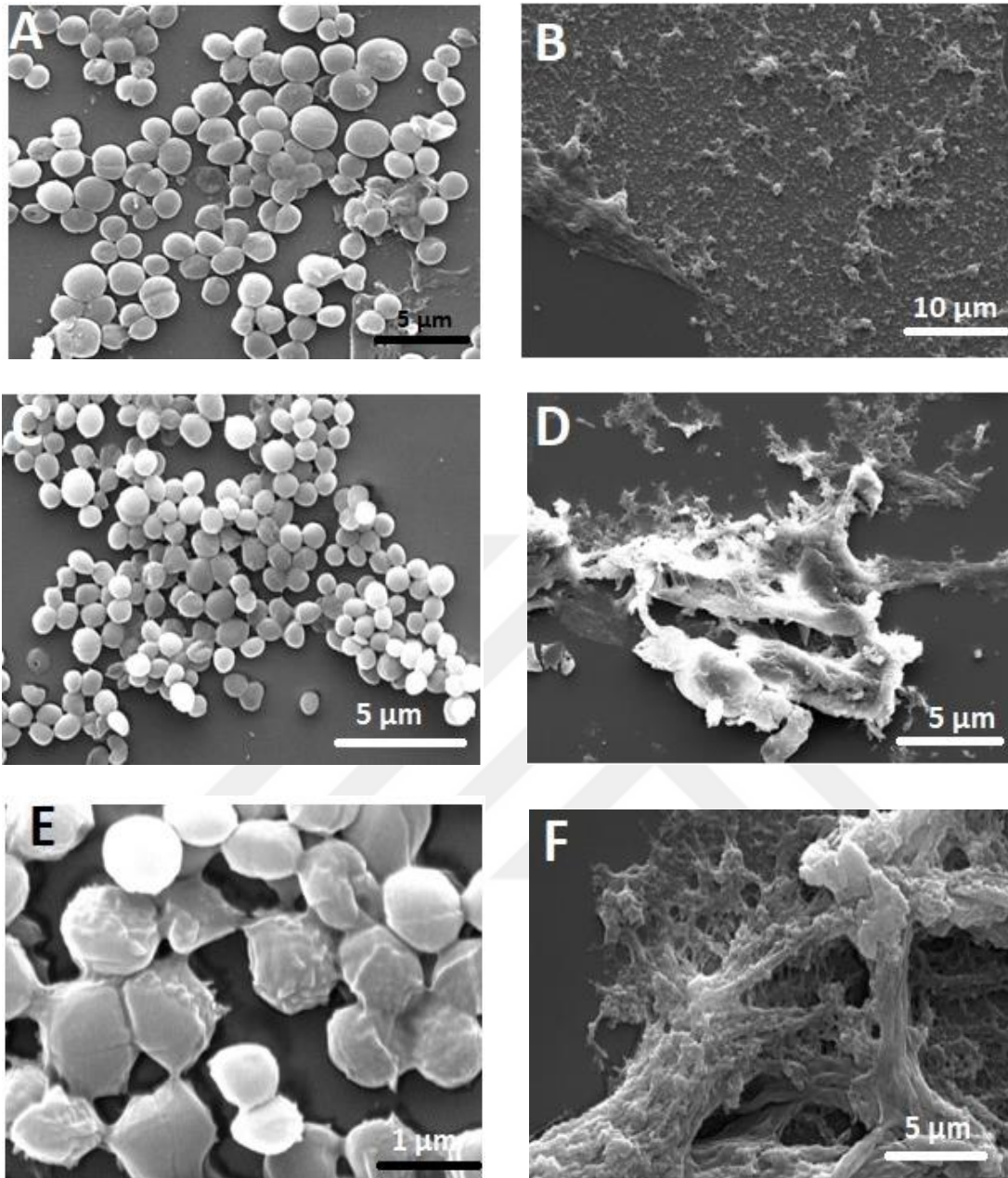


Figure 35. Scanning electron microscopy to show the effect of treatment with endolysin cocktail on 48 h old biofilms of *S. epidermidis* 30 (TRSE30) on coupons. The left side pictures (A, C, and E) are untreated biofilm imaged at different magnification (A, 16,000x; C, 16,000x; and E, 60,000x). The pictures on right-hand side are after endolysin treatment and imaged at different magnifications (B, 10,000x; D, 3,000x; and F, 20,000x).

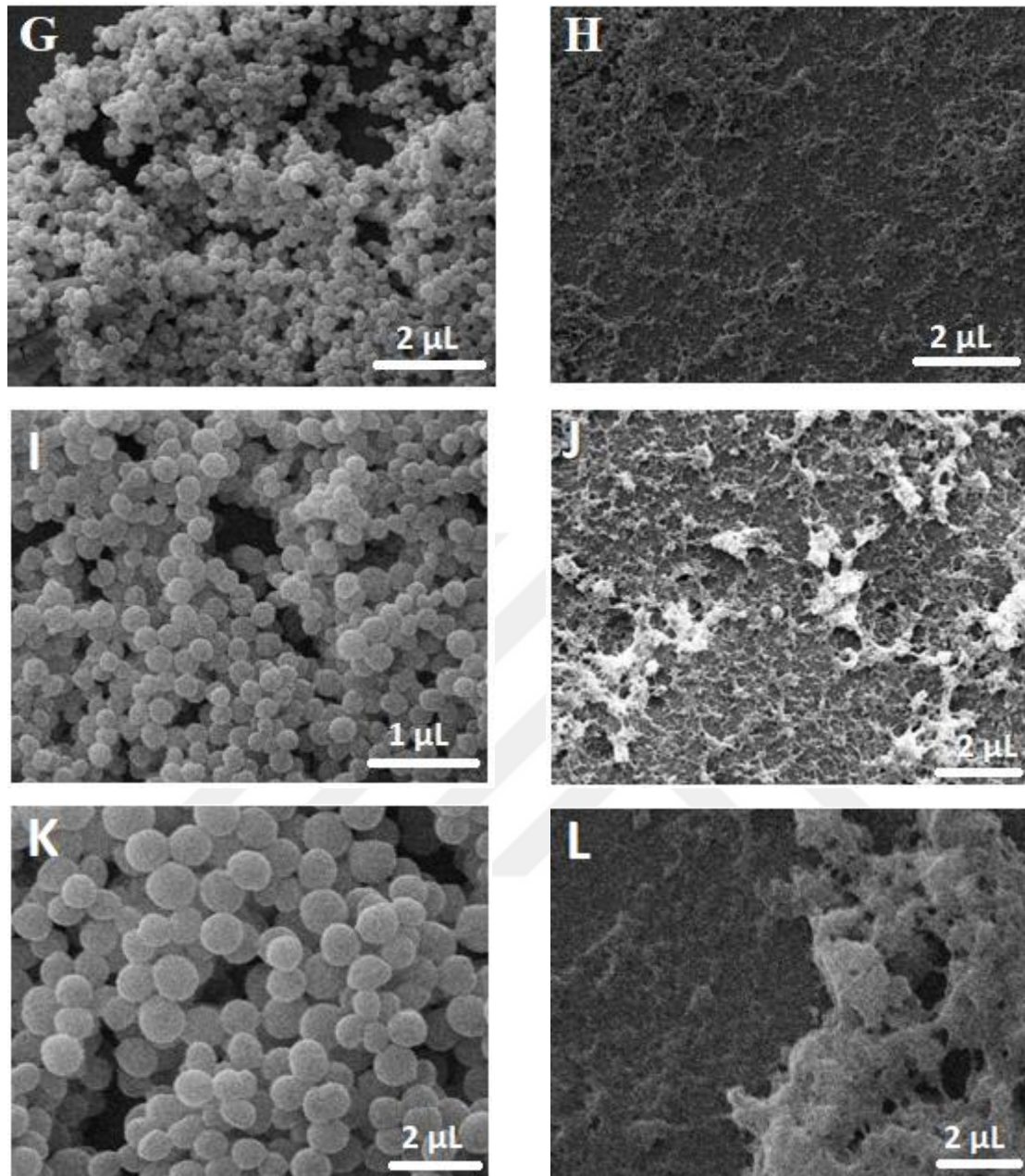


Figure 35. (Continued) scanning electron microscopy to show the effect of treatment with endolysin cocktail on 48 h old biofilms of *S. epidermidis* TRSE31 established on coupons. The pictures on the left (G, I and K) are untreated biofilm imaged at different magnifications (G, 5,000x; I, 10,000x, and K, 20,000x). The pictures on the right are after endolysin treatment and imaged at different magnifications (H, 15,000x and J, 10,000x; and, 10,000x).

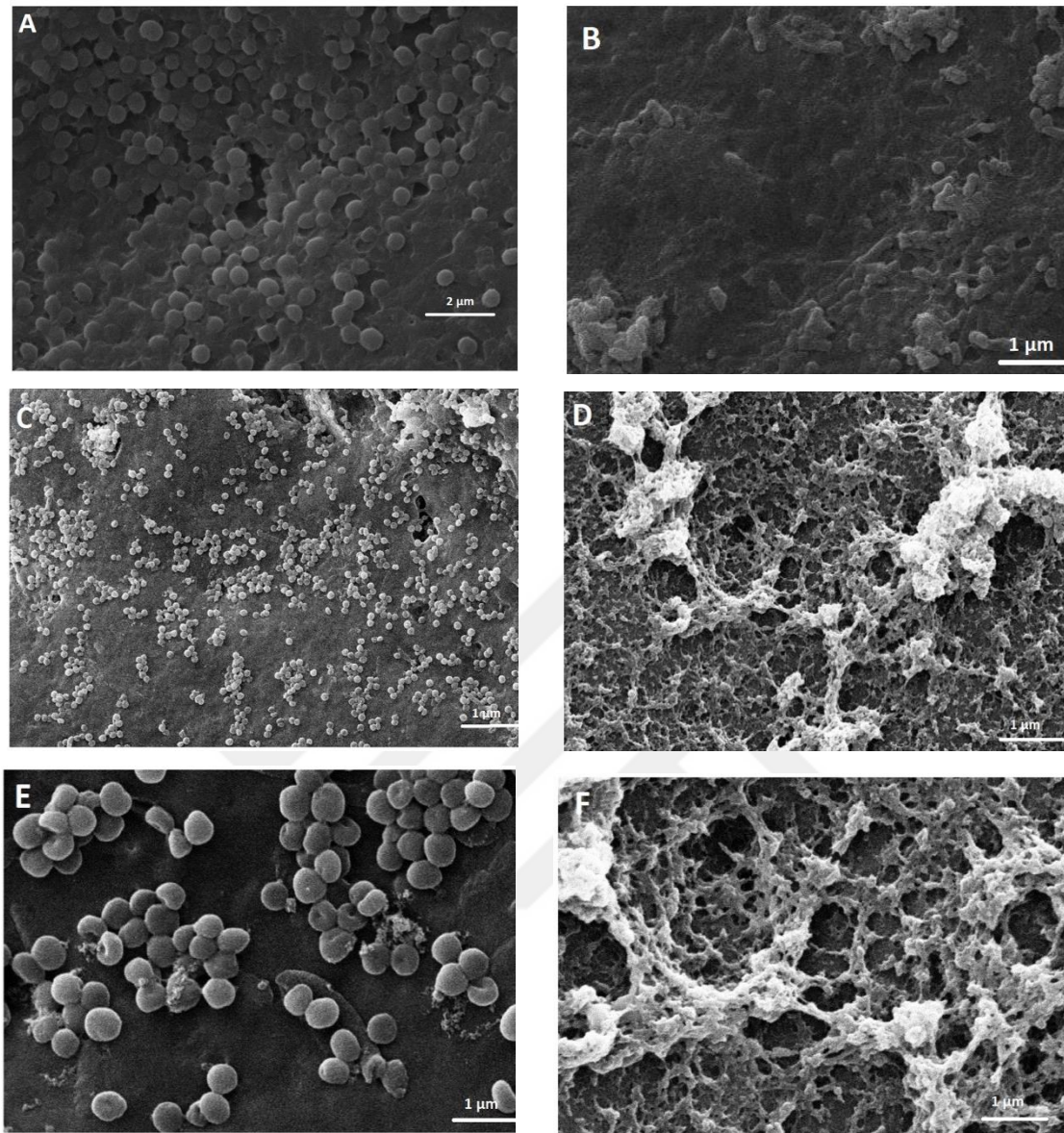


Figure 36. Scanning electron microscopy (SEM) images of treated and untreated *S. aureus* and *S. epidermidis* biofilms on catheter surfaces. Biofilms were formed on catheter sections and then treated with endolysin (0.50 mg/mL) for 12 h before analysis was performed with SEM. A, untreated *S. aureus* biofilm (10,000x); B, treated *S. aureus* biofilm (10,000x); C, untreated *S. epidermidis* biofilm (5,000x); D, treated *S. epidermidis* biofilm (10,000x); E, untreated *S. epidermidis* biofilm (20,000x); F, treated *S. epidermidis* biofilm (20,000x)

6.17. Cytotoxicity Assessment of Endolysin on Fibroblast Cells

To investigate the cytotoxicity of endolysins, a human fibroblast cell line was used. For this, confluent grown fibroblast cells were incubated at 37°C for 24 h in the presence of endolysins. The lethal effect of each endolysin was examined using the MTT assay method. The result of the MTT test is presented as percent survival in Figure 37 below. As can be seen in this figure, there is a little deviation in cell proliferation between endolysin treated and untreated cells.

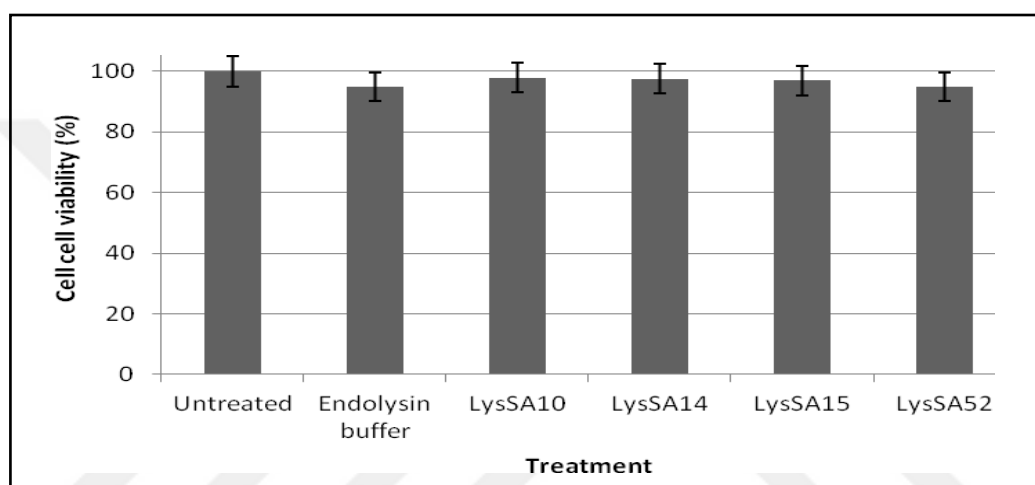


Figure 37. Assessment of cytotoxicity of four endolysins (LysSA10, LysSA14, LysSA15, and LysSA52) on human fibroblast cells. The viability of the fibroblast was determined using the MTT assay and the results were presented in percentage relative to non-treated fibroblast (100 %). Average and SD of triplicate experiments are shown here.

6.18. Bioinformatics Analysis.

6.18.1 Amino Acids Sequence Variation Analysis

The nucleic acid sequences of the four endolysins are translated into corresponding amino acid sequences using the MEGA 7 software. A total of 481 amino acids were obtained in each of the translated endolysin gene sequences. The resulted amino acid sequences of the four endolysins (LysSA10, LysSA14, LysSA15, and LysSA52) were compared using the Multiple Sequence Alignment program called ClustalW2 (Figure 38).

LysSA52	MQAKLTKKEFIEWLKTS	EGKQFNADLWYGFQCFDYANA	AWKVLFGLLKGLGAKDIPFAN	60
LysSA10	MQAKLTKKEFIEWLKTS	EGKQFNVDLWYGFQCFDYANA	GWKVLFGLLKGLGAKDIPFAN	60
LysSA14	MQAKQTKKEFIEWLKTS	EGKQFNVDLWYGFQCFDYANA	GWKVLFGLLKGLGAKDIPFAN	60
LysSA15	MQATLTKKEFIEWLKTS	EGKQFNVDLWYGFQCFDYANA	GWKVLFGLLKGLGAKDIPFAN	60
	***	. *****	. *****	. *****
LysSA52	NFDGLATVYQNTPDFL	AQPGDMVVFSGNYGAGYGH	VAWVIEATLIISLYMSRIGQAVAGL	120
LysSA10	NFDGLATVYQNTPDFL	AKPGDMVVFSGNYGAGYGH	VAWVIEATLDYIIVYEQN-WLGGGW	119
LysSA14	NFDGLATVYQNTPDFL	AKPGDMVVFSGNYGAGYGH	VAWVIEATLDYIIVYEQN-WLGGGW	119
LysSA15	NFDGLATVYQNTPDFL	AKPGDMVVFSGNYGAGYGH	VAWVIEATSDYIIVYEQN-WLGGGW	119
	*****	. *****	*****	: .:
LysSA52	TESNPA--GVGKKLQ	TTTCLRFPYVVYPPELQ	KRNSTHDSVQSPTQAPKKETAKPQPKA	178
LysSA10	TDRIEQPGWGW	EKVTRRQHALRFPYVVYPSYP	-KSETAPRSIQSPTQASKKETAKPQPKA	178
LysSA14	TDRIEQPGWGW	EKVTRRQHAYDFPMWFIRPNF	-KSETAPRSIQSPTQASKKETAKPQPKA	178
LysSA15	TDRIEQPGWGW	EKVTRRQHAYDFPMWFIRPNF	-KSETAPRSIQSPTQASKKETAKPQPKA	178
	*:	:	* * :	. ** . * :: * : *****
LysSA52	YVSGNTVMQALDESQ	VGWHTANQLGNKYYYGIE	VCQSMGADNATFLKNEQATFQECARLL	298
LysSA10	YVSGNTVMQALDESQ	VGWHTANQLGNKYYYGIE	VCQSMGADNATFLKNEQATFQECARLL	298
LysSA14	YVSGNTVMQALDESQ	VGWHTANQLGNKYYYGIE	VCQSMGADNATFLKNEQATFQECARLL	298
LysSA15	YVSGNTVMQALDESQ	VGWHTANQLGNKYYYGIE	VCQSMGADNATFLKNEQATFQECARLL	298
	*****	*****	*****	*****
LysSA52	KKWGLPANRNTIRL	HNEFTSTSCPHRSSV	LHTGFDPVTRGLLPEDKRLQLKDYFIKQIRA	358
LysSA10	KKWGLPANRNTIRL	HNEFTSTSCPHRSSV	LHTGFDPVTRGLLPEDKRLQLKDYFIKQIRA	358
LysSA14	KKWGLPANRNTIRL	HNEFTSTSCPHRSSV	LHTGFDPVTRGLLPEDKRLQLKDYFIKQIRA	358
LysSA15	KKWGLPANRNTIRL	HNEFTSTSCPHRSSV	LHTGFDPVTRGLLPEDKRLQLKDYFIKQIRA	358
	*****	*****	*****	*****
LysSA52	YMDGKIPVATVSND	SSASSNTVKPVASAWKRN	KYGTYYMEESARFTNGNQPITVRKVGPF	418
LysSA10	YMDGKIPVATVSNE	SSASSNTVKPVASAWKRN	KYGTYYMEESARFTNGNQPITVRKVGPF	418
LysSA14	YMDGKIPVATVSNE	SSASSNTVKPVASAWKRN	KYGTYYMEESARFTNGNQPITVRKVGPF	418
LysSA15	YMDGKIPVATVSNE	SSASSNTVKPVASAWKRN	KYGTYYMEESARFTNGNQPITVRKVGPF	418
	*****	. *****	*****	*****
LysSA52	LYCPVGYQFQPGGY	CDYTEVMLQDGHVWVGYT	WEGQRYLPIRTWNGSAPPNQILGDLWG	478
LysSA10	LSCPVGYYQFQPGGY	CDYTEVMLQDGHVWVGYT	WEGQRYLPIRTWNGSAPPNQILGDLWG	478
LysSA14	LSCPVGYYQFQPGGY	CDYTEVMLQDGHVWVGYT	WEGQRYLPIRTWNGSAPPNQILGDLWG	478
LysSA15	LSCPVGYYQFQPGGY	CDYTEVMLQDGHVWVGYT	WEGQRYLPIRTWNGSAPPNQILGDLWG	478
	* *****	*****	*****	*****
LysSA52	EIS*	481		
LysSA10	EIS*	481		
LysSA14	EIS*	481		
LysSA15	EIS*	481		

Figure 38. Amino acid sequence alignment of LysSA10, LysSA14, LysSA15, and LysSA52. “*” indicates identical amino acids

From the alignment results, the degree of similarity was obtained and the phylogenetic tree was constructed. As can be seen in Figure 39, LysSA52, which is derived

from commercial *S. aureus subsp. aureus* bacteriophage 52, is found in the same cluster with LysSA10 and they shared about 90.40 % similarity (Table 7). The LysSA52 also showed 88.73 % homology with LysSA14 and LysSA15. In general, the three endolysins (LysSA10, LysSA14, and LysSA15) derived from phages Φ trsa10, Φ trsa14, and Φ trsa15 isolated in this study, showed more than 97% amino acid sequence similarity to each other (Table 7).

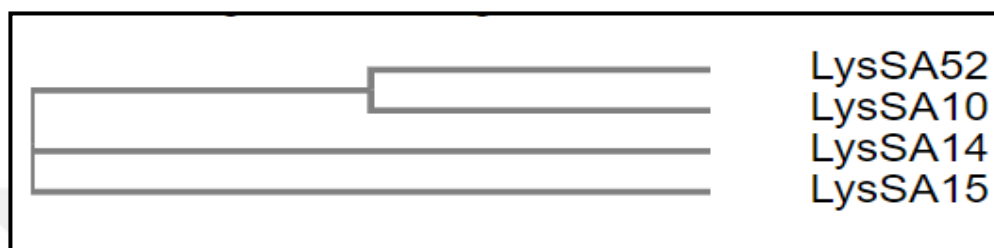


Figure 39. Neighbor-joining phylogenetic tree showing the relationship between the four endolysin protein sequences isolated from Φ trsa10, Φ trsa14, Φ trsa15, and *S. aureus subsp. aureus* bacteriophage 52. The phylogenetic tree was constructed based on multiple alignments of the protein sequences generated from ClustalW2

Table 7. Percent identity matrix of each endolysin obtained in this study.

Endolysin	LysSA52	LysSA10	LysSA14	LysSA15
LysSA52	100.00	90.40	88.73	88.73
LysSA10	90.40	100.00	97.51	97.51
LysSA14	88.73	97.51	100.00	99.17
LysSA15	88.73	97.51	99.17	100.00

6.18.2. Analysis of Modular Structures of Endolysins

In order to determine the modular structures of our newly identified endolysins, we analyzed the structures using the online software, SMART, and the results of the analysis indicated that all of the four endolysin proteins had three distinct domains: CHAP (cysteine, histidine-dependent) domain, amidase (Ami-2) domain, and SH3b domain (Figure 40). Of the total 481 amino acid of each endolysin (LysSA10, LysSA14, LysSA15, and LysSA52), amino acids 20 to 113 are involved in constituting CHAP (cysteine, histidine-dependent amidohydrolases /peptidases) catalytic domain, 138 to 338 amino

acids constitute a central amidase (Ami-2) domain, which also confers the lytic activity, and amino acids from 396 to 466 constitute the SH3b domain (Figure 40), which is thought to be involved in cell wall recognition and binding activity (166).

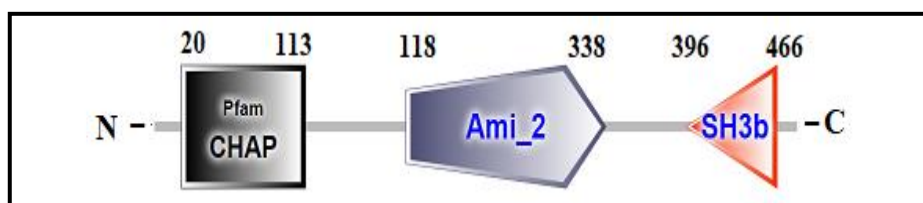


Figure 40. Domain organization of the four endolysins (LysSA10, LysSA14, LysSA15, and LysSA52) as displayed by SMART (<http://smart.embl-heidelberg.de/>) containing two catalytic domains (CHAP and Ami-2) and one cell wall binding domain (SH3b). Numbers indicate amino acid positions.

6.18.3. Structural Modeling

In addition to the most commonly used x-ray crystallography method for prediction of three-dimensional structures of proteins, another approach like homology modeling also has been reported (110, 136-138). In many cases, only one, enzymatically active domain of the endolysins was determined (110, 137, 139). In the present study, a homology or comparative modeling was performed to predict the three-dimensional structure of one catalytic domain (Ami-2) with 151 amino acids. In order to carry out this, the SWISS-MODEL was used. Template selection is the first criteria for homology modeling and based on the search results for the query sequence, we selected amidase-2 domain of LysGH15 (Protein Data Bank Id; 4ols), which previously was solved with by crystallography, as the template (110). The result of the modeling showed that all the four endolysins are similar to each other, and their enzymatic core is formed by a twisted, five-stranded β -sheet flanked by four helices linked through a loop region (Figure 41). In addition, one zinc cation is located at the center of the groove and interacts with different side chains.

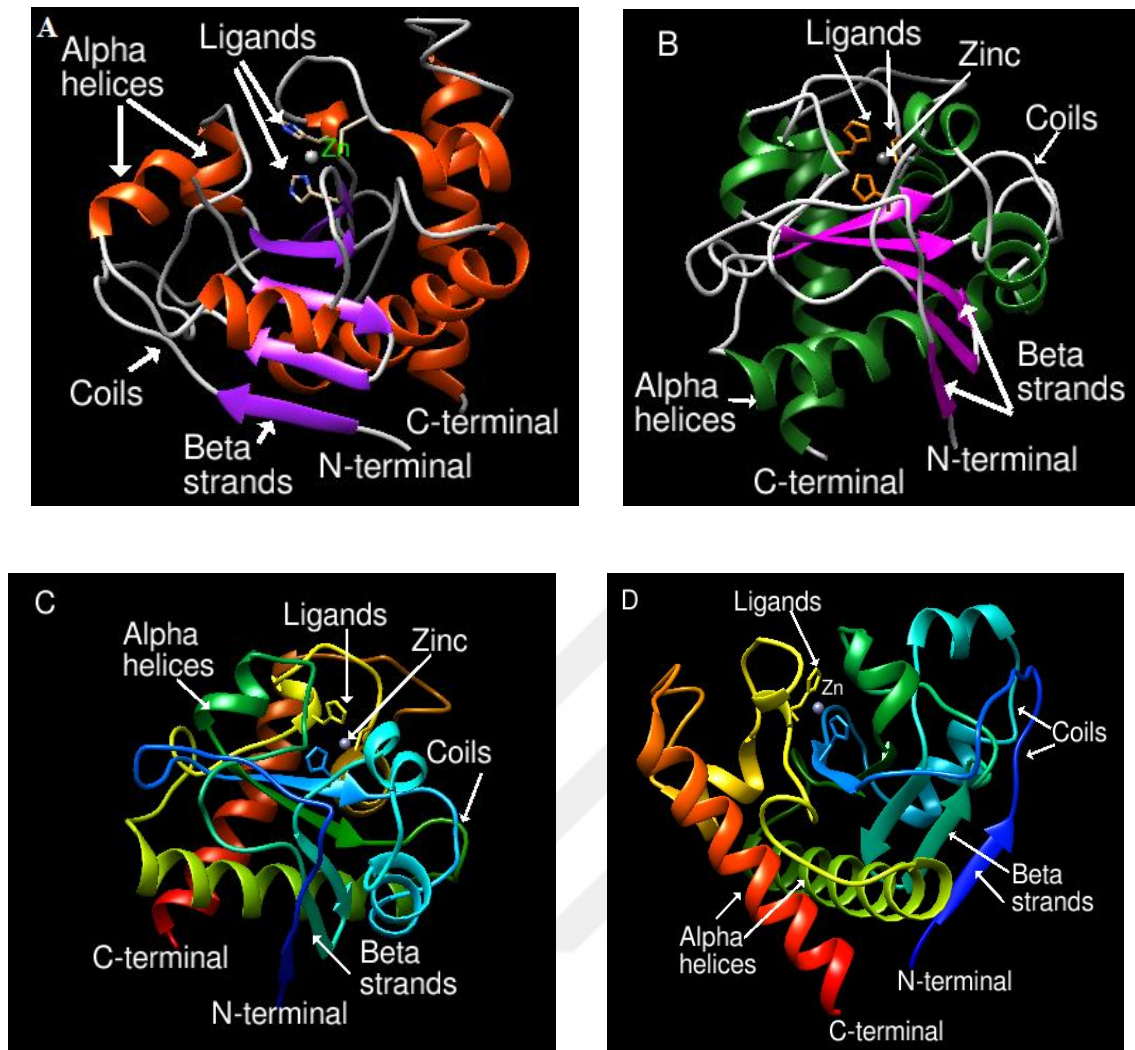


Figure 41. The predicted 3-D structures of endolysins using the SWISS-MODEL program available at <https://swissmodel.expasy.org/>. A, LysSA10; B, LysSA10; C, LysSA15; D, LysSA52. The Zn^{2+} ion in each endolysin is shown as a gray sphere.

7. DISCUSSION

Among coagulase positive *Staphylococci*, *S. aureus* is one of the most important human pathogens that produce local and systemic infections (140). *S. aureus* plays a major role in nosocomial infections. Difficulties in the treatment of these infections are reported due to the high rate of MRSA infections (141, 142). As an alternative to antibiotics, the use of phage endolysin has attracted the interest of scientists in combating pathogenic bacteria (7, 36, 93). In this study, we aimed to isolate and characterize new phages that can infect *S. aureus* and to produce its endolysin gene as a recombinant protein for combating staphylococcus strains. Initial attempts to isolate virulent phages from the environment were not successful. Due to the high prevalence of prophages in *S. aureus* genome (22), along with our sole interest in endolysin genes, use of virulent or temperate phages made no difference. We decided to isolate temperate phages (prophages) using the induction technique for our project.

Before induction of prophages from the genome of *S. aureus*, we screened for the presence of endolysin gene as a preliminary indicator of the availability of prophages by PCR using specific primers that we designed from *S. aureus* phage endolysins retrieved from the database. From the 60 chromosomal DNA of *S. aureus* screened for endolysin, only 17 were positive for presence endolysin genes (Figure 11). This result is very low since many strains of *S. aureus* harbor at least one or two prophages in its genome (22). The most probable reason for the small number or lack of endolysin positive *S. aureus* strains could be due to the primer set we used. Inclusion of different primer sets might increase the number. PCR positive strains were subsequently exposed to mitomycin C for the induction of prophages.

Using the induction technique, 7 functional phages were initially obtained by the spot test method (Figure 12 A and B), which was further verified by the plaque assay method (Figure 12 C and D) since clear zones can also be produced by bacteriocin (132). In the rest of the 10 lysates, no lytic phages were observed. This might be explained by inefficient induction of the culture and/or very low concentration of the phages that cannot infect host strains, or lack of appropriate hosts. In the phage positive lysates, plaques were obtained after incubation of plates at 37°C overnight. The sizes of the plaques for all the seven phages (Φ trsa10, Φ trsa14, Φ trsa15, Φ trsa205, Φ trsa207, Φ trsa220, and Φ trsa222) were small and ranged from 0.2 to 1 mm. Morphologically the newly identified phages

were investigated using transmission electron microscopy. The TEM analysis revealed that all seven phages have long tails with isometric and icosahedral heads (Figure 13). The isometric and icosahedral heads of Φ trsa10, Φ trsa14, and Φ trsa15 were measured and found to be 44.3 ± 1.0 , 43.1 ± 2.3 and 59.3 ± 0.3 nm in diameters, respectively (Table 4). These phages also had a non-contractile long tail, measuring 171.0 ± 2.8 , 213.9 ± 1.0 , and 156.2 ± 1.6 nm respectively (Table 4). Morphology is one of the most frequently used methods for the classification of bacteriophages. According to their morphological characteristics and based on the guidelines of the International Committee on Taxonomy of Viruses (143), all of the seven phages including Φ trsa10, Φ trsa14, and Φ trsa15, belong to *Siphoviridae* family in the order *Caudovirales* (Figure 13). Furthermore, as they have long tails, they belong to type B phages in Bradley's classification (132). More than 95 % of the phages reported so far in the literature belong to *Caudovirales* (144). About 60 % these phages have long and flexible tails and are assigned to the family of *Siphoviridae* (83). Therefore, all of the phages identified in the current study are categorized in *Siphoviridae* family.

With respect to host range, the seven newly isolated phages were further investigated for their lytic activity against all bacterial isolates (Table 6), in order to select the most virulent lytic phages. From these, three phages Φ trsa10, Φ trsa14, and Φ trsa15 had broad host ranges with lytic activities against 28 (46.6 %), 27 (45 %), and 26 (43.3 %) of the 60 *S. aureus* strains tested, respectively, were selected (Figure 14). As compared to the most known *S. aureus* phage K, which has a broad lytic activity (145), our phages have lower host ranges. The low lytic activity in our case may be associated with lysogenicity, which required induction for lytic activity (145) or with superinfection immunity by resident prophages (80), as this was also confirmed in the present study, in which, the addition of Φ trsa10, Φ trsa14, and Φ trsa15 did not infect their respective host in which they were originated. The host range differences of phages could be related to bacterial receptor mutation that can prevent the adsorption of phages (146) or through restriction modification system by which bacterial cells prevent foreign DNA from replicating, in particular, phage DNA leading to phage resistance (147).

To understand the growth of phage Φ trsa10, Φ trsa14, and Φ trsa15, the one-step growth curve was performed as the estimation of the burst size and burst period in the life cycle of phages has a great importance in phage therapy (85). The latent period, the timing

of phage-induced host cell lysis, which is typically under the control of holin, and any mutation in holin can significantly modify the timing of the latent period (148). According to the one step-growth curve experiments, the latent periods of phage Φ trsa10 and Φ trsa14 were found to be 20 min, followed by a 30 min rise period, and a burst size of 29 and 39 PFU per infected cell, respectively (Figure 15 A and B), whereas phage Φ trsa15 showed 25 min of latent period and burst size of 21 PFU per infected cell (Figure 15 C). Large burst size is considered as one of the major characteristics of effective phage that can be used as an antibacterial agent; because burst size is closely related to phage propagation (149) and can increase the initial dose of the phages several folds in short period of time (85, 150).

With regard to phage genome study, DNA was purified from phage Φ trsa10, Φ trsa14, and Φ trsa15 and in order to determine the approximate genome size of each phage, DNA was digested with four different restriction enzymes (Figure 17). After digestions with the above enzymes the molecular size of the genomic DNA of the three phages were estimated. The sum of the fragments resulted in the approximate genomic size of 37, 36 and 38 kb for Φ trsa10, Φ trsa14 and Φ trsa15, respectively. These results are close to the genome size of *Siphoviridae* family of phages established by Kwan and co-workers previously (151), who used genome size to classify the staphylococcal phages into different categories. For this, they conducted a comparative study on 27 genomes derived from *S. aureus* phage families (*Siphoviridae*, *Podoviridae*, and *Myoviridae*) and analyzed by a variety of bioinformatics tools, and then classified staphylococcal phages into three categories or classes based on their genome sizes (class I: < 20 kb; class II \approx 40 kb, class III > 125 kb). These categories were compared with morphological classification and similar results were found in which *Podoviridae* harboring the smallest genomes (class I), *Siphoviridae* containing medium size genome (class II), and *Myoviridae* harbors the largest ones (class III). This classification is in line with the estimation of our phage genome size since our phages belongs to *Siphoviridae* family.

Even though using of temperate phages as a whole have limited therapeutic potential (152), they each carry a gene encoding an essential enzyme called endolysin, with the ability to degrade bacterial cell wall when added exogenously (7, 103, 115). Thus, these proteins could be produced recombinantly and used as effective therapeutic agents against staphylococcal infections. However, in many cases, production of recombinant proteins

including phage endolysin faces many challenges such as misfolding of protein, poor solubility due to the formation of inclusion bodies, and purification difficulties (153-155). In order to overcome many of these challenges, gene fusion technologies have been developed to improve protein expression. Among these, pET SUMO plasmid (Figure 10), which is a cloning and at the same time expression vector, was developed to improve folding and solubility of target proteins (153). Considering these advantage, we selected this vector for cloning and expression of endolysin genes.

In the current study, a total of four endolysins genes (*LysSA10*, *LysSA14*, *LysSA15*, and *LysSA52*) having 1446 bp (Figure 18) were amplified from phage genome and cloned into pET SUMO expression vector successfully. The need to obtain the recombinant protein in the soluble fraction is of great importance, which is influenced by the expression system and induction temperature (156). Because of this, expression of cloned endolysin was conducted in *E. coli* BL 21 (DE3) at two different induction temperatures (37°C and 20°C). Following this, pellet and supernatant fractions were tested by SDS-PAGE. During induction at 37°C, the recombinant proteins were present in insoluble fractions or inclusion bodies (Figure 22 B). However, when the culture temperature was reduced to 20°C, the recombinant protein started to be found in the soluble fractions (Figure 23). This observation is supported by previous reports which showed that the low temperature reduces the formation of inclusion bodies (112, 157).

The SUMO (small ubiquitin-related modifier) fusion in the pET SUMO vector comprised of 100 amino acids has a hydrophobic core and hydrophilic surface; this characteristic makes it highly soluble (158). In addition to the low temperature, the SUMO fusion in the plasmid vector may also contribute to the solubility of our proteins. With this system, various bioactive peptides have been expressed as SUMO fusion proteins including but not limited to Brazzein, an edible fruit protein used as commercial sweetener (159), SARS-CoV (severe acute respiratory syndrome coronavirus) proteins (160), and human epidermal growth factor (hEGF) (161). In contrast to these, application of the SUMO fusion strategy to antimicrobial recombinant proteins has not been widely reported. Furthermore, to the best of our knowledge, this is the first report in cloning and expression of endolysin in this particular vector.

After expression, the purification approaches of proteins are necessary for continued structural and functional studies along with other applications. Affinity, hydrophobic

interaction, ion exchange, expanded bed adsorption, and size exclusion/gel filtrations are among the most commonly available techniques of the chromatographic purification system. The presence of his-tag (histidine-tag) in the SUMO fusion facilitates purification through affinity chromatography (153, 161). We tried to purify the crude lysate of expressed endolysins using Nickel-nitrilotriacetic acid (Ni-NTA) affinity chromatography. Though we obtained greater purity with less yield for LysSA10 (Figure 25 A), only partial purification was attained for LysSA14, LysSA15 and LysSA52 as shown in Figure 25 B and C. The reason for the appearance of non-specific bands on SDS-PAGE after purification may be due to the high salt or imidazole concentration that we have used. Careful choice of purification technique and an extensive phase of optimization are necessary to obtain satisfactory yields of the pure active enzymes (162); however, due to constraints of purification materials during this study, no further optimization was performed.

Currently, the demand for recombinant proteins has increased because of utilisation in various sectors such as healthcare, agriculture, food industry and others (86). Considering this, the presently produced endolysins (LysSA10, LysSA14, LysSA15, and LysSA52) tested for their biological activity. Both crude lysate and purified endolysin protein were used in activity test. The crude lysate prepared from *E. coli* BL21 cells harboring recombinant plasmids (endolysin containing plasmid) were exposed to exponential cultures of indicator strains resulted in the formation of clear zone (Figure 26). In contrast to this, no clear zone was formed upon spotting of lysate prepared from *E. coli* harboring plasmid without endolysin. This clearly demonstrated that the bacterial cells were lysed by the phage endolysins. Similar endolysin lytic activity test was reported in previous studies (26, 125, 163).

A significant activity loss was detected for purified or partially purified endolysins as compared to the crude lysate endolysin extracts. Similar results were also reported in a previous study (163) that described the purification of enzymes resulted in considerable activity loss. Certain reagents that have been used in purification procedure may impair the structure and thus, the activity of the protein of interest. In one study conducted by Fenton and colleagues (135), the use of NaCl at a final concentration of 300 mM greatly decreased the activity of endolysin. In our case, even a higher concentration of NaCl (500 mM) was applied in the elution buffer, and so this could be one factor for the partial activity loss of

our protein. In another study, the presence of high imidazole interfered with protein activity by forming aggregates (164). This could be another possible reason for the activity loss in our purified endolysins as we have used 500 mM imidazole in the elution buffer. Sometimes the N-terminal 6x His-tag sequence of the fusion protein has been shown to interfere with folding (165); which may, in turn, reduce the catalytic activity of the CHAP domain of endolysin.

Because the activities of several staphylococcal endolysins may or may not be enhanced by the addition of divalent metal ions such as calcium, magnesium, zinc and others were reported (110, 133-135), we examined the lytic activity of all of the four endolysins in the presence or absence of metal cations (Mg^{2+} , Ca^{2+} and Zn^{2+}). The analysis of this determinations indicated that addition of calcium or magnesium cations increases the lysine activity by 5 to 10 % as compared to control (Figure 29). The pH test for LysSA10, LysSA14, LysSA15, and LysSA52 analysis showed that all of the four endolysins were stable at a broad pH range (4.0 to 9.0) which is a desirable feature required for promising antibacterial agents. Optimal pH for LysSA10 and LysSA14 was found to be around 8.0, while for LysSA15 and LysSA52 was found to be around 7.0 (Figure 28). Heat sensitivity test of the four endolysins showed that all of them retained high activity (relative antibacterial activity > 90 %) against *S. aureus* at 60°C (Figure 27). Compared to some previously reported staphylococcal phage endolysin proteins (115), the endolysins identified in this study had a broader range of pH and thermostability.

The presence of one or two enzymatically active domains and one cell wall binding domain was reported for endolysins. Like many other staphylococcal endolysins described previously (8, 85, 115), the four endolysins identified in this study displayed three distinct domains: namely an N-terminal CHAP (Cysteine, histidine-dependent amidohydrolases/peptidases) domain, which has hydrolytic function, Ami-2 (N-acetylmuramoyl-L-alanine amidase) domain, which has also hydrolytic functions, and C-terminal SH3b domain, which is used for substrate recognition, were identified (Figure 40). In contrast to our endolysins, there are reports of staphylococcal endolysins with two domains. For instance, the endolysin of phage p68, Lys16, lacks the central N-acetylmuramoyl-L-alanine amidase domain (109).

The lytic spectrum of each endolysin produced in this study (LysSA10, LysSA14, LysSA15, and LysSA52) was evaluated by the spot assay method. Based on this assay, all

endolysins were found to be biologically active against a wide range of clinical *Staphylococcus* species including *S. aureus*, MRSA, *S. epidermidis*, and *S. haemolyticus* strains; whereas parental phages (Φ trsa10, Φ trsa14, and Φ trsa52) had antibacterial activity against only some of the *S. aureus* strains (Table 6). The results clearly showed that the host range of each endolysin was significantly broader than that of their respective parent phage (Table 6). This is in agreement with previous reports that described phage endolysin displayed a broader range of activity than the parent phages (8, 84). The differences for the host range between the endolysins and the parent phages are largely due to variability in phage receptor molecules on the staphylococcal cell surface, which is crucial for initial attachment during infection. In contrast to this, the phage endolysin have the advantage of targeting a part of the bacterial cell common to the entire genus *Staphylococcus* (167). Thus, these properties support the superior therapeutic potential of endolysins compared to whole phages.

Among the four endolysins, LysSA14 was more potent than LysSA10, LysSA15, and LysSA52 (Table 6). The potency against staphylococcal isolates increased when the combinations of the four enzymes applied. From a total of 88 staphylococcal strains tested, 78 (88.6 %) strains were at least sensitive to one of the four endolysins. However, they did not show any activity against other bacterial species including *Streptococcus spp.* and *E. coli*. This demonstrated that the newly identified endolysin in the present study had a broad spectrum within the *Staphylococcus* genus but no other bacterial species. This remarkable feature of endolysins has been also extended against staphylococcal biofilms in the present study.

In this study, the potential of LysSA10, LysSA14, LysSA15, and LysSA52 as a therapeutic agent for biofilm-associated *S. aureus* and *S. epidermidis* infections were evaluated. We considered that one of the valuable characteristics of the four endolysins was that they are effective against both *S. aureus* and *S. epidermis* biofilms because these types of bacteria are far more difficult to eradicate than their free-living (planktonic) counterparts (1, 168, 169). Different studies demonstrated biofilm removal ability of phage endolysins. Endolysin derived from phage phi11 hydrolyzed *S. aureus* biofilm established on polystyrene surface after 2 h treatment at 37°C (16). Similarly, endolysin SAL-2 derived from *S. aureus* phage SAP-2 eliminated *S. aureus* biofilms established in a microtiter well (84). Also, in another recent report, an endolysin, LysH5, showed

significant removal of *S. aureus* biofilms after 12 h treatments (110). Likewise, the newly identified endolysins in this study were also evaluated for their biofilm removal as well as biofilm inhibition capacity using crystal violet assay, plate count assay, and scanning electron microscopy.

his indicated that endolysin SAL-2 had a broader spectrum of activity within the *Staphylococcus* genus than bacteriophage SAP-2.

here's bacteriophage SAP-2 had antibacterial activity against only some *S. aureus* strains (Table 1)

For the biofilm established and treated in microtiter plates, the biofilm removal capacity was quantified by crystal violet assay. In this assay, we found that biofilms of both *S. aureus* and *S. epidermidis* were reduced in all tested concentration of each endolysin as compared to the control and the reduction was displayed in dose-dependent manner for each endolysin and significant removal of biofilm at 0.50 mg/mL was observed (Figure 30). At this particular concentration, treatments of both *S. aureus* and *S. epidermidis* biofilms reduced significantly by LysSA10 and endolysin cocktails, suggesting that these endolysins have a good potential in controlling biofilm infections caused by *S. aureus* and *S. epidermidis*. The removal activity of endolysins may be affecting individual sessile cells in the *S. aureus* biofilms. Similar biofilm removal activities have been reported in endolysin SAL-2 (84) and lysostaphin (127).

The explanation for the wider activity of the endolysin cocktail could be that these endolysins may have different cleavage sites on the peptidoglycan, as previously described that the catalytic domains of endolysins illustrate a large diversity and different chemical bonds of peptidoglycan are targeted (7). Eventhough there are two catalytic domains in the N-terminal of many staphylococcal endolysins, one might be dominant over the other. For instance, deletion analysis of 2638A endolysin derived from staphylococcal phage 2638A indicated that the amidase (Ami-2) domain confers most of the lytic activity over the other N-terminal peptidase (CHAP) domain of the same endolysin (166). In another study, maximum activity of antibacterial and antibiofilm properties have been reported with the combined action of endopeptidase and amidase domains of endolysins (16).

Since treatment of established biofilms of *S. aureus* and *S. epidermidis* by each endolysins exhibited reduction, we also determined the preventive capacity of biofilm formation. In this regard, the microtiter plate staining assay confirmed the reduction of biofilm growth in endolysin treated wells compared to the control setting (Figure 31). In this assay, the endolysin mixture was very effective in preventing the establishment of *S. aureus* and *S. epidermidis* biofilms compared to the individual endolysins. In general, the four endolysins were found to exhibit a strong synergy in killing staphylococcal strains as previously demonstrated for streptococcal phage λ SA2 and B30 endolysins against streptococci (170). This synergic effect can be explained by increased destructive effects on the three-dimensional peptidoglycan network when multiple unique bonds are attacked simultaneously, or by enhanced access to the cleavage site of one enzyme as a consequence of the catalytic action of the other (171)

To extend our understanding of LysSA10, LysSA14, LysSA15, and LysSA52 as anti-biofilm agents and their potential as disinfectants, we established *S. aureus* and *S. epidermidis* biofilm on foley catheter (well Lead[®]) and glass coupons, and then treated each with endolysin individually and in combination. Based on the plate count assay, the addition of endolysin on the matured biofilms resulted in decreasing colonized *S. aureus* and *S. epidermidis* by approximately up to 2.6 log compared to the control setting (Figure 32). Notably, scanning electron microscopy confirmed the reduction in total biomass in biofilms and highly induced morphological changes, which are an indication of bacterial cell damage (Figure 34-36). Similar to this, one recent study conducted by Lood and colleague (26), described the efficacy of phage lysine (PlyF307) on biofilm of *Acinetobacter baumannii* established on a catheter tube. According to their report, 2-hour treatment of the 3-day old biofilm resulted in a reduction of 1.6 log unit of *A. baumannii* in *in vitro* setting and about 2 log reduction of two days old biofilm in an *in vivo* model.

Initial attachment of bacteria to a solid surface, especially on medical devices like a catheter, is the first step in biofilm formation. Coating biomaterial surfaces with bactericidal or bacteriostatic substances in such a way that no bacterial adhesion can occur is one of the strategies to decrease the incidence of medical device-related infections among many (169). For instance, antibiotics have been commonly used to impregnate catheters to prevent biofilm formation (172, 173). Even though the result is promising, it could lead to the selection of antibiotic resistance (174). For this reason, investigating of

potential natural antimicrobial agents that can prevent and control microbial biofilm development on a range of medical devices has great importance. In the present study coating catheter with endolysin and subsequent prevention of biofilm formation on the catheter by *S. aureus* and *S. epidermidis* were also investigated using viable cell count assay. In this assay, an inhibition of biofilm formation by approximately 1 to 1.5 log unit was achieved (Figure 33). This result is low as compared to the result of biofilm removal assay of the same strains in this study, in which about 2.5 log reductions were achieved. The low result of preventing the initial attachment on coating catheter is most likely due to the instability of the enzymes on the catheter or leaching out from catheter sections. Thus, a strategy for the enzyme stability on the catheter surface is required in order to sustain their biofilm inhibition potential.

Catheter-related infections are one of a number of significant problems in healthcare (59). For example, catheter-related infections are responsible for bloodstream infection, and urinary tract infections in bladder catheters, which accounts for an estimated 20 % of the episodes of nosocomial infections in acute care and more than 50 % in long-term care facilities (175). Prevention of infections related to these biomaterials is an important goal. In view of the results of the biofilm formation and disruption assays in the present study, LysSA10, LysSA14, LysSA15, and LysSA52 endolysins could potentially be used as coating agents on medical devices to prevent staphylococcal adherence and biofilm formation. The validity of this approach has been previously demonstrated in lysostaphin-coated catheters for killing *S. aureus* (128) and Dispersin B (enzyme produced by oral Gram-negative bacterium *Actinobacillus actinomycetemcomitans*) coated catheters together with triclosan (an antiseptic present in many household products). These showed significant protection against colonization of *S. aureus* and *S. epidermidis*, *E. coli*, and *C. albicans* (176).

For the bioactivity evaluation of any protein, cytotoxicity test is one of the most important methods for preclinical research (177). *In vitro* cytotoxicity test makes use of mammalian cell culture. This is more advantageous over *in vivo* assays in some aspects such as cost efficiency, time and ethics (178). Among the various approaches of *in vitro* cytotoxicity tests, we selected the MTT assay method for testing of our newly produced endolysins against a human fibroblast cell line, in order to examine the concept whether they can be applied in the treatment of superficial infection caused by staphylococcal

species. This method is very sensitive, quantitative, and a reliable colorimetric assay which is used in evaluating cell viability as a function of redox potential (179). The evaluation of the cytotoxicity of the four endolysins (LysSA10, LysSA14, LysSA15, and LysSA52) revealed that there is a maximum of 8 % decrease in cell viability in LysSA52 treated cells compared to the untreated cells (Figure 37). For LysSA10, LysSA14, and LysSA15 only 4 to 5 % cell viability decrease was detected. The reduction of cell viability could result from the endolysin buffer that we used during the preparation of endolysins. The decreased in cell viability after endolysin buffer treatment supports this assumption. Another possibility for the apparent cytotoxicity could be due to the endotoxin transferred from the host cells during endolysin productions.



8. CONCLUSIONS AND RECOMMENDATIONS

- The result of the current study showed that prophage carriage is a common event for clinical isolates of *S. aureus*. PCR screening of the endolysin gene for identification and isolation of potential prophage in clinical isolates is required. With this approach new phages that infect *S. aureus* strains were isolated and characterized in this study.
- Genes encoding endolysins were amplified from the genomes of four phages and cloned into the pET SUMO expression vector. Four endolysins (LysSA10, LysSA14, LysSA15, and LysSA52), with a molecular mass of 66.22 kDa were over-expressed in *E. coli* BL21 (DE3) successfully.
- The putative genes of the four endolysins identified in this study were sequenced, and the resulting sequence data were submitted to the GenBank database and assigned the accession numbers MH025825, MH025826, and MH025827 for LysSA10, LysSA14, and LysSA15 respectively.
- The functionality of each endolysin was evaluated by spot test on a range of staphylococcal strains. The combination of the four endolysins showed activity against 78 (88.6 %) of the 88 total clinical staphylococcal strains including *S. aureus*, *S. epidermidis*, and *S. heamolyticus*. The lytic activities of each endolysin was 67 (83.7%) for LysSA14, 53 (62.3%) for LysSA10, 51 (60%) for LysSA15, and 48 (56.5%) for LysSA52 against 88 staphylococcal clinical isolates including *S. aureus*, *S. epidermidis*, and *S. heamolyticus*.
- The expressed endolysins were also characterized in terms of pH range and thermostability, and results revealed that all the four endolysins had a good stability over a broad range of pH (5.0-9.0) and retained high activity up to 50°C.
- In addition, the effects of endolysins on biofilm removal and biofilm inhibition of *S. aureus* and *S. epidermidis* on microtiter plates and on catheter sections were examined through crystal violet staining, viable bacterial counts, and scanning electron microscopy.

- Quantification of biofilms using crystal violet assay after 12 h treatment with endolysin cocktail revealed that there is decreased biofilm masses by up to 60 %. On catheter sections, the addition of endolysin at a concentration of 0.50 mg/mL, separately and in combination, resulted reduction of colonization by *S. aureus* and *S. epidermidis* by approximately 1.5 to 2.5 log units compared to the control.
- Notably, scanning electron microscopy confirmed that reduction in total biomass in *S. aureus* and *S. epidermidis* biofilm, and highly induced morphological changes were observed in both strains upon addition of endolysin, which is an indicative of bacterial cell damage.
- Analysis of cytotoxicity of each endolysin on mammalian fibroblast cells using the MTT assay indicated that their toxicity is tolerable.
- Certainly, all of the four endolysins (LysSA10, LysSA14, LysSA15, and LysSA52) characterized here provide starting point for further formulation of each endolysin to enhance their antimicrobial activities. Overall, our results show that LysSA10, LysSA14, LysSA15, and LysSA52 have a potential for application for decontamination, and could be utilized as coating agents on biomaterials including catheter to prevent the adherence and subsequent biofilm formation by staphylococcal strains.
- Further *in vitro* and *in vivo* studies are needed to be undertaken to assess their efficacy in the complex biological environments. Therefore, the following recommendations are made as future guidance.
- Determining the activity of each endolysin in combination with various antimicrobial drugs with an aim to identify the synergistic effects on eliminating both planktonic and biofilm forms of staphylococcal species.
- Development of an adequate formulation and stabilization of endolysins for various purposes such as spray, ointment, and other anti-staphylococcal agents.
- Improvement of the stability of the endolysin on a range of medical devices including catheters with various approaches such as enzyme immobilization (attachment of enzyme molecules onto or into a large surface) via nanoparticles, or through simple adsorption and covalent attachment.

- Furthermore, enhancing the activity of recombinant endolysins by modifying their structure can be considered.



9. REFERENCES

1. Otto M (2008). Staphylococcal biofilms. *Curr Top Microbiol Immunol* 322: 207-228.
2. Arciola, C. R., Campoccia, D., Speziale, P., Montanaro, L., & Costerton, J. W. (2012). Biofilm formation in *Staphylococcus* implant infections. A review of molecular mechanisms and implications for biofilm-resistant materials. *Biomaterials* 33 (26), 5967-5982.
3. Esposito S, Purrello S, Bonnet E, Novelli A, Tripodi F, Pascale R, Unal S, Milkovich G (2013). Central venous catheter-related biofilm infections: An up-to-date focus on methicillin-resistant *Staphylococcus aureus*. *J Glob Antimicrob Resist* 1(2): 71-78.
4. Francolini I, Donelli G (2010). Prevention and control of biofilm-based medical-device-related infections. *FEMS Immunol Med Microbiol* 59 (3): 227-238.
5. Sulakvelidze A, Alavidze Z, Morris JG (2001). Bacteriophage therapy. *Antimicrob Agents Chemother* 45(3): 649-659.
6. Drulis-Kawa Z, Majkowska-Skrobek G, Maciejewska B, Delattre A-S, Lavigne R (2012). Learning from bacteriophages—advantages and limitations of phage and phage-encoded protein applications. *Curr Protein Pept Sci* 13(8): 699-722.
7. Nelson DC, Schmelcher M, Rodriguez-Rubio L, Klumpp J, Pritchard DG, Dong S, Donovan DM (2012). Endolysins as antimicrobials. *Adv Virus Res* 83: 299-365
8. O'flaherty S, Coffey A, Meaney W, Fitzgerald G, Ross R (2005). The recombinant phage lysin LysK has a broad spectrum of lytic activity against clinically relevant staphylococci, including methicillin-resistant *Staphylococcus aureus*. *J Bacteriol* 187 (20): 7161-7164.
9. Schmelcher M, Donovan DM, Loessner MJ (2012). Bacteriophage endolysins as novel antimicrobials. *Future Microbiol* 7(10): 1147-1171.
10. Loessner MJ (2005). Bacteriophage endolysins—current state of research and applications. *Curr Opin Microbiol* 8(4): 480-487.
11. Becker SC, Dong S, Baker JR, Foster-Frey J, Pritchard DG, Donovan DM (2009). LysK CHAP endopeptidase domain is required for lysis of live staphylococcal cells. *FEMS Microbiol Lett* 294(1): 52-60.

12. Fenton M, McAuliffe O, O'Mahony J, Coffey A (2010). Recombinant bacteriophage lysins as antibacterials. *Bioeng Bugs* 1(1): 9-16.
13. Rashel M, Uchiyama J, Ujihara T, Uehara Y, Kuramoto S, Sugihara S, Yagyu K-I, Muraoka A, Sugai M, Hiramatsu K (2007). Efficient elimination of multidrug-resistant *Staphylococcus aureus* by cloned lysin derived from bacteriophage ϕ MR11. *J Infect Dis* 196(8): 1237-1247.
14. Szweda P, Schielmann M, Kotlowski R, Gorczyca G, Zalewska M, Milewski S (2012). Peptidoglycan hydrolases-potential weapons against *Staphylococcus aureus*. *Appl Microbiol Biotechnol* 96(5): 1157-1174.
15. Pastagia M, Euler C, Chahales P, Fuentes-Duculan J, Krueger JG, Fischetti VA (2011). A novel chimeric lysin shows superiority to mupirocin for skin decolonization of methicillin-resistant and sensitive *Staphylococcus aureus* strains. *Antimicrob Agents Chemother* 55(2): 738-744.
16. Sass P, Bierbaum G (2007). Lytic activity of recombinant bacteriophage ϕ 11 and ϕ 12 endolysins on whole cells and biofilms of *Staphylococcus aureus*. *Appl Environ Microbiol* 73(1): 347-352.
17. Rodríguez-Rubio L, Martínez B, Rodríguez A, Donovan DM, Götz F, García P (2013). The phage lytic proteins from the *Staphylococcus aureus* bacteriophage vB_SauS-phiPLA88 display multiple active catalytic domains and do not trigger staphylococcal resistance. *PLoS One* 8(5): e64671.
18. Hendrix RW (2002). Bacteriophages: evolution of the majority. *Theor Popul Biol* 61(4): 471-480.
19. Ashelford KE, Day MJ, Fry JC (2003). Elevated abundance of bacteriophage infecting bacteria in soil. *Appl Environ Microbiol* 69(1): 285-289.
20. Sharp R (2001). Bacteriophages: biology and history. *J Chem Technol Biotechnol* 76(7): 667-672.
21. Deghorain M, Van Melderen L. (2012). The staphylococci phages family: an overview. *Viruses* 4: 3316–3335.

22. Goerke C, Pantucek R, Holtfreter S, Schulte B, Zink M, Grumann D, Bröker BM, Doskar J, Wolz C (2009). Diversity of prophages in dominant *Staphylococcus aureus* clonal lineages. *J Bacteriol* 191(11): 3462-3468.
23. Carson L, Gorman SP, Gilmore BF (2010). The use of lytic bacteriophages in the prevention and eradication of biofilms of *Proteus mirabilis* and *Escherichia coli*. *FEMS Immunol Med Microbiol* 59(3): 447-455.
24. Curtin JJ, Donlan RM (2006). Using bacteriophages to reduce formation of catheter-associated biofilms by *Staphylococcus epidermidis*. *Antimicrob Agents Chemother* 50(4): 1268-1275.
25. Fu W, Forster T, Mayer O, Curtin JJ, Lehman SM, Donlan RM (2010). Bacteriophage cocktail for the prevention of biofilm formation by *Pseudomonas aeruginosa* on catheters in an in vitro model system. *Antimicrob Agents Chemother* 54(1): 397-404.
26. Lood R, Winer BY, Pelzek AJ, Diez-Martinez R, Thandar M, Euler CW, Schuch R, Fischetti VA (2015). Novel phage lysin capable of killing the multidrug-resistant gram-negative bacterium *Acinetobacter baumannii* in a mouse bacteremia model. *Antimicrob Agents Chemother* 59(4): 1983-1991.
27. Harris LG, Richards RG (2006). Staphylococci and implant surfaces: a review. *Injury* 37(2): S3-S14.
28. Orenstein A (2011). The discovery and naming of *Staphylococcus aureus*. *Periodical [serial online]* Date Available from.
29. Kloos WE, Bannerman TL (1994). Update on clinical significance of coagulase-negative staphylococci. *Clin Microbiol Rev.*7(1): 117-140.
30. Foster, T. (1996). *Staphylococcus*. *Medical Microbiology*. 4th edition. Galveston (TX): University of Texas Medical Branch at Galveston.
31. Taylor TA, Unakal CG (2017). *Staphylococcus aureus*.
32. Harris L, Foster S, Richards R (2002). An introduction to *Staphylococcus aureus*, and techniques for identifying and quantifying *S. aureus* adhesins in relation to adhesion to biomaterials: *Eur Cell Mater.* 4(3).

33. Tong, S. Y., Davis, J. S., Eichenberger, E., Holland, T. L., & Fowler, V. G. (2015). *Staphylococcus aureus* infections: epidemiology, pathophysiology, clinical manifestations, and management. *Clin microbiol Rev.* 28(3), 603-61.
34. Lucet J, Herrmann M, Rohner P, Auckenthaler R, Waldvogel F, Lew DP (1990). Treatment of experimental foreign body infection caused by methicillin-resistant *Staphylococcus aureus*. *Antimicrob Agents Chemother* 34(12): 2312-2317.
35. Dmitriev BA, Toukach FV, Holst O, Rietschel E, Ehlers S (2004). Tertiary structure of *Staphylococcus aureus* cell wall murein. *J Bacteriol* 186(21): 7141-7148.
36. Kashani HH, Schmelcher M, Sabzalipour H, Hosseini ES, Moniri R (2018). Recombinant endolysins as potential therapeutics against antibiotic-resistant *Staphylococcus aureus*: current status of research and novel delivery strategies. *Clin Microbiol Rev.*31(1): e00071-00017.
37. Brown S, Santa Maria Jr JP, Walker S (2013). Wall teichoic acids of gram-positive bacteria. *Annu Rev Microbiol* 67: 313-336.
38. Liu GY (2009). Molecular pathogenesis of *Staphylococcus aureus* infection. *Pediatr Res* 65(5): 71-77.
39. Wertheim HF, Van Kleef M, Vos MC, Ott A, Verbrugh HA, Fokkens W (2006). Nose picking and nasal carriage of *Staphylococcus aureus*. *Infect Control Hosp Epidemiol* 27(8): 863-867.
40. Chessa D, Ganau G, Spiga L, Bulla A, Mazzarello V, Campus GV, Rubino S (2016). *Staphylococcus aureus* and *Staphylococcus epidermidis* virulence strain as causative agents of persistent infections in breast implants. *PLoS One* 11(1): e0146668.
41. Todar K. (2005). *Todar's online textbook of bacteriology*. University of Wisconsin-Madison Department of Bacteriology.
42. Plano LR, Gutman DM, Woischnik M, Collins CM (2000). Recombinant *Staphylococcus aureus* Exfoliative Toxins are Not Bacterial Superantigens. *Infect Immun* 68(5): 3048-3052.
43. Gordon RJ, Lowy FD (2008). Pathogenesis of methicillin-resistant *Staphylococcus aureus* infection. *Clin Infect Dis* 46(Suppl 5): S350-S359.

44. Kong EF, Johnson JK, Jabra-Rizk MA (2016). Community-associated methicillin-resistant *Staphylococcus aureus*: an Enemy amidst Us. *PLoS Pathog* 12(10): e1005837.
45. Costa AR, Batistão DW, Ribas RM, Sousa AM, Pereira MO, Botelho CM (2013). *Staphylococcus aureus* virulence factors and disease. *Microbial pathogens and strategies for combating them: science, technology and education* 1: 702-710.
46. Kluytmans J, Van Belkum A, Verbrugh H (1997). Nasal carriage of *Staphylococcus aureus*: epidemiology, underlying mechanisms, and associated risks. *Clin Microbiol Rev* 10(3): 505-520.
47. Song X, Perencevich E, Campos J, Short BL, Singh N (2010). Clinical and economic impact of methicillin-resistant *Staphylococcus aureus* colonization or infection on neonates in intensive care units. *Infect Control Hosp Epidemiol* 31(2): 177-182.
48. Schleifer KH, Kloos WE (1975). Isolation and characterization of Staphylococci from human skin I. Amended descriptions of *Staphylococcus epidermidis* and *Staphylococcus saprophyticus* and descriptions of three new species: *Staphylococcus cohnii*, *Staphylococcus haemolyticus*, and *Staphylococcus xylosus*. *Int J Syst Evol Microbiol* 25(1): 50-61.
49. Becker K, Heilmann C, Peters G (2014). Coagulase-negative staphylococci. *Clinical microbiology reviews* 27(4): 870-926.
50. Landini P, Antoniani D, Burgess JG, Nijland R (2010). Molecular mechanisms of compounds affecting bacterial biofilm formation and dispersal. *Appl Microbiol Biotechnol* 86(3): 813-823.
51. Heilmann C, Schweitzer O, Gerke C, Vanittanakom N, Mack D, Götz F (1996). Molecular basis of intercellular adhesion in the biofilm-forming *Staphylococcus epidermidis*. *Mol Microbiol* 20(5): 1083-1091.
52. Zhao, X., Zhao, F., Wang, J., & Zhong, N. (2017). Biofilm formation and control strategies of foodborne pathogens: food safety perspectives. *RSC Advances*, 7(58): 36670-36683.
53. Hammer BK, Bassler BL (2003). Quorum sensing controls biofilm formation in *Vibrio cholerae*. *Mol Microbiol* 50(1): 101-104.

54. Stewart PS (2002). Mechanisms of antibiotic resistance in bacterial biofilms. *International J Med Microbiol* 292(2): 107-113.
55. Percival SL, Suleman L, Vuotto C, Donelli G (2015). Healthcare-associated infections, medical devices, and biofilms: risk, tolerance and control. *J Med Microbiol* 64(4): 323-334.
56. O'Toole G, Kaplan HB, Kolter R (2000). Biofilm formation as microbial development. *Annu Rev Microbiol* 54(1): 49-79.
57. Kaplan Já (2010). Biofilm dispersal: mechanisms, clinical implications, and potential therapeutic uses. *J Dent Res* 89(3): 205-218.
58. Flemming H-C, Wingender J, Szewzyk U, Steinberg P, Rice SA, Kjelleberg S (2016). Biofilms: an emergent form of bacterial life. *Nat Rev Microbiol* 14(9): 563.
59. Von Eiff C, Jansen B, Kohnen W, Becker K (2005). Infections associated with medical devices. *Drugs* 65(2): 179-214.
60. Shirliff, M., & Leid, J. G. (2009). *The role of biofilms in device-related infections (Vol. 2)*. New York: Springer.
61. Von Eiff C, Heilmann C, Peters G (1999). New aspects in the molecular basis of polymer-associated infections due to staphylococci. *Eur J Clin Microbiol Infect Dis* 18(12): 843-846.
62. Veenstra G, Cremers F, Van Dijk H, Flier A (1996). Ultrastructural organization and regulation of a biomaterial adhesin of *Staphylococcus epidermidis*. *J Bacteriol* 178(2): 537-541.
63. Heilmann C, Hussain M, Peters G, Götz F (1997). Evidence for autolysin-mediated primary attachment of *Staphylococcus epidermidis* to a polystyrene surface. *Mol Microbiol* 24(5): 1013-1024.
64. Shintani H (2004). Modification of medical device surface to attain anti-infection. *Trends Biomater Artif Organs* 18(1): 1-8.
65. Ren W, Sheng X, Huang X, Zhi F, Cai W (2013). Evaluation of detergents and contact time on biofilm removal from flexible endoscopes. *Am J Infect Control* 41(9): 89-92.

66. Gawande PV, Leung KP, Madhyastha S (2014). Antibiofilm and antimicrobial efficacy of DispersinB®-KSL-W peptide-based wound gel against chronic wound infection associated with bacteria. *Curr Microbiol* 68(5): 635-641.
67. Kaplan JB, Rangunath C, Ramasubbu N, Fine DH (2003). A Detachment of *Actinobacillus actinomycetemcomitans* biofilm cells by an endogenous β -hexosaminidase activity. *J Bacteriol* 185(16): 4693-4698.
68. Ackermann H-W (2001). Frequency of morphological phage descriptions in the year 2000. *Arch Virol* 146(5): 843-857.
69. Orlova E (2012). Bacteriophages and their structural organization InTech.
70. Summers WC (2001). Bacteriophage therapy. *Annu Rev Microbiol* 55(1): 437-451.
71. Guttman B, Raya R, Kutter E (2005). Basic phage biology. *Bacteriophages: Biology and applications* 4.
72. Elbreki M, Ross RP, Hill C, O'Mahony J, McAuliffe O, Coffey A (2014). Bacteriophages and their derivatives as biotherapeutic agents in disease prevention and treatment. *J Viruses* 2014.
73. McDaniel L, Paul J (2005). Effect of nutrient addition and environmental factors on prophage induction in natural populations of marine *Synechococcus* species. *Appl Environ Microbiol* 71(2): 842-850.
74. Barnhart B, Cox S, Jett J (1976). Prophage induction and inactivation by UV light. *J Virol* 18(3): 950-955.
75. Seeley N, Primrose S (1982). A review: the isolation of bacteriophages from the environment. *J Appl Microbiol* 53(1): 1-17.
76. Tomasz M (1995). Mitomycin C: small, fast and deadly (but very selective). *Chem Biol* 2(9): 575-579.
77. Little JW (2005). Lysogeny, prophage induction, and lysogenic conversion. *Phages. ASM*, 37-54.
78. Bae T, Baba T, Hiramatsu K, Schneewind O (2006). Prophages of *Staphylococcus aureus* Newman and their contribution to virulence. *Mol Microbiol* 62(4): 1035-1047.

79. Biddappa AC, Sundarrajan S, Ramalinga AB, Sriram B, Padmanabhan S (2012). *Staphylococcus* bacteriophage tails with bactericidal properties: New findings. *Biotechnol Appl Biochem* 59(6): 495-502.
80. Gutiérrez D, Martínez B, Rodríguez A, García P (2010). Isolation and characterization of bacteriophages infecting *Staphylococcus epidermidis*. *Curr Microbiol* 61(6): 601-608.
81. Summers WC (2006). Phage and the early development of molecular biology. *The bacteriophages* 2: 3-8.
82. Ackermann H-W, Prangishvili D (2012). Prokaryote viruses studied by electron microscopy. *Arch Virol* 157(10): 1843-1849.
83. Ackermann H-W (2007). 5500 Phages examined in the electron microscope. *Arch Virol* 152(2): 227-243.
84. Son J-S, Lee S-J, Jun SY, Yoon SJ, Kang SH, Paik HR, Kang JO, Choi Y-J (2010). Antibacterial and biofilm removal activity of a *podoviridae* *Staphylococcus aureus* bacteriophage SAP-2 and a derived recombinant cell-wall-degrading enzyme. *Appl Microbiol Biotechnol* 86(5): 1439-1449.
85. Nilsson AS (2014). Phage therapy—constraints and possibilities. *Ups J Med Sci* 119(2): 192-198.
86. Palomares LA, Estrada-Moncada S, Ramírez OT (2004). Production of recombinant proteins: challenges and solutions. *Methods Mol Biol* 267: 15-52
87. O'Mahony J, Fenton M, Henry M, Sleator RD, Coffey A (2011). Lysins to kill—a tale of viral weapons of mass destruction. *Bioeng Bugs* 2(6): 306-308.
88. Gräslund S, Nordlund P, Weigelt J, Hallberg BM, Bray J, Gileadi O, Knapp S, Oppermann U, Arrowsmith C, Hui R (2008). Protein production and purification. *Nat Methods* 5(2): 135-46
89. Porowińska, D., Wujak, M., Roszek, K., & Komoszyński, M. (2013). Prokaryotic expression systems. *Postepy Higi Med Dosw (Online)*, 67: 119-129.
90. Eiberle MK, Jungbauer A (2010). Technical refolding of proteins: do we have freedom to operate? *Biotechnol J* 5(6): 547-559.

91. Gaeng S, Scherer S, Neve H, Loessner MJ (2000). Gene Cloning and Expression and Secretion of *Listeria monocytogenes* Bacteriophage-Lytic Enzymes in *Lactococcus lactis*. *Appl Environ Microbiol* 66(7): 2951-2958.
92. Fischetti VA (2008). Bacteriophage lysins as effective antibacterials. *Curr Opin Microbiol* 11(5): 393-400.
93. Keary R, McAuliffe O, Ross R, Hill C, O'Mahony J, Coffey A (2013). Bacteriophages and their endolysins for control of pathogenic bacteria. Méndez-Vilas A *Microbial pathogens and strategies for combating them: science, technology, and education*, Formatex Research Center, Badajoz, Spain: 1028-1040.
94. Briers Y, Volekaert G, Cornelissen A, Lagaert S, Michiels CW, Hertveldt K, Lavigne R (2007). Muralytic activity and modular structure of the endolysins of *Pseudomonas aeruginosa* bacteriophages ϕ KZ and EL. *Mol Microbiol* 65(5): 1334-1344.
95. Fenton M, Ross P, McAuliffe O, O'Mahony J, Coffey A. (2010). Recombinant bacteriophage lysins as antibacterials. *Bioeng Bugs*1: 9–16.
96. Nelson D, Loomis L, Fischetti VA (2001). Prevention and elimination of upper respiratory colonization of mice by group A streptococci by using a bacteriophage lytic enzyme. *Proc Natl Acad Sci USA* 98(7): 4107-4112.
97. Hermoso JA, García JL, García P (2007). Taking aim on bacterial pathogens: from phage therapy to enzybiotics. *Curr Opin Microbiol*. 10(5): 461-472.
98. Loeffler JM, Nelson D, Fischetti VA (2001). Rapid killing of *Streptococcus pneumoniae* with a bacteriophage cell wall hydrolase. *Science* 294(5549): 2170-2172.
99. Yoong P, Schuch R, Nelson D, Fischetti VA (2004). Identification of a broadly active phage lytic enzyme with lethal activity against antibiotic-resistant *Enterococcus faecalis* and *Enterococcus faecium*. *J Bacteriol* 186(14): 4808-4812
100. Djurkovic S, Loeffler JM, Fischetti VA (2005). Synergistic killing of *Streptococcus pneumoniae* with the bacteriophage lytic enzyme Cpl-1 and penicillin or gentamicin depends on the level of penicillin resistance. *Antimicrob Agents Chemother* 49(3): 1225-1228.

101. Entenza J, Loeffler J, Grandgirard D, Fischetti V, Moreillon P (2005). Therapeutic effects of bacteriophage Cpl-1 lysin against *Streptococcus pneumoniae* endocarditis in rats. *Antimicrob Agents Chemother.* 49(11): 4789-4792.
102. Mao J, Schmelcher M, Harty WJ, Foster-Frey J, Donovan DM (2013). Chimeric Ply187 endolysin kills *Staphylococcus aureus* more effectively than the parental enzyme. *FEMS Microbiol Lett* 342(1): 30-36.
103. Becker SC, Foster-Frey J, Donovan DM (2008). The phage K lytic enzyme LysK and lysostaphin act synergistically to kill MRSA. *FEMS Microbiol Lett* 287(2): 185-191.
104. Daniel A, Euler C, Collin M, Chahales P, Gorelick KJ, Fischetti VA (2010). Synergism between a novel chimeric lysin and oxacillin protects against infection by methicillin-resistant *Staphylococcus aureus*. *Antimicrob Agents Chemother* 54(4): 1603-1612.
105. Loeffler JM, Djurkovic S, Fischetti VA (2003). Phage lytic enzyme Cpl-1 as a novel antimicrobial for pneumococcal bacteremia. *Infect Immun* 71(11): 6199-6204.
106. Wang Y, Sun J, Lu C (2009). Purified recombinant phage lysin LySMP: an extensive spectrum of lytic activity for swine streptococci. *Curr Microbiol* 58(6): 609-615.
107. Mayer MJ, Narbad A, Gasson MJ (2008). Molecular characterization of a *Clostridium difficile* bacteriophage and its cloned biologically active endolysin. *J Bacteriol* 190(20): 6734-6740.
108. Porter CJ, Schuch R, Pelzek AJ, Buckle AM, McGowan S, Wilce MC, Rossjohn J, Russell R, Nelson D, Fischetti VA (2007). The 1.6 Å crystal structure of the catalytic domain of PlyB, a bacteriophage lysin active against *Bacillus anthracis*. *J Mol Biol* 366(2): 540-550.
109. Takáč M, Witte A, Bläsi U (2005). Functional analysis of the lysis genes of *Staphylococcus aureus* phage P68 in *Escherichia coli*. *Microbiology* 151(7): 2331-2342.
110. Gu J, Feng Y, Feng X, Sun C, Lei L, Ding W, Niu F, Jiao L, Yang M, Li Y (2014). Structural and biochemical characterization reveals LysGH15 as an unprecedented “EF-hand-like” calcium-binding phage lysin. *PLoS Pathog.*10(5): e1004109.

111. Yokoi K-j, Kawahigashi N, Uchida M, Sugahara K, Shinohara M, Kawasaki K-I, Nakamura S, Taketo A, Kodaira K-I (2005). The two-component cell lysis genes holWMY and lysWMY of the *Staphylococcus warneri* M phage ϕ WMY: cloning, sequencing, expression, and mutational analysis in *Escherichia coli*. *Gene* 351: 97-108.
112. Zimmer M, Vukov N, Scherer S, Loessner MJ (2002). The murein hydrolase of the bacteriophage ϕ 3626 dual lysis system is active against all tested *Clostridium perfringens* strains. *Appl Environ Microbiol* 68(11): 5311-5317.
113. Son J, Jun S, Kim E, Park J, Paik H, Yoon S, Kang S, Choi YJ (2010). Complete genome sequence of a newly isolated lytic bacteriophage, EFAP-1 of *Enterococcus faecalis*, and antibacterial activity of its endolysin EFAL-1. *J Appl Microbiol* 108 (5): 1769-1779.
114. Domenech M, García E, Moscoso M (2011). In vitro destruction of *Streptococcus pneumoniae* biofilms with bacterial and phage peptidoglycan hydrolases. *Antimicrob Agents Chemother* 55 (9): 4144-4148.
115. Obeso JM, Martínez B, Rodríguez A, García P (2008). Lytic activity of the recombinant staphylococcal bacteriophage Φ H5 endolysin active against *Staphylococcus aureus* in milk. *Int J Food Microbiol* 128(2): 212-218.
116. Garcia P, Madera C, Martinez B, Rodriguez A, Evaristo Suarez J (2009). Jul. Prevalence of bacteriophages infecting *Staphylococcus aureus* in dairy samples and their potential as biocontrol agents. *J Dairy Sci* 92(7): 3019-3026.
117. Zhang H, Bao H, Billington C, Hudson JA, Wang R (2012). Isolation and lytic activity of the *Listeria* bacteriophage endolysin LysZ5 against *Listeria monocytogenes* in soya milk. *Food Microbiol* 31(1): 133-136.
118. Solanki K, Grover N, Downs P, Paskaleva EE, Mehta KK, Lee L, Schadler LS, Kane RS, Dordick JS (2013). Enzyme-based listericidal nanocomposites. *Sci Rep* 3: 1584.
119. Englen M, Kelley L (2000). A rapid DNA isolation procedure for the identification of *Campylobacter jejuni* by the polymerase chain reaction. *Lett Appl Microbiol* 31(6): 421-426.

120. Carey-Smith GV, Billington C, Cornelius AJ, Hudson JA, Heinemann JA (2006). Isolation and characterization of bacteriophages infecting *Salmonella* spp. FEMS Microbiol Lett 258(2): 182-186.
121. Sahin F, Karasartova D, Ozsan TM, Gerçeker D, Kıyan M (2013). Identification of a novel lytic bacteriophage obtained from clinical MRSA isolates and evaluation of its antibacterial activity. Mikrobiyol Bul 47(1): 27-34.
122. Synnott AJ, Kuang Y, Kurimoto M, Yamamichi K, Iwano H, Tanji Y (2009). Isolation from sewage influent and characterization of novel *Staphylococcus aureus* bacteriophages with wide host ranges and potent lytic capabilities. Appl Environ Microbiol 75(13): 4483-4490.
123. Li L, Zhang Z (2014). Isolation and characterization of a virulent bacteriophage SPW specific for *Staphylococcus aureus* isolated from bovine mastitis of lactating dairy cattle. Mol Biol Rep 41(9): 5829-5838.
124. Chung, C. T., & Miller, R. H. (1993). Preparation and storage of competent *Escherichia coli* cells. Methods Enzymol. Vol. 218, pp. 621-627.
125. Mishra AK, Rawat M, Viswas KN, Kumar S, Reddy M (2013). Expression and lytic efficacy assessment of the *Staphylococcus aureus* phage SA4 lysin gene. J Vet Sci 14(1): 37-43.
126. Schmelcher M, Waldherr F, Loessner MJ (2012). Listeria bacteriophage peptidoglycan hydrolases feature high thermoresistance and reveal increased activity after divalent metal cation substitution. Appl Microbiol Biotechnol 93(2): 633-643.
127. Gutierrez, D., Ruas-Madiedo, P., Martínez, B., Rodríguez, A., & García, P. (2014). Effective removal of staphylococcal biofilms by the endolysin LysH5. PLoS One, 9(9): e107307.
128. Shah A, Mond J, Walsh S (2004). Lysostaphin-coated catheters eradicate *Staphylococcus aureus* challenge and block surface colonization. Antimicrob Agents Chemother 48(7): 2704-2707.
129. Watters CM, Burton T, Kirui DK, Millenbaugh NJ (2016). Enzymatic degradation of in vitro *Staphylococcus aureus* biofilms supplemented with human plasma. Infect Drug Resist 9: 71.

130. Mosmann T (1983). Rapid colorimetric assay for cellular growth and survival: application to proliferation and cytotoxicity assays. *J Immunol Methods* 65(1-2): 55-63.
131. Pettersen EF, Goddard TD, Huang CC, Couch GS, Greenblatt DM, Meng EC, Ferrin TE (2004). UCSF Chimera a visualization system for exploratory research and analysis. *J Comput Chem* 25(13): 1605-1612.
132. Bradley DE (1967). Ultrastructure of bacteriophage and bacteriocins. *Bacteriol Rev* 31(4): 230.
133. Chang Y, Kim M, Ryu S (2017). Characterization of a novel endolysin LysSA11 and its utility as a potent biocontrol agent against *Staphylococcus aureus* on food and utensils. *Food Microbiol* 68: 112-120.
134. Donovan DM, Lardeo M, Foster-Frey J (2006). Lysis of staphylococcal mastitis pathogens by bacteriophage phi11 endolysin. *FEMS Microbiol Lett* 265(1): 133-139.
135. Fenton M, Ross R, McAuliffe O, O'Mahony J, Coffey A (2011). Characterization of the staphylococcal bacteriophage lysin CHAPK. *J Appl Microbiol* 111(4): 1025-1035.
136. Oakley BB, Talundzic E, Morales CA, Hiatt KL, Siragusa GR, Volozhantsev NV, Seal BS (2011). Comparative genomics of four closely related *Clostridium perfringens* bacteriophages reveals variable evolution among core genes with therapeutic potential. *BMC Genomics* 12(1): 282.
137. Sharma RD, Goswami N, Lynn AM (2009). A modeled structure for amidase-03 from *Bacillus anthracis*. *Bioinformation* 4(6): 242.
138. Zou Y, Hou C (2010). Systematic analysis of an amidase domain CHAP in 12 *Staphylococcus aureus* genomes and 44 staphylococcal phage genomes. *Comput Biol Chem* 34(4): 251-257.
139. Fenton M, Cooney JC, Ross RP, Sleator RD, McAuliffe O, O'Mahony J, Coffey A (2011). In silico modeling of the staphylococcal bacteriophage-derived peptidase CHAPK. *Bacteriophage* 1(4): 198-206.

140. Gutiérrez D, Fernández L, Rodríguez A, García P (2018). Are Phage Lytic Proteins the Secret Weapon To Kill *Staphylococcus aureus*? *MBio* 9(1): e01923-01917.
141. Denis O, Nonhoff C, Dowzicky MJ (2014). Antimicrobial susceptibility among Gram-positive and Gram-negative isolates collected in Europe between 2004 and 2010. *J Glob Antimicrob Resist* 2(3): 155-161.
142. Schneider-Lindner V, Delaney J, Dial S, Dascal A, Suissa S (2007). Antimicrobial drugs and community-acquired methicillin-resistant *Staphylococcus aureus*, United Kingdom. *Emerg Infect Dis* 13(7): 994.
143. Fauquet CM, Mayo MA, Maniloff J, Desselberger U, Ball LA (2005). Virus taxonomy: VIIIth report of the International Committee on Taxonomy of Viruses Elsevier Academic Press.p35.
144. Bebeacua C, Tremblay D, Farenc C, Chapot-Chartier M-P, Sadovskaya I, Van Heel M, Veesler D, Moineau S, Cambillau C (2013). Structure, adsorption to host, and infection mechanism of virulent lactococcal phage p2. *J Virol* 87(22): 12302-12312.
145. Estrella, L.A., Quinones, J., Henry, M., Hannah, R. M., Pope, R. K., Hamilton, T., & Biswajit, B. (2016). Characterization of novel *Staphylococcus aureus* lytic phage and defining their combinatorial virulence using the OmniLog® system. *Bacteriophage*, 6(3), e1219440.
146. Sturino JM, Klaenhammer TR (2006). Engineered bacteriophage-defense systems in bioprocessing. *Nat Rev Microbiol* 4(5): 395.
147. Deveau H, Garneau JE, Moineau S (2010). CRISPR/Cas system and its role in phage-bacteria interactions. *Annu Rev Microbiol* 64: 475-493.
148. Young R, Wang N, Roof WD (2000). Phages will out: strategies of host cell lysis. *Trends Microbiol* 8(3): 120-128.
149. Gallet R, Kanno S, Wang N (2011). Effects of bacteriophage traits on plaque formation. *BMC Microbiol* 11(1): 181.
150. Choi C, Kuatsjah E, Wu E, Yuan S (2010). The effect of cell size on the burst size of T4 bacteriophage infections of *Escherichia coli* B23. *J Exp Microbiol Immunol* 14: 85-91.


151. Kwan T, Liu J, DuBow M, Gros P, Pelletier J (2005). The complete genomes and proteomes of 27 *Staphylococcus aureus* bacteriophages. *Proc Natl Acad Sci U S A* 102(14): 5174-5179.
152. Keary, R., McAuliffe, O., Ross, R. P., Hill, C., O'Mahony, J., & Coffey, A. (2014). Genome analysis of the staphylococcal temperate phage DW2 and functional studies on the endolysin and tail hydrolase. *Bacteriophage*, 4(1): e28451.
153. Butt TR, Edavettal SC, Hall JP, Mattern MR (2005). SUMO fusion technology for difficult-to-express proteins. *Protein Expr Purif* 43(1): 1-9.
154. Rosano GL, Ceccarelli EA (2014). Recombinant protein expression in *Escherichia coli*: advances and challenges. *Front Microbiol* 5: 172.
155. Tripathi NK (2016). Production and purification of recombinant proteins from *Escherichia coli*. *ChemBioEng Reviews* 3(3): 116-133.
156. Dhalluin A, Bourgeois I, Pestel-Caron M, Camiade E, Raux G, Courtin P, Chapot-Chartier M-P, Pons J-L (2005). Acd, a peptidoglycan hydrolase of *Clostridium difficile* with N-acetylglucosaminidase activity. *Microbiology* 151(7): 2343-2351.
157. Niiranen L, Espelid S, Karlsten CR, Mustonen M, Paulsen SM, Heikinheimo P, Willassen NP (2007). Comparative expression study to increase the solubility of cold-adapted *Vibrio* proteins in *Escherichia coli*. *Protein Expr Purif* 52(1): 210-218.
158. Li Y (2009). Carrier proteins for fusion expression of antimicrobial peptides in *Escherichia coli*. *Biotechnol Appl Biochem* 54(1): 1-9.
159. Assadi-Porter FM, Patry S, Markley JL (2008). Efficient and rapid protein expression and purification of small high disulfide containing sweet protein brazzein in *E. coli*. *Protein Expr Purif* 58(2): 263-268.
160. Zuo X, Mattern MR, Tan R, Li S, Hall J, Sterner DE, Shoo J, Tran H, Lim P, Sarafianos SG (2005). Expression and purification of SARS coronavirus proteins using SUMO-fusions. *Protein Expr Purif* 42(1): 100-110.
161. Su Z, Huang Y, Zhou Q, Wu Z, Wu X, Zheng Q, Ding C, Li X (2006). High-level expression and purification of human epidermal growth factor with SUMO fusion in *Escherichia coli*. *Protein Pept Lett* 13(8): 785-792.

162. Coffey A, Fenton M, O'Mahony J, Henry M (2012). Purification and applications of bacteriophage lytic enzymes. Nova Science publisher 117-146.
163. Wittmann J, Eichenlaub R, Dreiseikelmann B (2010). The endolysins of bacteriophages CMP1 and CN77 are specific for the lysis of *Clavibacter michiganensis* strains. *Microbiology*. 156(8): 2366-2373.
164. Bornhorst JA, Falke JJ (2000). Purification of proteins using polyhistidine affinity tags. *Methods Enzymol* 326:245-54.
165. Hefti MH, Dixon R, Vervoort J (2001). A novel purification method for histidine-tagged proteins containing a thrombin cleavage site. *Anal Biochem* 295(2): 180-185.
166. Abaev I, Foster-Frey J, Korobova O, Shishkova N, Kiseleva N, Kopylov P, Pryamchuk S, Schmelcher M, Becker SC, Donovan DM (2013). Staphylococcal phage 2638A endolysin is lytic for *Staphylococcus aureus* and harbors an inter-lytic-domain secondary translational start site. *Appl Microbiol Biotechnol* 97(8): 3449-3456.
167. O'Flaherty S, Ross RP, Coffey A (2009). Bacteriophage and their lysins for the elimination of infectious bacteria. *FEMS Microbiol Rev* 33(4): 801-819.
168. Stewart PS, Costerton JW (2001). Antibiotic resistance of bacteria in biofilms. *The lancet* 358(9276): 135-138.
169. Chen, M., Yu, Q., & Sun, H. (2013). Novel strategies for the prevention and treatment of biofilm related infections. *Int J Mol Sci* 14(9):18488-18501.
170. Schmelcher, M., Powell, A. M., Camp, M. J., Pohl, C. S., & Donovan, D. M. (2015). Synergistic streptococcal phage λ SA2 and B30 endolysins kill streptococci in cow milk and in a mouse model of mastitis. *Appl Microbiol Biotechnol*, 99(20), 8475-8486.
171. Loeffler J, Fischetti V (2003). Synergistic lethal effect of a combination of phage lytic enzymes with different activities on penicillin-sensitive and-resistant *Streptococcus pneumoniae* strains. *Antimicrob Agents Chemother* 47(1): 375-377.

172. Casey AL, Mermel LA, Nightingale P, Elliott TS (2008). Antimicrobial central venous catheters in adults: a systematic review and meta-analysis. *Lancet Infect Dis* 8(12): 763-776.
173. Hockenhull JC, Dwan KM, Smith GW, Gamble CL, Boland A, Walley TJ, Dickson RC (2009). The clinical effectiveness of central venous catheters treated with anti-infective agents in preventing catheter-related bloodstream infections: a systematic review. *Crit Care Med* 37(2): 702-712.
174. Hoffman LR, D'argenio DA, MacCoss MJ, Zhang Z, Jones RA, Miller SI (2005). Aminoglycoside antibiotics induce bacterial biofilm formation. *Nature* 436(7054): 1171.
175. Nicolle LE (2014). Catheter associated urinary tract infections. *Antimicrob Resist Infect Control* 3(1): 23.
176. Darouiche, R. O., Mansouri, M. D., Gawande, P. V., & Madhyastha, S. (2009). Antimicrobial and antibiofilm efficacy of triclosan and DispersinB® combination. *J Antimicrob Chemother*, 64(1), 88-93.
177. Kunzmann A, Andersson B, Thurnherr T, Krug H, Scheynius A, Fadeel B (2011). Toxicology of engineered nanomaterials: focus on biocompatibility, biodistribution, and biodegradation. *Biochimica et Biophysica Acta (BBA)-General Subjects* 1810(3): 361-373.
178. Li W, Zhou J, Xu Y (2015). Study of the in vitro cytotoxicity testing of medical devices. *Biomed Rep* 3(5): 617-620.
179. Senthilraja P, Kathiresan K (2015). In vitro cytotoxicity MTT assay in Vero, HepG2, and MCF-7 cell lines study of Marine Yeast. *JAPS* 5 (03): 080-084.

10. ETHICAL COUNCIL APPROVAL

T.C. KARADENİZ
TEKNİK ÜNİVERSİTESİ
TIP FAKÜLTESİ BİLİMSEL
ARAŞTIRMALAR
ETİK KURUL BAŞKANLIĞI



KARADENİZ
TECHNICAL UNIVERSITY
FACULTY OF MEDICINE
ETHIC COUNCIL

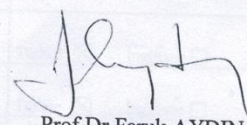
Sayı: 24237859- 616
Konu: Onay Belgesi

Tarih:16/11/2015

Sayın; Prof.Dr.İlknur TOSUN
Tıbbi Mikrobiyoloji ABD.


“Faj Kaynaklı Endolizinin Rekombinant Olarak Üretilmesi ve *Staphylococcus* Biyofilmleri Üzerine Etkisinin Araştırılması” başlıklı etik kurul 2015/120 no.lu tez çalışması raportör ve etik kurul görüşleri doğrultusunda; tıbbi etik açıdan uygun olduğuna karar verilmiştir.

Bilginizi ve gereğini rica ederim.


Prof.Dr.Faruk AYDIN
Etik Kurul Başkanı

Eki : 1 onay belgesi

ASLININ AYNIYDUR


Mehmet
KTÜ-1
Fakülte Sekreteri

KTÜ TIP FAKÜLTESİ BİLİMSEL ARAŞTIRMALAR
ETİK KURULU KARAR FORMU

BAŞVURU BİLGİLERİ	ARAŞTIRMANIN AÇIK ADI	“Faj Kaynaklı Endolizinin Rekombinant Olarak Üretilmesi ve <i>Staphylococcus</i> Biyofilmleri Üzerine Etkisinin Araştırılması”		
	ARAŞTIRMANIN PROTOKOL/PLAN KODU	2015/120		
	KOORDİNATÖR/SORUMLU ARAŞTIRMACI UNVANI/ADI/SOYADI	Prof.Dr.İlknur TOSUN		
	KOORDİNATÖR/SORUMLU ARAŞTIRMACININ UZMANLIK ALANI	Tıbbi Mikrobiyoloji		
	TEZ SAHİBİ/DİĞER ARAŞTIRICILAR, UNVANI/ADI/SOYADI	Doktora Öğr.Mujib *Abdulkadir ABDURRAHMAN, Prof.Dr.Ali Osman KILIÇ		
	DESTEKLEYİCİ			
	ARAŞTIRMANIN NİTELİĞİ			
	ARAŞTIRMANIN TÜRÜ	TEZ <input checked="" type="checkbox"/> AKADEMİK AMAÇLI <input type="checkbox"/>		
	ARAŞTIRMAYA KATILAN MERKEZLER	TEK MERKEZ <input checked="" type="checkbox"/>	ÇOK MERKEZLİ <input type="checkbox"/>	- ULUSAL <input type="checkbox"/>

DEĞERLENDİRİLEN BELGELER	Belge Adı	Tarihi	Versiyon Numarası	Dili	
		ARAŞTIRMA PROTOKOLÜ/PLANI			Türkçe <input checked="" type="checkbox"/> İngilizce <input type="checkbox"/> Diğer <input type="checkbox"/>
	BİLGİLENDİRİLMİŞ GÖNÜLLÜ OLUR FORMU			Türkçe <input checked="" type="checkbox"/> İngilizce <input type="checkbox"/> Diğer <input type="checkbox"/>	
	OLGU RAPOR FORMU			Türkçe <input checked="" type="checkbox"/> İngilizce <input type="checkbox"/> Diğer <input type="checkbox"/>	
DEĞERLENDİRİLEN DİĞER BELGELER	Belge Adı	Açıklama			
	TÜRKÇE ETİKET ÖRNEĞİ	<input type="checkbox"/>			
	SİGORTA	<input type="checkbox"/>			
	ARAŞTIRMA BÜTÇESİ	<input type="checkbox"/>			
	BIYOLOJİK MATERYEL TRANSFER FORMU	<input type="checkbox"/>			
	İLAN	<input type="checkbox"/>			
	YILLIK BİLDİRİM	<input type="checkbox"/>			
	SONUÇ RAPORU	<input type="checkbox"/>			
	GÜVENLİLİK BİLDİRİMLERİ	<input type="checkbox"/>			
DİĞER:	<input type="checkbox"/>				



Sayfa 1

Mehmet AYDIN
KTÜ TIP FAKÜLTESİ
Fakülte Sekreteri

KTÜ TIP FAKÜLTESİ BİLİMSEL ARAŞTIRMALAR
ETİK KURULU KARAR FORMU

KARAR BİLGİLERİ	Karar No: 4	Tarih: 09/11/2015.
	Prof.Dr.İlknur TOSUN'un sorumluluğunda yürütülen Doktora Öğr.Mujib Abdulkadir ABDURRAHMAN'a ait "Faj Kaynaklı Endolizinin Rekombinant Olarak Üretilmesi ve <i>Staphylococcus</i> Biyofilmleri Üzerine Etkisinin Araştırılması" başlıklı 2015/120 no.lu ve yukarıda başvuru bilgileri verilen araştırma/tez başvuru dosyası ile ilgili belgeler araştırmanın gerekçe, amaç, yaklaşım ve yöntemleri dikkate alınarak incelenmiş, gerçekleştirilmesinde etik sakınca bulunmadığına; toplantıya katılan etik kurul üyelerinin oy birliği ile karar verilmiştir.	

KTÜ TIP FAKÜLTESİ BİLİMSEL ARAŞTIRMALAR ETİK KURULU KARAR FORMU	
ÇALIŞMA ESASI	Klinik Araştırmalar Hakkında Yönetmelik, İyi Klinik Uygulamaları Kılavuzu
BAŞKANIN UNVANI / ADI / SOYADI:	Prof.Dr.Faruk AYDIN

Unvanı/Adı/Soyadı	Uzmanlık Alanı	Kurumu	Cinsiyet		İlişki *		Katılım **		İmza
Prof.Dr.Faruk AYDIN Başkan:	Tıbbi Mikrobiyoloji	KTÜ Tıp Fakültesi	E <input checked="" type="checkbox"/>	K <input type="checkbox"/>	E <input type="checkbox"/>	H <input checked="" type="checkbox"/>	E <input checked="" type="checkbox"/>	H <input type="checkbox"/>	
Prof.Dr.Gamze ÇAN Başkan Yrd.	Halk Sağlığı	KTÜ Tıp Fakültesi	E <input type="checkbox"/>	K <input checked="" type="checkbox"/>	E <input type="checkbox"/>	H <input checked="" type="checkbox"/>	E <input checked="" type="checkbox"/>	H <input type="checkbox"/>	
Prof.Dr.S.Caner KARAHAN Üye:	Tıbbi Biyokimya	KTÜ Tıp Fakültesi	E <input checked="" type="checkbox"/>	K <input type="checkbox"/>	E <input type="checkbox"/>	H <input checked="" type="checkbox"/>	E <input checked="" type="checkbox"/>	H <input type="checkbox"/>	
Prof.Dr.S. Murat KESİM Raportör:	Farmakoloji	KTÜ Tıp Fakültesi	E <input checked="" type="checkbox"/>	K <input type="checkbox"/>	E <input type="checkbox"/>	H <input checked="" type="checkbox"/>	E <input checked="" type="checkbox"/>	H <input type="checkbox"/>	
Prof.Dr.Yılmaz BÜLBÜL Üye:	Göğüs Hastalıkları	KTÜ Tıp Fakültesi	E <input checked="" type="checkbox"/>	K <input type="checkbox"/>	E <input type="checkbox"/>	H <input checked="" type="checkbox"/>	E <input checked="" type="checkbox"/>	H <input type="checkbox"/>	
Doç.Dr. Murat LİVAOĞLU Üye:	Plastik, Rekons. ve Estetik Cer	KTÜ Tıp Fakültesi	E <input checked="" type="checkbox"/>	K <input type="checkbox"/>	E <input type="checkbox"/>	H <input checked="" type="checkbox"/>	E <input type="checkbox"/>	H <input checked="" type="checkbox"/>	
Doç.Dr.Şafak ERSÖZ Üye:	Patoloji	KTÜ Tıp Fakültesi	E <input type="checkbox"/>	K <input checked="" type="checkbox"/>	E <input type="checkbox"/>	H <input checked="" type="checkbox"/>	E <input checked="" type="checkbox"/>	H <input type="checkbox"/>	
Doç.Dr. Evrim Ö. KARAGÜZEL Üye:	Ruh Sağlığı ve Hastalıkları	KTÜ Tıp Fakültesi	E <input type="checkbox"/>	K <input checked="" type="checkbox"/>	E <input type="checkbox"/>	H <input checked="" type="checkbox"/>	E <input checked="" type="checkbox"/>	H <input type="checkbox"/>	
Prof.Dr.Murat ÇAKIR Üye:	Çocuk Sağlığı ve Hastalıkları	KTÜ Tıp Fakültesi	E <input checked="" type="checkbox"/>	K <input type="checkbox"/>	E <input type="checkbox"/>	H <input checked="" type="checkbox"/>	E <input checked="" type="checkbox"/>	H <input type="checkbox"/>	

* :Araştırma ile İlişki
** :Toplantıda Bulunma



11. CURRICULUM VITAE

Name: Mujib Abdulkadir Abdurrahman

Sex: Male

Date of Birth: 1984

Place of Birth: Assendabo, Ethiopia

Nationality: Ethiopian

Marital Status: Married

E-mail: mujibe07@gmail.com

Educational Informations

Education level	Graduated Institution Name	Graduation Year
MSc in Microbiology	Haramaya University	2011
BSc in Applied Biology	Hawasa University	2005
Secondary School	Jimma Senior Secondary School	2002

Others Diploma

- Higher Diploma in Teachers Education (On duty training for about one year in Dire Dawa University, Ethiopia (September 25, 2011 to June 30, 2012)
- Diploma in Turkish Language from Ankara University TÖMER, Turkey (Attended From October 2012 to June 2013)

Language

- English, Amharic. Afan Oromo
- Turkish

Work Experience

Profession/duties	Institution	Duration
Lecturer	Dire Dawa University	August 2011- September 2012
Graduate Assistant	Dire Dawa University	November 2006-January 2008

Papers

1. Kiliç, A. O., I. Tosun, **M. A. Abdurrahman**. Anti-staphylococcal and anti-biofilm properties of three recombinant endolysins derived from *Staphylococcus aureus* bacteriophages, trsa10, trsa15, and 52. In the 28th ECCMID, the European Congress of Clinical Microbiology and Infectious Diseases, Madrid, Spain, 21-24 April 2018,
2. **Abdurahman, M. A.**, I. Tosun, A. O. Kiliç. Cloning, Expression and Antibacterial Activity Assessment of Lysin From *Staphylococcus aureus* Bacteriophage, Φ trsa14. In 10th Balkan Congress of Microbiology, Sofia, Bulgaria, 16-18 November 2017, pp.129-129.
3. **Abdurahman, M. A.**, İ. Tosun, A.O Kiliç. Cloning and expression of endolysin genes from Three *Staphylococcus aureus* Phages: ϕ SA10, ϕ SA15 and phage 52. In 37th Turkish Microbiology Congress, Antalya, Turkey, 16-20 November 2016, pp.190-190.
4. **Abdurahman, M. A.**, İ. Tosun, M. Khorshidtalab, İ. Durukan, G. Bayramoğlu, A.O. Kiliç. Isolation and Host Range determination of Temperate Bacteriophages from clinical isolates of *Staphylococcus aureus*. In 37th Turkish Microbiology Congress, Antalya, Turkey, 16-20 November 2016, pp.350-350.
5. M.Khorshidtalab, S.S. Nas, İ. Durukan, E.F. Tüfekci, **M. A. Abdurrahman**, A. O. Kiliç. Isolation and characterization of Lytic bacteriophages from Waste waters. In 37th Turkish Microbiology Congress, Antalya, Turkey, 16-20 November 2016, pp.183-183.
6. M.Khorshidtalab , I. Durukan , S.S.Nas , E.F.Tufekçi, **M.Abdurrahman**, A. O. Kiliç. Isolation and Characterization of a Lytic Bacteriophage From Wastewater Infecting *Enterobacter* spp., 3rd Congress of Baltic Microbiologists 2016, Vilnius, Lithuania, 18-21 October 2016, pp.77-77.
7. Tabbouche, S., Tüfekci E. F., Samanje, J., **Abdurrahman, M.**, Reis, A., Kiliç, A.O. Morphological and Genetic Characterization and Antimicrobial Susceptibility Determination of Bacteria Isolated from *Callosobruchus maculatus* (Bean Beetle's) Intestinal Flora. In 36th Turkish Microbiology Congress, Antalya, Turkey, 12-16 November 2014, pp 243-244.

Project

- Recombinant Phage Endolysins Production and Investigation of their Efficacy against Staphylococcal Biofilms, which was supported by Scientific Research Project unit from Karadeniz Technical University grant No. TDK-2015-5340, Turkey.

Hobbies:

Playing football, reading magazines and being engaged in Social works.

